

TWO DIMENSIONAL FINITE ELEMENT MODELING FOR THE MULTI TIER  
PILE WALL WITH ANCHOR SHORING SYSYTEM

A THESIS SUBMITTED TO  
THE GRADUATE SCHOOL OF NATURAL AND APPLIED SCIENCES  
OF  
MIDDLE EAST TECHNICAL UNIVERSITY

BY

YUNUS EMRE ÖZYÜREK

IN PARTIAL FULFILLMENT OF THE REQUIREMENTS  
FOR  
THE DEGREE OF MASTER OF SCIENCE  
IN  
CIVIL ENGINEERING

SEPTEMBER 2019



Approval of the thesis:

**TWO DIMENSIONAL FINITE ELEMENT MODELING FOR THE MULTI  
TIER PILE WALL WITH ANCHOR SHORING SYSYTEM**

submitted by **YUNUS EMRE ÖZYÜREK** in partial fulfillment of the requirements  
for the degree of **Master of Science in Civil Engineering Department, Middle East  
Technical University** by,

Prof. Dr. Halil Kalıpçılar  
Dean, Graduate School of **Natural and Applied Sciences**

\_\_\_\_\_

Prof. Dr. Ahmet Türer  
Head of Department, **Civil Engineering**

\_\_\_\_\_

Assoc. Prof. Dr. Nejan Huvaj Sarıhan  
Supervisor, **Civil Engineering, METU**

\_\_\_\_\_

**Examining Committee Members:**

Assoc. Prof. Dr. Zeynep Gülerce  
Civil Engineering, METU

\_\_\_\_\_

Assoc. Prof. Dr. Nejan Huvaj Sarıhan  
Civil Engineering, METU

\_\_\_\_\_

Assist. Prof. Dr. Onur Pekcan  
Civil Engineering, METU

\_\_\_\_\_

Prof. Dr. Nihat Sinan Işık  
Civil Engineering, Gazi University

\_\_\_\_\_

Assist. Prof. Dr. Gence Genç  
Civil Engineering, Çankaya University

\_\_\_\_\_

Date: 06.09.2019

**I hereby declare that all information in this document has been obtained and presented in accordance with academic rules and ethical conduct. I also declare that, as required by these rules and conduct, I have fully cited and referenced all material and results that are not original to this work.**

Name, Surname: Yunus Emre Özyürek

Signature:

## **ABSTRACT**

### **TWO DIMENSIONAL FINITE ELEMENT MODELING FOR THE MULTI TIER PILE WALL WITH ANCHOR SHORING SYSYTEM**

Özyürek, Yunus Emre  
Master of Science, Civil Engineering  
Supervisor: Assoc. Prof. Dr. Nejan Huvaj Sarıhan

September 2019, 129 pages

For deep excavations (such as greater than 20-25 m excavation depths) in urban areas, where there is strict deformation limits, multi-tier pile wall shoring system with soil anchors is becoming more widely used, since the system with one level of piles becomes insufficient or unfeasible. In this study, parameters affecting the behavior of multi-tier pile wall retaining system is investigated via two-dimensional finite element method. Firstly, a 30 m excavation is carried out with a multi-tier shoring system supported by prestressed ground anchors in an area with Ankara clay soil. This shoring system is analyzed by two-dimensional finite element method and the results are compared with the inclinometer measurements in the field. General deformation behavior measured by inclinometer could not be captured by any of the constitutive models. The “closest” pile horizontal deformation behavior to inclinometer measurements is obtained by using the Hardening Soil Model and drained geotechnical material parameters. Furthermore, the effects and the importance of overconsolidation ratio of clay in the results is demonstrated.

Then the effects of various parameters by using two - dimensional finite element method (using Plaxis 2D software) on multi-tier shoring systems supported by prestressed ground anchors are investigated. These parameters are embedded length of upper pile, embedded length of the lower pile (socket length), effect of having an

anchor at the overlap zone between two piles, the horizontal distance between upper and lower piles, interface friction coefficient between pile and soil, higher and lower intensity anchor placement (i.e. anchors per m<sup>2</sup> plan area of wall). When the anchor in overlap length of upper and lower piles is canceled, displacements increase significantly in the socket zone of upper pile and in top of lower pile. Therefore, in the multi-tier pile wall retaining system, construction of the last row anchors of upper pile must be completed (together with pre-stressing and cross beam construction) before starting to the forage of the lower pile. It is concluded that for horizontal distances greater than or equal to  $H/3$  (where  $H$  is the total depth of excavation) anchor lengths of two walls can be designed separately. The results of this study could be useful for safe design of multi-tier pile walls.

Keywords: Multi-Tier Pile Wall, Anchor, Plaxis 2D, Deep Excavation.

## ÖZ

### ÇOK SEVİYELİ KAZIKLI ANKRAJLI İKSA SİSTEMLERİNİN İKİ BOYUTLU SONLU ELEMANLAR YÖNTEMİ İLE ANALİZİ

Özyürek, Yunus Emre  
Yüksek Lisans, İnşaat Mühendisliği  
Tez Danışmanı: Doç. Dr. Nejan Huvaj Sarıhan

Eylül 2019, 129 sayfa

Deformasyon sınırlarının olduğu kentsel alanlarda derin kazılar (20-25 m'den fazla kazı derinliği gibi) için, zemin ankrajlı çok katmanlı kazık duvarı iksa sistemi yaygın olarak kullanılmaktadır, çünkü bir tek sıra kazık sistemi yetersiz ya da imkansız hale gelmektedir. Bu çalışmada, çok seviyeli kazıklı ankrajlı iksa sisteminin davranışını etkileyen parametreler iki boyutlu sonlu elemanlar yöntemi ile incelenmiştir. İlk olarak, Ankara kili bulunan bir alanda öngermeli zemin ankrajları ile desteklenen çok seviyeli bir iksa sistemi ile 30 metrelik bir kazı yapılmıştır. Bu iksa sistemi iki boyutlu sonlu elemanlar yöntemi ile analiz edilmiş ve sonuçlar, alandaki inklinometre ölçümleriyle karşılaştırılmıştır. İnklinometre ile ölçülen genel deformasyon davranışı, zemin modellerin hiçbiri ile elde edilememiştir. İnklinometre ölçümlerine “en yakın” kazık yatay deformasyon davranışı, “Hardening Soil” Modeli ve drenajlı zemin geoteknik parametreleri kullanılarak elde edilmiştir. Ayrıca aşırı konsolidasyon oranının sonuçlara etkisi ve önemi ortaya konmuştur.

Daha sonra, iki boyutlu sonlu elemanlar yöntemi (Plaxis 2D yazılımı) kullanılarak çeşitli parametrelerin, öngermeli zemin ankrajları tarafından desteklenen çok katmanlı iksa sistemleri üzerindeki etkileri incelenmiştir. Bu parametreler üst kazığın soket uzunluğu, alt kazığın soket uzunluğu, iki kazık arasında üst üste binme bölgesinde bir ankraj bulunup bulunmamasının etkisi, üst ve alt kazıklar arasındaki yatay mesafe, kazık ve zemin arasında arayüz sürtünme katsayısı, daha yüksek ve daha düşük yoğunluklu ankraj yerleşimi (duvarın m<sup>2</sup> plan alanı başına düşen ankraj sayısı). Üst ve alt sıra kazıkların üst üste binme bölgesindeki ankraj iptal edildiğinde, yatay deplasmanlar üst sıra kazık soket bölgesinde ve alt sıra kazıkların üst bölgesinde önemli ölçüde artmıştır. Bu nedenle, çok katmanlı kazık duvarlı iksa sistemlerinde, alt

kazığın foraj işlemine başlamadan önce üst sıra kazıkların son sıra ankrajların yapımı (öngerme ve kuşak kiriş yapısı ile birlikte) tamamlanmalıdır. Yatay mesafe analizlerinde ise,  $H/3$ 'e eşit veya daha büyük yatay mesafeler için (H toplam kazı derinliği) iki duvarın ankraj uzunluklarının ayrı ayrı tasarlanabileceği sonucuna varılmıştır. Bu çalışmanın sonuçları, çok seviyeli kazıklı ankrajlı İksa sistemlerinin güvenli tasarımı için faydalı olabilir.

Anahtar Kelimeler: Çok Seviyeli Kazıklı İksa Sistemi, Ankraj, Plaxis 2D, Derin Kazı.

To My Family

## ACKNOWLEDGEMENTS

First of all, I would like to appreciate to my supervisor Assoc. Prof. Dr. Nejan Huvaj Sarihan for her guidance, experience, technical support and encouragement throughout all process of this thesis.

I would like to express my gratitude the faculty members of the Geotechnical Department of Middle East Technical University, who helped me gain the knowledge, and experience that I have now.

I would also like to thank to my co-workers at İksa Engineering Co. for their valuable knowledge and support.

I would like to express my special thanks to my friend Gamze Yılmaz for her endless patience and help.

Finally, I would like to thank my family for all their love, motivation and support.

Yunus Emre ÖZYÜREK  
(Civil Engineer)

## TABLE OF CONTENTS

ABSTRACT .....	v
ÖZ .....	vii
ACKNOWLEDGEMENTS .....	x
TABLE OF CONTENTS .....	xi
LIST OF TABLES .....	xvi
LIST OF FIGURES .....	xviii
LIST OF ABBREVIATIONS .....	xxiii
1. INTRODUCTION .....	1
1.1. Problem Statement .....	4
1.2. Research Objectives .....	5
1.3. Scope of Thesis .....	6
2. OVERVIEW OF DEEP EXCAVATION SUPPORT SYSTEM AND LITERATURE REVIEW .....	7
2.1. Review of Deep Excavation Support System.....	7
2.1.1. Brief Information on Lateral Earth Pressures .....	7
2.1.2. Earth Pressure at Rest .....	8
2.1.3. Rankine Theory .....	9
2.1.4. Coulomb Theory .....	10
2.1.5. Earth Pressures Acting on Braced Excavations.....	11
2.2. Prestressed Anchored Pile Wall Design.....	13
2.2.1. Prestressed Soil Anchor Details.....	14
2.2.1.1. Types of Ground Anchors.....	14

2.2.1.2. Parts of Ground Anchor.....	15
2.2.1.3. Free (unbonded) length.....	16
2.2.1.4. Bonded Length.....	16
2.3. Location of Critical Potential Failure Surface .....	17
2.4. Failure Mechanism of Anchor System.....	19
2.4.1. Failure of Steel Tendon .....	20
2.4.2. Failure of Steel Tendon & Grout Body .....	20
2.4.3. Failure of Ground & Grout Body .....	20
2.4.4. Failure of Wall.....	21
2.4.5. Slip Failure .....	21
2.4.6. Rotational Failure .....	21
2.4.7. Wall Deformation Criteria.....	21
2.5. Literature Review of Other Studies on Deep Excavations .....	22
2.6. Finite Element Method and Plaxis 2D Analysis .....	27
2.6.1. Plaxis 2D .....	27
2.6.1.1. Graphical Model Input.....	27
2.6.1.2. Define Idealized Soil Profile .....	28
2.6.1.3. Plate .....	28
2.6.1.4. Interface .....	28
2.6.1.5. Ground Anchor .....	28
2.6.1.6. Embedded Beam Row .....	28
2.6.1.7. Loads.....	28
2.6.1.8. Auto Mesh Establishment.....	29
2.6.1.9. Staged Construction.....	29

3. CASE STUDY .....	31
3.1. Introduction .....	31
3.2. Project Information.....	31
3.3. General Geology and Soil Properties .....	32
3.3.1. Field Tests.....	33
3.3.1.1. Standard Penetration Test (SPT).....	34
3.3.1.2. Pressuremeter Test (PMT) .....	35
3.3.2. Laboratory Tests .....	36
3.3.3. Determination of Undrained (Short Term) Parameters .....	38
3.3.3.1. Undrained Shear Strength .....	38
3.3.3.2. Undrained Friction Angle .....	41
3.3.3.3. Undrained Elastic Modulus.....	41
3.3.4. Determination of Drained (Long Term) Parameters.....	44
3.3.4.1. Drained Friction Angle .....	44
3.3.4.2. Drained Cohesion.....	46
3.3.4.3. Drained Elastic Modulus.....	48
3.4. Soil Models.....	50
3.4.1. Mohr Coulomb Material Model (MC).....	50
3.4.2. Hardening Soil Material Model (HS) .....	51
3.5. Shoring System.....	54
3.5.1. Section Details .....	55
3.5.2. Anchor Details and Bond Length Capacity .....	57
3.5.3. Tensile Capacity of Anchorages .....	59
3.6. Finite Element Modelling of Multi-Tier Pile Wall .....	59

3.7. Inclinometer Measurements .....	65
3.8. The Effect of Overconsolidation Ratio On the Behavior of Shoring System.	66
3.9. Comparison of Results .....	68
4. PARAMETRIC STUDIES.....	69
4.1. Introduction.....	69
4.2. Description of Model .....	69
4.3. Soil Properties .....	71
4.4. Material Properties.....	71
4.5. Parametric Analysis .....	72
4.5.1. Determination of Upper Pile Socket Length .....	72
4.5.2. Determination of Lower Pile Socket Length.....	79
4.5.3. Effect of pile-soil interface friction .....	86
4.5.4. Effect of having an anchor on the overlap zone of two piles .....	88
4.5.5. Effect of Horizontal Distance Between Upper and Lower Pile .....	90
5. CONCLUSIONS .....	105
5.1. Scope of the case study and results .....	105
5.2. Scope of the parametric study and results.....	106
5.3. Limitations of the study and recommendations for future research.....	108
REFERENCES .....	109
A. BORING LOGS .....	113
B. SHORING SYSTEM PROJECT.....	117
C. CONSTRUCTION PHOTOS.....	120
D. PLAXIS 2D RESULTS.....	123
E. PLAXIS 2D RESULTS OF PARAMETRIC STUDIES .....	128



## LIST OF TABLES

### TABLES

Table 3.1 Locations and depth of boreholes .....	33
Table 3.2 Idealized soil profile and their properties, including $c_u$ (kPa) values .....	40
Table 3.3 Variation of undrained elastic modulus with OCR (Jamiolkowski et al. 1979).....	41
Table 3.4 Overconsolidation and undrained shear strength ratio (after Ladd et al. 1977) .....	42
Table 3.5 Over consolidation from undrained strength ratio (after Mayne et al., 2001). .....	43
Table 3.6 Over consolidation from undrained strength ratio (after Mayne et al., 2001). .....	43
Table 3.7 Undrained Elastic Modulus, $E_u$ (kPa) Values.....	44
Table 3.8 Drained friction angle $\phi'$ values .....	46
Table 3.9 Possible values of $\alpha$ factor in different soil types (Lunne et al. 1997) .....	47
Table 3.10 Drained Shear Strength, $c'$ (kPa) Values.....	48
Table 3.11 Drained Elastic Modulus, $E'$ (MPa) Values .....	48
Table 3.12 Drained and Undrained Parameters of Ankara Clay used in this study area .....	49
Table 3.13 Pile and Anchor Details of Deep Excavation .....	56
Table 3.14 Anchor details of the deepest excavation section.....	57
Table 3.15 Obtained results from Plaxis 2D analysis (1-continues) .....	64
Table 3.16 Obtained results from Plaxis 2D analysis (2) .....	64
Table 3.17 Obtained results from Plaxis 2D analysis (1-continues) .....	67
Table 3.18 Obtained results from Plaxis 2D analysis (2) .....	67
Table 4.1 PLAXIS 2D input parameters of bored piles.....	72
Table 4.2 PLAXIS 2D input parameters of anchors free length.....	72

Table 4.3 PLAXIS 2D input parameters of anchors bonded length .....	72
Table 4.4 Summary table of parametric studies for socket length of upper pile .....	73
Table 4.5 Plaxis 2D analyses results with higher intensity anchors (1-continues) ....	74
Table 4.6 Plaxis 2D analyses results with higher intensity anchors (2).....	75
Table 4.7 PLAXIS analyses results with lower intensity anchors (1-continues).....	75
Table 4.8 PLAXIS analyses results with lower intensity anchors (2).....	75
Table 4.9 Summary table of parametric studies for socket length of lower pile .....	80
Table 4.10 PLAXIS analyses results with higher intensity anchors (1-continues)....	81
Table 4.11 Plaxis 2D analyses results with higher intensity anchors (2).....	81
Table 4.12 Plaxis 2D analyses results with lower intensity anchors (1-continues) ...	82
Table 4.13 PLAXIS analyses results with lower intensity anchors (2).....	82
Table 4.14 Plaxis 2D analyses results of interface effect (1-continues) .....	87
Table 4.15 PLAXIS 2D analyses results of interface effect (2).....	87
Table 4.16 Plaxis 2D analyses result of with and without anchor on overlap zone (1-continues).....	89
Table 4.17 Plaxis 2D analyses result of with and without anchor on overlap zone (2).....	89
Table 4.18 PLAXIS analyses results of effect of horizontal distance (when the failure wedge of the whole 30-m deep excavation is considered) (1-continues) .....	91
Table 4.19 PLAXIS analyses results of effect of horizontal distance (when the failure wedge of the whole 30-m deep excavation is considered) (2).....	91
Table 4.20 Plaxis 2D analyses results of effect of horizontal distance (when the failure wedge of the individual, two separate walls, is considered) (1-continues).....	96
Table 4.21 PLAXIS analyses results of effect of horizontal distance (when the failure wedge of the individual, two separate walls, is considered) (2) .....	96
Table 4.22 Interaction coefficient vs horizontal distance .....	101

## LIST OF FIGURES

### FIGURES

Figure 1.1 Constructed multi-tier bored pile wall with anchors system in İstanbul Skyland project .....	2
Figure 1.2 Cross section view of the design of a multi-tier pile wall with anchors for a 30 m deep excavation in Ankara clay, in 2018 .....	3
Figure 1.3 Two-tier pile wall in Kuşadası (2014), (a) front view, (b) side view (N. Huvaj, personal communication) .....	5
Figure 2.1 Nature of lateral earth pressure on retaining wall .....	8
Figure 2.2 Coulomb's active earth pressure (Das 2007) .....	10
Figure 2.3 Apparent-pressure envelope (a) for cuts in sand, (b) for cuts in soft to medium clay, (c) for cuts in stiff clay (Peck 1969) .....	13
Figure 2.4 Main types of grouted ground anchors (FHWA-IF-99-015, 1999) .....	15
Figure 2.5 Components of a ground anchor (FHWA-IF-99-015, 1999) .....	15
Figure 2.6 Critical failure surface in ground anchor wall system (FHWA-IF-99-015, 1999) .....	17
Figure 2.7 Critical potential failure surface a: (FHWA-IF-99-015, 1999), b: BS 8081 (1989) .....	18
Figure 2.8 Potential failure conditions to be considered in design of anchored walls (FHWA-IF-99-015, 1999) .....	19
Figure 2.9 (a) Multi-tier pile wall with anchors for an excavation in İstanbul (Aktan, 2014), (b) Double-row excavation support system in China by Fang et al. (2013). .	26
Figure 2.10 Description of the interaction between two walls .....	26
Figure 3.1 Foundation formwork plan and pile layout plan .....	32
Figure 3.2 Locations of boreholes .....	32
Figure 3.3 Change in SPT-N values with depth .....	34
Figure 3.4 Pressuremeter modulus ( $E_M$ ) values with depth .....	35

Figure 3.5 Net limit pressure ( $P_{LN}$ ) values with depth.....	36
Figure 3.6 Laboratory test results (liquid limit, %, with depth).....	37
Figure 3.7 Laboratory test results (liquid limit, %, with depth).....	37
Figure 3.8 Laboratory test results (plasticity index, %, with depth).....	38
Figure 3.9 SPT- $N_{60}$ – $C_u$ ( $C_u = f_1 \times \text{SPT-}N_{60}$ ) – PI Correlations (Stroud 1974) .....	39
Figure 3.10 Undrained shear strength values using Stroud (1974) correlation with SPT- $N_{60}$ .....	39
Figure 3.11 Undrained shear strength values from pressuremeter test (Briaud, 1992) .....	40
Figure 3.12 Plasticity index and $E_u / N$ correlations (Poulos and Small, 2000).....	44
Figure 3.13 $\phi'_{nc}$ vs. $I_p$ for primarily normally consolidated reconstituted and undisturbed clays (Sorensen and Okkels, 2013) .....	45
Figure 3.14 Variation of $\sin \phi'$ with plasticity index for normally consolidated clays (Das 2007).....	46
Figure 3.15 Relation between $c'_{oc}$ and $c_u$ for overconsolidated clays (Sorensen and Okkels, 2013).....	47
Figure 3.16 Idealized Soil Profile .....	49
Figure 3.17 Mohr–Coulomb failure criterion: a) linear envelope in the Mohr diagram; b) pyramidal surface in principal stress space and cross-section in the equipressure plane .....	50
Figure 3.18 Hyperbolic stress-strain relation in primary loading for a standard drained triaxial test (after Schanz et al., 1999).....	52
Figure 3.19 Power law exponent $m$ related to a) Plasticity Index PI (Viggiani and Atkinson, 1995) and b) liquid limit $w_L$ (Hicker, 1996).....	53
Figure 3.20 Definition of $E_{oedref}$ in oedometer test results (Plaxis Material Models Manual, 2011) .....	54
Figure 3.21 Facade view of constructed bored piles.....	55
Figure 3.22 Top view of piles .....	56
Figure 3.23 Cross section details of the deep excavation .....	56

Figure 3.24 4×0,6” Temporary anchor typical cross section.....	58
Figure 3.25 Skin friction in cohesive soils for various fixed anchor lengths, with and without post-grouting (after Ostermayer, 1974).....	58
Figure 3.26 a) Initial phase, b) upper pile construction, c) upper part of anchors and excavation works, d) upper pile horizontal displacement. ....	61
Figure 3.27 Lower pile construction, lower part of anchors and excavation works, horizontal displacement of shoring system, bending moments of piles. ....	62
Figure 3.28 Shear forces on piles, horizontal displacement of shoring system, factor of safety, incremental deviatoric strain.....	63
Figure 3.29 Horizontal deformations on piles in Plaxis 2D .....	65
Figure 3.30 Inclinometer measurements.....	66
Figure 4.1 Geometry of multi-Tier pile wall shoring system that is used in parametric study.....	70
Figure 4.2 Cross section of shoring system (Upper pile socket length) .....	74
Figure 4.3 Horizontal displacement results ((1) indicates higher intensity anchor per m <sup>2</sup> area).....	76
Figure 4.4 Moment values on piles ((1) indicates higher intensity anchor per m <sup>2</sup> area) .....	76
Figure 4.5 Shear forces on piles ((1) indicates higher intensity anchor per m <sup>2</sup> area)	77
Figure 4.6 Maximum Anchor Load ((1) indicates higher intensity anchor per m <sup>2</sup> area) .....	77
Figure 4.7 Factor of Safety Values ((1) indicates higher intensity anchor per m <sup>2</sup> area) .....	78
Figure 4.8 Cross section of shoring system (lower pile socket length).....	80
Figure 4.9 Horizontal displacement results ((1) indicates higher intensity anchor per m <sup>2</sup> area).....	83
Figure 4.10 Moment forces on piles ((1) indicates higher intensity anchor per m <sup>2</sup> area) .....	83
Figure 4.11 Shear forces on piles ((1) indicates higher intensity anchor per m <sup>2</sup> area) .....	84

Figure 4.12 Maximum Anchor Load ((1) indicates higher intensity anchor per m <sup>2</sup> area)	84
Figure 4.13 Factor of Safety Values ((1) indicates higher intensity anchor per m <sup>2</sup> area)	85
Figure 4.14 Cross section of shoring system (7th Row Anchor)	88
Figure 4.15 Cross section of shoring system (Horizontal Distance)	90
Figure 4.16 Horizontal displacement results (when the failure wedge of the whole 30-m deep excavation is considered)	92
Figure 4.17 Moment values on piles (when the failure wedge of the whole 30-m deep excavation is considered)	93
Figure 4.18 Shear forces on piles (when the failure wedge of the whole 30-m deep excavation is considered)	93
Figure 4.19 Maximum anchor loads (when the failure wedge of the whole 30-m deep excavation is considered)	94
Figure 4.20 Factor of safety values (when the failure wedge of the whole 30-m deep excavation is considered)	94
Figure 4.21 Cross section of shoring system (Horizontal Distance) (when the failure wedge of the individual, two separate walls, is considered)	96
Figure 4.22 Horizontal displacement results (when the failure wedge of the individual, two separate walls, is considered)	97
Figure 4.23 Moment values on piles (when the failure wedge of the individual, two separate walls, is considered)	98
Figure 4.24 Shear forces on piles (when the failure wedge of the individual, two separate walls, is considered)	98
Figure 4.25 Maximum anchor loads (when the failure wedge of the individual, two separate walls, is considered)	99
Figure 4.26 Factor of safety values (when the failure wedge of the individual, two separate walls, is considered)	99
Figure 4.27 Interaction coefficient vs horizontal distance	102
Figure 4.28 Description of the interaction between two walls	102



## LIST OF ABBREVIATIONS

<b>ASSHTO</b>	American Association of State Highway and Transportation Officials
<b>ASTM</b>	American Society for Testing and Materials
<b>BS</b>	British Standards
<b>CAD</b>	Computer Aided Design
<b>FEM</b>	Finite Element Modelling
<b>FHWA</b>	Federal Highway Administration
<b>FS</b>	Factor of Safety
<b>HSM</b>	Hardening Soil Model
<b>LL</b>	Liquid Limit
<b>MC</b>	Mohr Coulomb
<b>NAVFAC</b>	Naval Facilities Engineering Command
<b>PI</b>	Plasticity Index
<b>PL</b>	Plastic Limit
<b>OCR</b>	Over consolidation Ratio
<b>PMT</b>	Pressuremeter Test
<b>SPT</b>	Standard Penetration Test



## **CHAPTER 1**

### **INTRODUCTION**

Nowadays, the rapid increase in the population has started to change the urbanization requirements all over the city centers, significantly. The land value is getting costly day by day, so land efficient designs and solutions related to the underground constructions have higher importance. Designs focusing on deep excavations become essential for almost every project in cities. The main principle of deep excavation support systems is to ensure not only the safety of the retaining system but also the safety of the surrounding structures such as existing buildings, roads and infrastructural facilities.

A common shoring system of deep excavations is composed of bored piles supported by soil anchors. The performance of the shoring system is dependent on soil and groundwater conditions, as well as other factors. For relatively deeper excavations (such as greater than 20-25 m excavation depths) in urban areas, where there are strict deformation limits, multi-tier pile wall shoring system with soil anchors (examples in Figure 1.1 and Figure 1.2) is becoming more widely used, since the system with one level of piles becomes insufficient, uneconomical or unfeasible. In this study, parameters affecting the behavior of multi-tier pile wall shoring system is investigated via two-dimensional finite element method.

More than 70 m deep excavation project is completed in Istanbul (Skyland Project); composed of multi-tier shoring system, in a soil profile consisting of sandstone and claystone layers. In fact, this project is reportedly the deepest excavation project supported by pile walls with anchors, not only in Europe, but also in the World. The foundation excavation project consisted of multi-tier bored pile – mini pile for vertical elements and pre-tensioned anchors for horizontal elements.

Bored pile lengths were ranging between 20 m - 27 m and prestressed anchor lengths were between 28 m – 56 m. In the design, there were 5 berms (multi-tiers), 4 of which used anchors and bored piles and 1 berm used anchors and shotcrete. When the final excavation depth was reached, the measured maximum horizontal deformations were about 30 mm in this project. Facade view of constructed multi-tier bored piles and anchors can be seen in Figure 1.1 published by Kasktaş Co. in 2015.



Figure 1.1 Constructed multi-tier bored pile wall with anchors system in İstanbul Skyland project

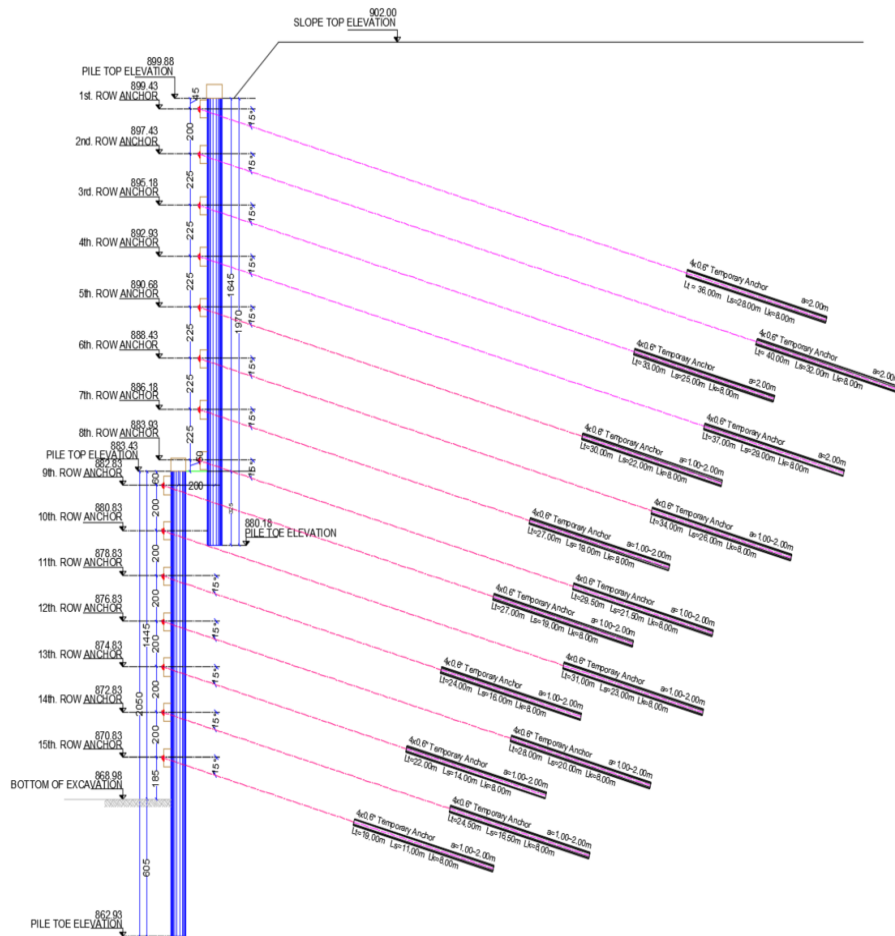


Figure 1.2 Cross section view of the design of a multi-tier pile wall with anchors for a 30 m deep excavation in Ankara clay, in 2018

Some of the reasons for choosing a multi-tier pile wall as a shoring system for a deep excavation, instead of a single wall are:

- (1) Construction of bored piles that are longer than 30 m requires piling machines with larger torque capacity and is very difficult and expensive as compared to construction of shorter piles,
- (2) When constructing bored piles longer than 30 m, accuracy in the verticality of the pile decreases. In multi-tier pile wall systems, due to the shorter length of

pile, the deviations that may occur from the pile vertical axis decrease and defects in the pile decrease, as compared to longer pile construction.

- (3) It takes a lot of time in the 30-meter forage pile hole to unload soil from boom cylinder and back into the pit. The reason is that boom cylinder covers a longer distance and repeats it many times. Therefore; construction time is longer for the longer piles. In multi-tier pile system, the construction of shorter piles can be completed more quickly in the field, and this provides time savings because, the other stages (such as the removal of the soil in front of the pile) can start earlier than long-single-pile system construction. While pile construction can continue over a large area, there are opportunities to start excavation, anchoring and construction on other facades.

### **1.1. Problem Statement**

Numerous successful applications of multi-tier pile wall systems have been published by several researchers (Aktan, 2014) and also constructed in the field (Figure 1.1). However, cases of failures and instabilities have also been reported in multi-tier shoring systems in recent years. For example, excessive deformations were observed and emergency fill was placed in front of piles, in a two-tiered pile wall system with anchors in Kuşadası, in 2014 (Figure 1.3.), when the excavation depth was about 16 m (which is even before reaching to the final depth of excavation of 27 m). The profile was composed of claystone and clayey limestone and the ground surface behind the piles had 15-degree slope angle, where 4-5 story buildings were located.

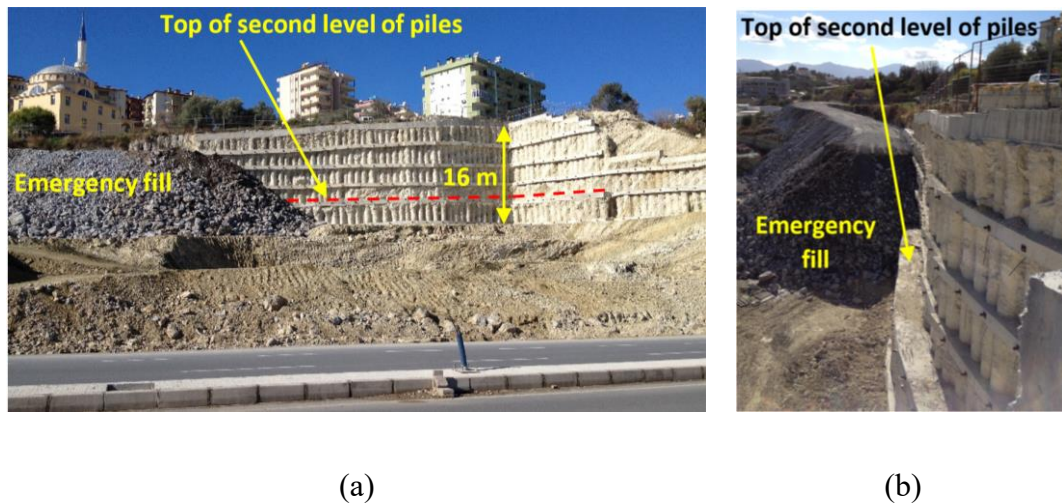


Figure 1.3 Two-tier pile wall in Kuşadası (2014), (a) front view, (b) side view (N. Huvaj, personal communication)

Interaction among bored piles, anchors and soil is a complex mechanism that involves significant number of variables by the nature of the problem. Pile spacing, pile embedment depth, pile rigidity, geotechnical properties of soils, pile head fixity conditions are some of the important factors in design for a typical project. Investigating the effects of these factors, revealing interrelation between them and understanding actual behavior have a vital importance because of lack of comprehensive and widespread design guideline about multi-tier bored piles with soil anchors.

## 1.2. Research Objectives

The main objective of this study is to investigate the factors affecting the behavior of multi-tier bored pile walls with anchors by using two-dimensional finite element method.

The effects of factors such as (1) the embedded length of lower and upper pile (i.e. does the overlap length of two piles, or the embedment length of the lower pile influence the behavior?), (2) the level of anchor intensity per  $m^2$  area of wall (is the shoring system behavior different at different anchor intensity levels?), (3) horizontal spacing between the two pile walls (at which horizontal spacing the system behaves like two individual,

separate, walls? And when they should be designed like individual pile walls with their own anchors?), (4) existence of an anchor at the overlap zone of two piles (is the behavior of wall system influenced by having an anchor at the overlap zone?), (5) coefficient of interface friction between pile and soil.

Firstly, verification study needs to be carried out to check the accuracy of two-dimensional finite element model and soil constitutive models used, by investigating the compatibility of the results with the full-scale measurements in the field in a multi-tier wall system. Then via a parametric study using two-dimensional finite element modeling, a two-tier pile wall system in Ankara clay is analyzed, to evaluate the effects of above-mentioned factors.

Results obtained from this study can be useful to evaluate the behavior of the multi-tier pile wall in-depth, to establish a better understanding about actual mechanism of the system and to develop comprehensive design procedures.

### **1.3. Scope of Thesis**

This study investigates the behavior of multi-tier pile wall supported by soil anchors system via finite element analyses (using finite element software Plaxis 2D 2019). Chapter 2 represents the literature review and describe geometry and length of piles and soil anchors studied by 2D finite element model. In Chapter 3, a case study is analyzed to verify the accuracy of the proposed finite element models and constitutive soil models. Afterwards, in Chapter 4, a parametric study is carried out to investigate the factors affecting multi-tier shoring system. Results and suggestions for future research is given in Chapter 5.

## **CHAPTER 2**

### **OVERVIEW OF DEEP EXCAVATION SUPPORT SYSTEM AND LITERATURE REVIEW**

Excavating deep into the ground has become an attractive option for contractors in recent years, especially in big cities, for reasons such as developing required parking lots, number of floor restrictions, constraints at the construction sites, creating more sellable building area, for dealing with high land costs, and/or for reducing the net foundation pressure on the ground. Variables such as depth of excavation, soil properties, permanent or temporary shoring system, nature of groundwater, all of these factors change excavation costs considerably. For this reason, deep excavation systems must be well-designed and appropriate construction techniques must be used.

#### **2.1. Review of Deep Excavation Support System**

##### **2.1.1. Brief Information on Lateral Earth Pressures**

Vertical or near vertical slopes of soil are supported by retaining walls, cantilever sheet pile walls, braced cuts and other similar retaining structures. The proper design of these structures requires an estimation of lateral earth pressure which is a function of factors such as type and amount of wall movement, shear strength parameters of soil, unit weight of soil and drainage condition in the backfill. The nature and different types of lateral pressures, at-rest, active and passive lateral earth pressure conditions are illustrated in Figure 2.1. The ratio of the horizontal effective stress to vertical effective stress identifies lateral earth pressure coefficient.

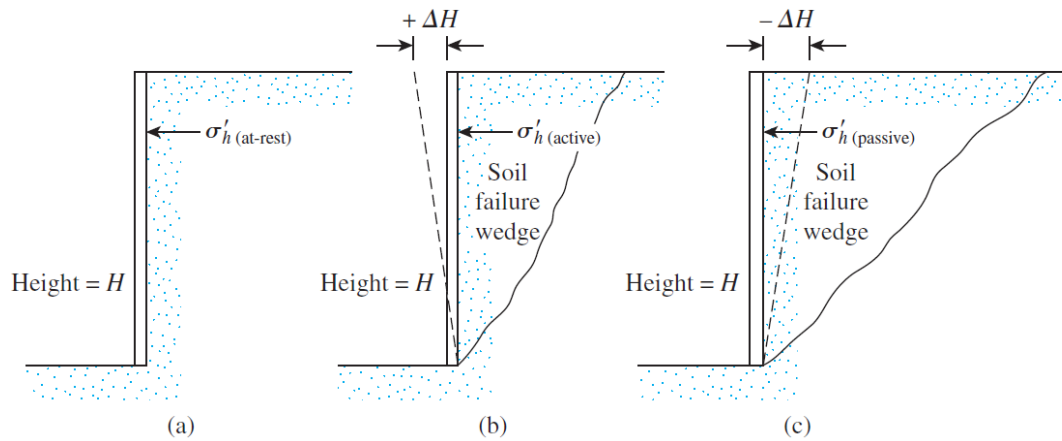


Figure 2.1 Nature of lateral earth pressure on retaining wall

### 2.1.2. Earth Pressure at Rest

If the retaining wall is not allowed to move to any direction, the lateral pressure at a depth  $z$  is

$$\sigma_h = K_0 * \sigma'_0 + u \quad (2.1)$$

where

$\sigma_h$ : Total horizontal stress

$\sigma'_0$ : Effective vertical stress

$u$  : Pore water pressure

$K_0$ : Coefficient of at rest earth pressure

For normally consolidated soil, the relation for  $K_0$  (Jacky, 1944) is

$$K_0 = 1 - \sin\phi' \quad (2.2)$$

For over-consolidated soil, at rest earth pressure coefficient can be expressed as (Mayne and Kulhawy, 1982)

$$K_0 = (1 - \sin\phi')OCR^{\sin\phi'} \quad (2.3)$$

Where;

OCR : Over-consolidation ratio

### 2.1.3. Rankine Theory

Following assumptions are required for Rankine Theory to be valid (Coduto, 2001);

- ✓ Soil is homogeneous and isotropic.
- ✓ The length of the wall is limitless and wall is examined in two dimensions.
- ✓ The wall can move enough to satisfy prerequisites of active or passive pressure.
- ✓ The friction between the wall and soil is insignificant.

In this theory, active lateral earth pressure is determined by Equation 2.4 and passive lateral earth pressure is obtained via equation 2.5:

$$\sigma'_a = (\gamma'z + q)K_a - 2c'\sqrt{K_a} \quad (2.4)$$

$$\sigma'_p = (\gamma'z + q)K_p + 2c'\sqrt{K_p} \quad (2.5)$$

$\sigma'_a$  : Active lateral earth pressure, and  $\sigma'_p$  : Passive lateral earth pressure,

$c'$  : cohesion,

$K_a$  : Active lateral earth pressure coefficient,  $K_p$  : Passive lateral earth pressure coefficient

$\gamma'$  : buoyant unit weight of soil,

$z$  : depth

$q$  : surcharge

Lateral earth pressure coefficient in the active and passive state (if the soil behind the wall is horizontal) are calculated by equations given in equation 2.6 and equation 2.7, respectively:

$$K_a = \tan^2(45 - \Phi/2) \quad (2.6)$$

$$K_p = \tan^2(45 + \Phi/2) \quad (2.7)$$



3. The active force per unit length of the wall, which will be inclined at an angle  $\delta$  to the normal drawn to the back face of the wall.

Coulomb active forces are calculated by Equation 2.8;

$$P_a = \frac{1}{2} \gamma H^2 K_a \quad (2.8)$$

where,

$$K_a = \frac{\sin^2(\beta + \phi')}{\sin^2(\beta) \sin(\beta - \delta) \left[ 1 + \sqrt{\frac{\sin(\delta' + \phi') \sin(\phi' - \alpha)}{\sin(\beta - \delta) \sin(\alpha + \beta)}} \right]^2} \quad (2.9)$$

and H: height of the wall.

Coulomb passive force is calculated by Equation 2.10

$$P_p = \frac{1}{2} \gamma H^2 K_p \quad (2.10)$$

where,

$$K_p = \frac{\sin^2(\beta - \phi')}{\sin^2(\beta) \sin(\beta + \delta) \left[ 1 - \sqrt{\frac{\sin(\delta' + \phi') \sin(\phi' + \alpha)}{\sin(\beta + \delta) \sin(\alpha + \beta)}} \right]^2} \quad (2.11)$$

and H : height of the wall.

$\alpha$ : Slope angle above the retaining wall (Figure 2.2)

$\beta$ : Angle of the back-face of the retaining wall from horizontal

$\phi$ : Angle of resultant force with normal to the failure plane in soil

$\delta$ : Angle of friction between the wall and backfill

$\gamma$ : Unit weight of soil

### 2.1.5. Earth Pressures Acting on Braced Excavations

In the excavations supported by shoring systems, soil pressures cannot be calculated by classical earth pressure theories. The reason for that is, the soil movement and failure criteria does not correspond in the Rankine and Coulomb theories mentioned in the previous chapters. It is known that shoring system has to move a little from the

bottom to form active earth pressure. If classical earth pressure theories are used in the shoring system, the design will be made by considering lower lateral earth pressures in the upper parts of the wall and the support system will be weaker. Therefore, distribution of soil pressure must be calculated with different methods.

The modified pressure envelope shows a uniform earth pressure distribution in sand, as in Figure 2.3(a) and the active earth pressure for sands is given as:

$$\sigma_a = 0.65\gamma HK_a \quad (2.12)$$

where

$K_a$ : Rankine active pressure coefficient =  $\tan^2(45 - \phi'/2)$

$\phi'$ : Effective friction angle of sand

H : Height of cut

$\gamma$  : Unit weight of soil

In soft to medium clays and in stiff clays, Peck (1969) provided envelopes of apparent-lateral-pressure diagrams for cuts. The pressure envelope for soft to medium clay is shown in Figure 2.3(b) and is applicable to the condition

$$\frac{\gamma H}{c} > 4$$

Where c is undrained shear strength ( $\phi = 0$ )

The pressure,  $\sigma_a$ , is the larger of

$$\sigma_a = \gamma H \left[ \left( 1 - \frac{4c}{\gamma H} \right) \right] \quad (2.13)$$

$$\sigma_a = 0.3\gamma H \quad (2.14)$$

The pressure envelope for cuts in stiff clay is;

$$\sigma_a = 0.2\gamma H \text{ to } 0.4\gamma H \quad (\text{with an average of } 0.3\gamma H) \quad (2.15)$$

Soil pressure diagrams described by Peck (1969) are given in following figures.

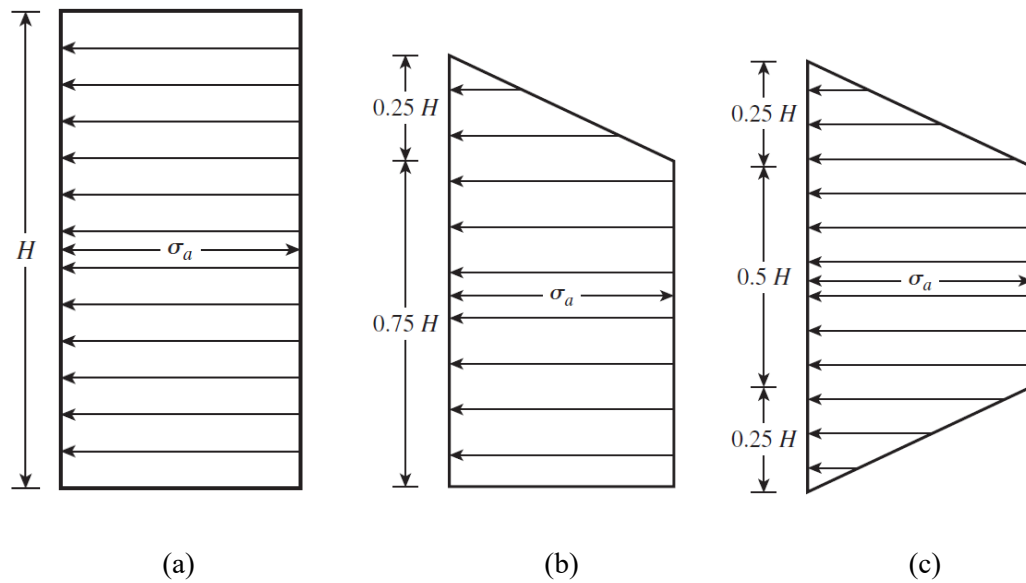


Figure 2.3 Apparent-pressure envelope (a) for cuts in sand, (b) for cuts in soft to medium clay, (c) for cuts in stiff clay (Peck 1969)

When using lateral earth pressure envelopes in Figure 2.3., it should be kept in mind that:

1. They are applicable to excavations with depths greater than 6 m.
2. They depend on the assumption that the water table is below bottom of excavation.
3. Sand is assumed to be drained.
4. Clay is assumed to be undrained and pore water pressure is not considered.

## 2.2. Prestressed Anchored Pile Wall Design

In Turkey, the most widely used construction method is bored reinforced concrete piles with prestressed soil anchors. The typical design procedure and calculation steps for pre-stressed anchored wall is as follows (FHWA-IF-99-015, 1999).

Step 1. Determine project requirements, including all geometry, external loading conditions (seismic loads, etc.), temporary or permanent anchors, performance criteria and construction restrictions.

Step 2. Evaluate both laboratory and in-situ tests to determine relevant soil properties.

Step 3. For the final wall height, select the lateral soil pressure distribution acting on the back of the wall. Furthermore, surface loads and water loads must be determined.

Step 4. Calculate horizontal soil anchor loads and wall bending moments. Adjust the vertical anchors until an optimum wall bending moment distribution is achieved.

Step 5. Determine required anchor inclination taking consideration of limitations

Step 6. Assess horizontal spacing of anchors based on wall type. Calculate individual anchor loads.

Step 7. Assess vertical and lateral capacity of shoring system below excavation subgrade.

Step 8. Check the stability of shoring system

Step 9. Estimate maximum horizontal wall displacement and ground surface settlements

Step 10. Design waler beam, facing drainage systems, and connected devices.

### **2.2.1. Prestressed Soil Anchor Details**

Prestressed ground anchor is installed in soil that is used to transfer an applied prestressed load into the ground.

#### **2.2.1.1. Types of Ground Anchors**

There are four ground anchor types, which were listed below and shown in Figure 2.4:

- 1) Straight shaft gravity-grouted ground anchors (Type A),
- 2) Straight shaft pressure-grouted ground anchors (Type B),
- 3) Post-grouted ground anchors (Type C).
- 4) Underreamed anchor (Type D)

Anchor types currently used in practice in Turkey are Type A – Type B and Type C.

Main types of grouted ground anchors are given in Figure 2.4.

In general, in rocks, fine grained cohesionless soils and firm to hard cohesive soils, most suitable technique is straight shaft gravity grouted anchor.

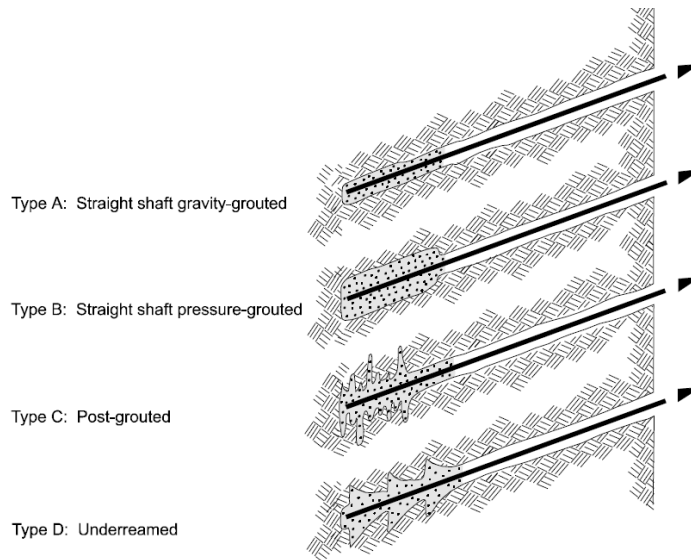


Figure 2.4 Main types of grouted ground anchors (FHWA-IF-99-015, 1999)

### 2.2.1.2. Parts of Ground Anchor

Ground anchor is typically separated into 3 parts which are anchorage, free length (unbonded) length and bonded length. These components of a ground anchor are given schematically in Figure 2.5.

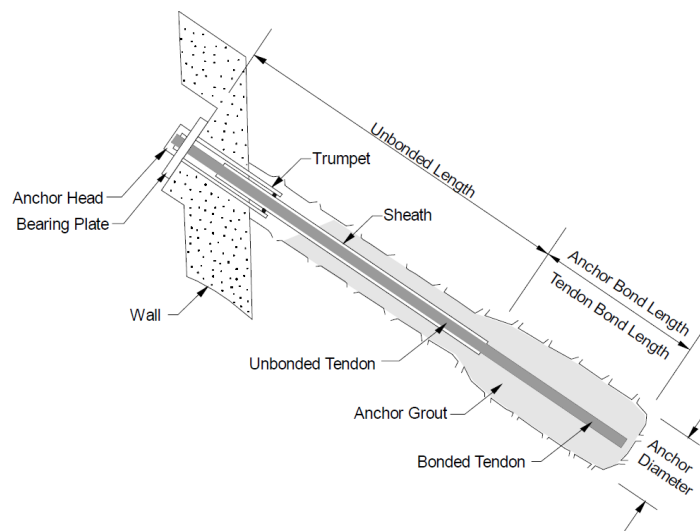


Figure 2.5 Components of a ground anchor (FHWA-IF-99-015, 1999)

### 2.2.1.3. Free (unbonded) length

The length of the anchor between the critical potential failure plane and the wall is defined as unbonded length or free length. Free length consist of multiple seven-wire strands. The load in the strand tendons is transferred to grout body. The common strand diameters are 0.5 inch (12.70 mm) and 0.6 inch (15.24 mm). Minimum length of unbonded part of anchor is 4.5 m for strand tendons. Material specifications for strand tendons is specified in American Society for Testing and Materials (ASTM) A416. Properties of 15-mm diameter and Grade 1860 [270] prestressing steel strands are given in Table 2.1.

Table 2.1 Properties of 15-mm diameter steel strands (ASTM A416)

Number of 15-mm diameter strands	Cross Section Area (mm <sup>2</sup> )	Ultimate Strength (kN)	Pressressing Force		
			Maximum Test Load 0.8 $f_{pu}$ x $A_{ps}$	Lock off Load 0.7 $f_{pu}$ x $A_{ps}$	Design Load 0.6 $f_{pu}$ x $A_{ps}$
1	140	260.7	209	182	156
2	280	521.4	417	365	313
3	420	782.1	626	548	469
4	560	1042.8	834	730	626

### 2.2.1.4. Bonded Length

Bonded length consists of strands and grout. The load is transferred to the ground by friction between grout body and ground. Grout is composed of cement, water, and admixtures. There is no aggregate in anchor grout (ASTM C150). A water/cement ratio of anchor grout must be between 0.4 to 0.55 by weight. Type I cement has a minimum 28-day compressive strength of 21 MPa at the time of anchor stressing. Ultimate load capacity of bonded length  $T_f$  in kN can be estimated from Equation 2.16. (BS 8081, 1989)

$$T_f = \pi D L \alpha c_u \quad (2.16)$$

where:

$c_u$  : average undrained shear strength over fixed anchor length (kN/m<sup>2</sup>)

$\alpha$  : adhesion factor

D : diameter of borehole (m)

L : length of fixed anchor (m)

Exceeding bonded length beyond 10 m is useless for transferring load effectively. For this reason, optimum bonded length can be considered as 10 m (BS 8081, 1989).

### 2.3. Location of Critical Potential Failure Surface

Anchor bonded length must be situated adequately behind critical potential failure surface, so that load can be transferred from anchor bond to ground. Critical potential failure surface of anchored pile wall system can be seen in Figure 2.6. For shoring system, critical potential failure surface can be assumed to extend up from point of a zero-shear force on wall at an angle of  $45 + \phi'/2$  from horizontal (Figure 2.7b). Unbonded length is typically extended either a minimum distance of  $H/5$ , where H is height of the wall, or 1.50 m behind the critical potential failure surface (Figure 2.7).

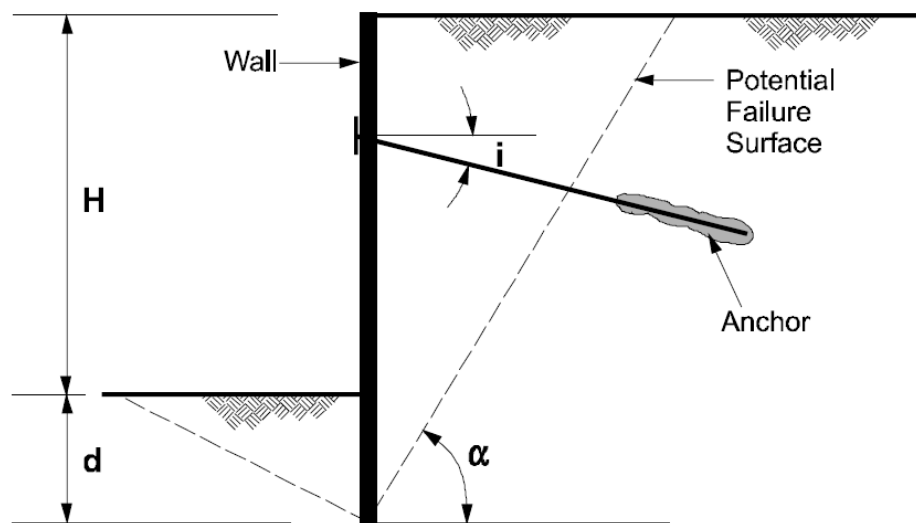
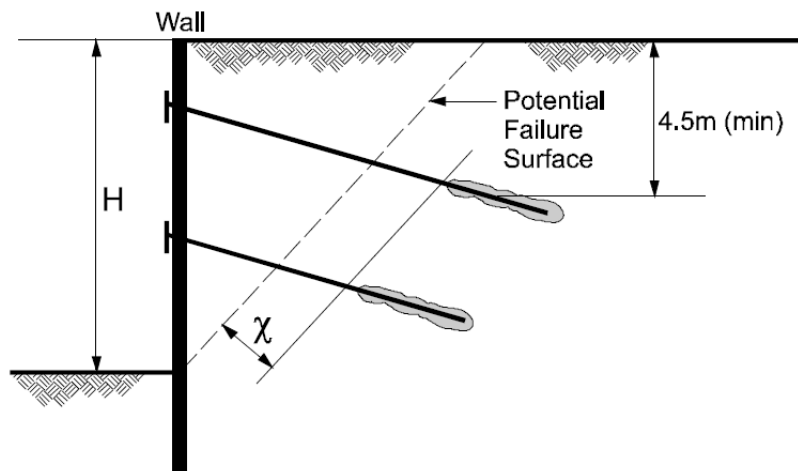


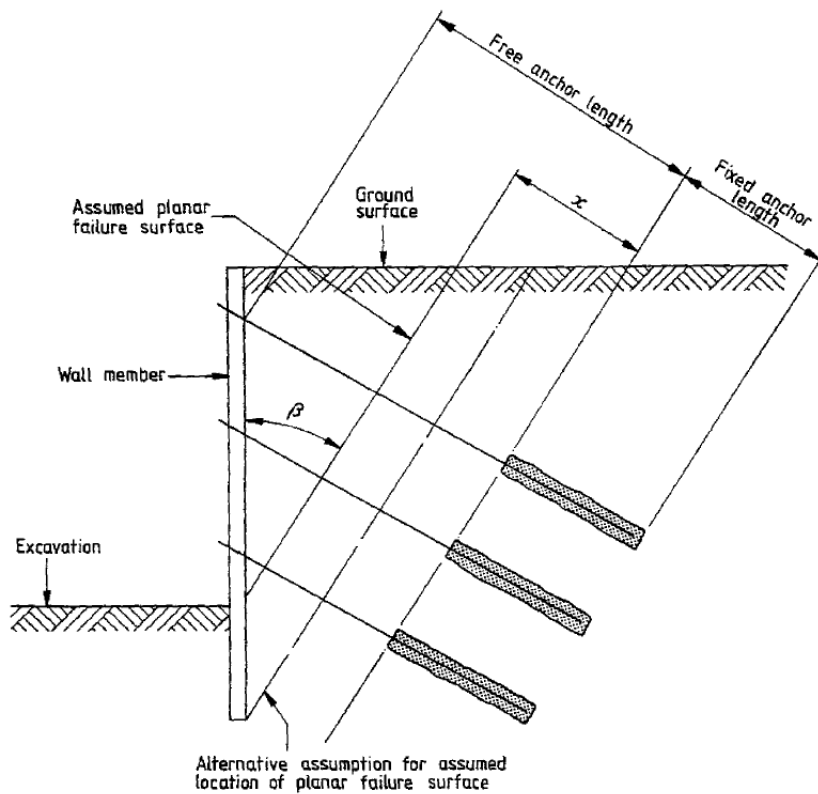
Figure 2.6 Critical failure surface in ground anchor wall system (FHWA-IF-99-015, 1999)



Minimum unbonded length = 3m (bar)  
4.5m (strand)

$\chi = 1.5\text{m}$  or  $0.2H$ , whichever is greater

(a)



(b)

Figure 2.7 Critical potential failure surface a: (FHWA-IF-99-015, 1999), b: BS 8081 (1989)

The spacing of anchors (horizontal and vertical) will depend on specific requirements and constraints of the project. For example, (1) necessity for a very stiff system may require closely-spaced anchors to control horizontal wall movements; (2) positioning and inclination of the anchors may be influenced by the existing underground structures or infrastructure; and (3) type of vertical wall elements selected for the design (FHWA-IF-99-015, 1999). For ground anchors installed in soil, a minimum overburden of 4.5 m over the center of the anchor bond zone is required.

#### 2.4. Failure Mechanism of Anchor System

Due to project and application faults in anchor systems, it is possible to create failure mechanisms which are shown schematically in Figure 2.8. Comments on the some of the factors that cause failure and the consequences of failure are summarized below:

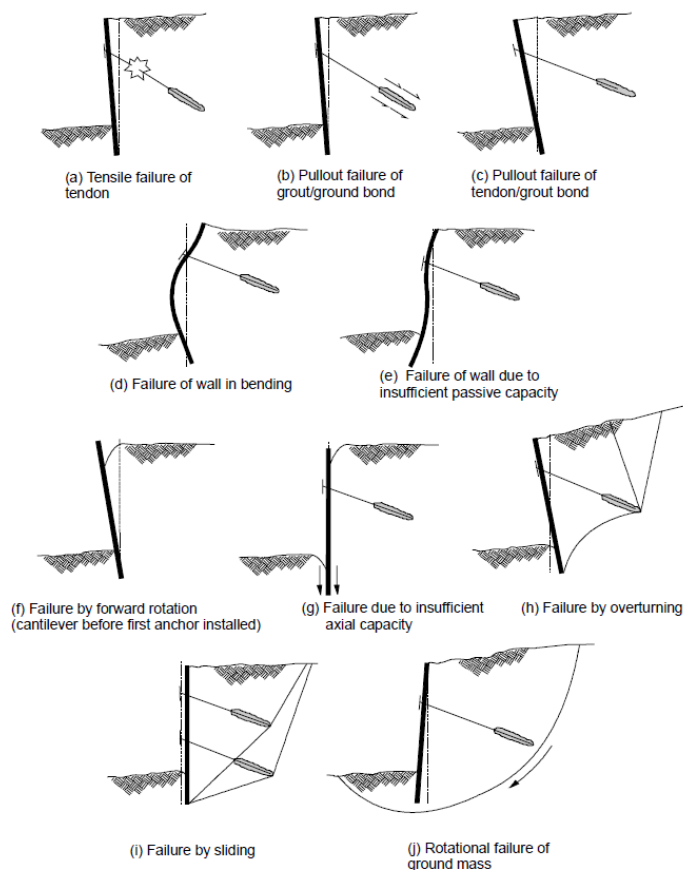


Figure 2.8 Potential failure conditions to be considered in design of anchored walls (FHWA-IF-99-015, 1999)

#### **2.4.1. Failure of Steel Tendon**

If load applied is greater than axial capacity of the tendon, failure is unavoidable. Therefore, factor of safety is utilized in calculation of tensile capacity of steel. It is suggested that steel tendon load should not exceed 60% of specified minimum tensile strength for final design for temporary conditions.

#### **2.4.2. Failure of Steel Tendon & Grout Body**

Friction resistance between anchor and grout body is ensured by adhesion of the materials. Failure of steel tendon and grout body is due to the loss of adherence between the anchorage tendon and injection. Adhesion can be described as relationship between grout and rough steel tendon. Friction resistance occurs because of movement of the anchor changes according to the magnitude of force applied to the anchor, roughness of the anchor tendon and also the amount of movement. It is observed in the rocks and soils with high shear strength where the adherence force between soil and the injection is high. If tendons are not covered by adequate thickness with injection, this type of failure can be observed.

#### **2.4.3. Failure of Ground & Grout Body**

If applied pre-stress load is greater than friction resistance between soil and grout body, anchor may pull out. Firstly, since anchor is stretched, the part of the nearest bond length is extended and transfers load to the ground. Once the stress is transferred to the end of the bond zone and the ultimate ground-grout bond is exceeded, anchor failure by pullout occurs. Generally, this type of failure occurs in soil with low shear strength. Therefore, in the loading tests, anchors should be tested at 1.25 to 1.33 times of the design load. Experience has shown that for typical soil anchors, increasing the bond length beyond 9 to 12 m does not lead to increases in resistance.

#### **2.4.4. Failure of Wall**

The collapse of the vertical support element results from the inability to carry the cross-sectional forces (moment forces, shear forces) formed by the loading of the shoring system.

#### **2.4.5. Slip Failure**

Slip failure is a rigid way to shift the shoring system along the base. If the anchor forces and passive resistance which are resisting to slip are lower than the forces which try to slide, slip failure is expected. If the anchor force is insufficient or the anchor grout body is located within the slip key, resistance to slide is reduced. It usually shows itself during excavation, but if precautions are not taken, it leads to significant loss of stability.

#### **2.4.6. Rotational Failure**

Rotational failure (or global external failure) develops when the whole shoring system (including the bonded length of anchors) moves in a failure plane underneath/behind it. Anchors are usually dimensioned by taking into account the potential slip wedges behind the wall. However, if there is an unstable sliding plane that includes the entire shoring system, there will be a global collapse no matter how often and how strong the anchors in the system are. In case a global instability occurs, its irreversibility (or difficulty for remedial measures) leads to major loss of stability and cost.

#### **2.4.7. Wall Deformation Criteria**

Maximum lateral wall movements for anchored walls constructed in sands and stiff clays average approximately 0.2%H, with a maximum value of approximately 0.5%H, where H is the height of the wall. The maximum vertical settlements behind a wall constructed in these materials average 0.15%H, with a maximum value of about 0.5%H (FHWA-IF-99-015, 1999).

## **2.5. Literature Review of Other Studies on Deep Excavations**

There are many kinds of research in the literature regarding the deep excavation problems of geotechnical engineering. However, there are very limited number of studies in the literature on multi-tier anchored wall systems in Turkey (Aktan 2014) and around the world (in China by Fang et al. 2013). In the following paragraphs, brief information is provided about some of the recent studies in Turkey on excavation support systems.

Sincil (2006) studied deep excavation project of the Gazino station within the scope of the Ulus-Keçiören Metro project, supported by anchored pile walls. The comparison of the inclinometer measurement and numerical data of soil stability for deep excavation was the main scope of this study. The excavation was modelled and analyzed by using the Plaxis finite element software. Anchored and non-anchored behavior for wall displacements were compared. The results of the numerical analysis were considered satisfactory considering the distribution and reliability of the field measurements, although the horizontal wall displacements above the excavation level were larger than the measured ones and the displacements below the excavation level were lower than those measured. It is stated that the results would be more accurate and valid with more detailed and careful field and laboratory tests and would result better soil parameters.

In Ermanlar (2009) study; within the scope of the Istanbul Metro Project, a supported deep excavation project with inclinometer observations was examined. In this study, displacement analysis was performed with two different sections using the Plaxis software. In both sections, drainage analyses were performed due to duration between the excavation period and completing of the structure, and Mohr Coulomb soil structure model was chosen. In field studies; elasticity modulus changes were determined according to the pressuremeter tests performed at each 5 m. It was observed that horizontal displacement values obtained from instrumental observations and analyses results were close to each other. For the second section, finite element

analysis was repeated by reducing the modulus of elasticity by 50% and 75% in order to understand the inconsistency of the displacement of up to 145 mm observed in the inclinometer measurements with a maximum of 45 mm displacement. However, numerical changes were not able to approach the observed values. The results gathered from inclinometer tests, did not give valid data for reality, especially in rock layers.

Özberk (2009) investigated the deformation behavior of a project as a case study, by carrying out analyses using the Plaxis 8.2 software. In the deep excavation project bored pile and mini pile with anchors were modelled, and the inclinometer measurements were compared with the results obtained numerically. As a result, it was seen that horizontal displacement values obtained by instrumental observations and horizontal displacement values were compatible for three of the sections between each other. In one of the sections, it was observed that there was a discrepancy between the results of numerical analysis and inclinometer measurements. The reason for that was reported as the estimated material parameters for greywacke in the first 10 m did not represent the actual lithology well. To overcome this problem, analysis was repeated by taking one third of the current elastic modulus value of the first 10 m of greywacke layer to satisfy a better fit between the calculated and the measured value. After the final excavation depth was reached in each section,  $\phi / c$  reduction analysis was performed and the safety values of the excavation against the failure were calculated and the sections were found to be sufficiently safe against failure.

Aktan (2014) investigated the behavior of shoring system (mini-piled wall with prestressed anchors) within the scope of Hilton Istanbul Bomonti Hotel project (Fig. 2.9a). Project was modeled by using the Plaxis 8.2 finite element software and the effects of various parameters are investigated. In addition to classical earth pressure calculation methods, various earth pressure distributions developed for preliminary design calculations for deep excavations were given in detail. The effects of soil engineering characteristics, ground/structure interface element and prestressed anchors used as horizontal support elements on the rigidity of the shoring system were investigated on the same geometry model, provided that other parameters were kept

constant. According to the stress level of ground stiffness in the calculations, with increased pressure, hardening soil model was used. At the first stage, loading-reloading modulus of elasticity ( $E_{ur}$ ) of soil was changed between 60 MPa and 450 MPa, and the displacements occurring in the shoring system were reduced by about 25%. Internal friction angle was more effective and decisive value than the modulus of elasticity for displacement values. At the second stage, the aim was to understand effect of interface reduction factor, which is a characteristic value according to the type of material and soil, on pile displacements. At the final stage, the effect of the anchor grout length, anchor placement angle, anchor tendon diameter and anchor horizontal spacing on lateral displacements were investigated. Anchor grout lengths were determined as 8 m-10 m and they were determined that more than 8 m of grout length did not cause any reduction in pile displacement. While the inclination of the anchor was  $15^\circ$  in case study, the increase in the slope increased the displacements and the stability of the system was deteriorated at  $45^\circ$  slope. The calculations for the 0.5 inch, 0.6 inch and 0.7 inch anchor tendon diameters given in the standards did not make a significant difference in displacements. The horizontal spacing of the anchor was changed between 1 m and 2 m and the most suitable range for the project was determined to be 1.5 m.

Aktaş (2019) carried out a back analysis of a 25-m deep excavation in Ankara, and compared the results obtained from finite element analyses with the measurements obtained from inclinometers. A Python code was written for the back-analyses of parameters used, specifically to correlate stiffness parameters with SPT  $N_{60}$  values. To be more precise in numerical analysis, soil is divided into layers according to SPT- $N_{60}$  measurements. As a result of analyses, soil models were compared with each other and displacements obtained from the MC model could not converge to reality. HSsmall model results are closest to real displacements. Moreover, displacement curves obtained from HS and HSsmall models are very close to each other. Linear correlation formula is stated as  $E_{50ref} = 780 \times N_{60}$  kPa for this excavation of the case study in Ankara clay.

Fang et al. (2013) studied via 2D plane strain finite element analyses, “a special double-row” support structure for braced excavation with diaphragm wall and bracing struts. For a deep excavation in Hangzhou city in China, the authors noted that the performance of the excavation support system depends on the interaction between two walls. The major factors in influencing the behavior of the system are noted as: the overlap length of two piles, embedment depth of the lower pile wall and the horizontal spacing between the two piles (Fig. 2.9b). Fang et al. (2013) reported that the earth pressure against the lower (inner) wall is significantly influenced by the passive earth pressure in the passive zone of the upper (outer) wall. If the spacing between the two walls is greater than the influence distance,  $L$  (in Fig. 2.9b), then it can be assumed that the interaction between two walls will be negligible. Analyses were also carried out for overlap length of two walls,  $h_3$  (in Fig. 2.9b), in the range of 8 to 12 m (0.4 to 0.6 of upper wall length) and total length of inner (lower) wall being constant as 15 m. As the overlap length of two walls increased, the horizontal movement of the outer (upper) wall decreased and that of inner (lower) wall increased. When the embedment ratio of the inner (lower) wall increased, horizontal deflections of both walls decreased. The effects of the horizontal spacing between the two walls was also studied, by changing the spacing in the range of 1 to 17 m. It was noted that both walls’ horizontal movements decreased when the spacing between the two walls increased, which means by increasing the spacing between two walls the interaction between the walls reduced. Fang et al. (2013) defined an interaction coefficient, which is equal to 1 and 0, when the distances between the two walls are 1 m and 17 m respectively. Interaction coefficient was described as the ratio of the “difference between the maximum horizontal deflections when the horizontal distance between walls is  $x$  m ( $\Delta_x$ ) and when it is 17 m ( $\Delta_{17}$ )” to the “difference between the maximum horizontal deflections when the horizontal distance between walls is 1 m ( $\Delta_1$ ) and when it is 17 m ( $\Delta_{17}$ )”. It is reported that the interaction coefficient decreases linearly with increasing spacing between two walls.

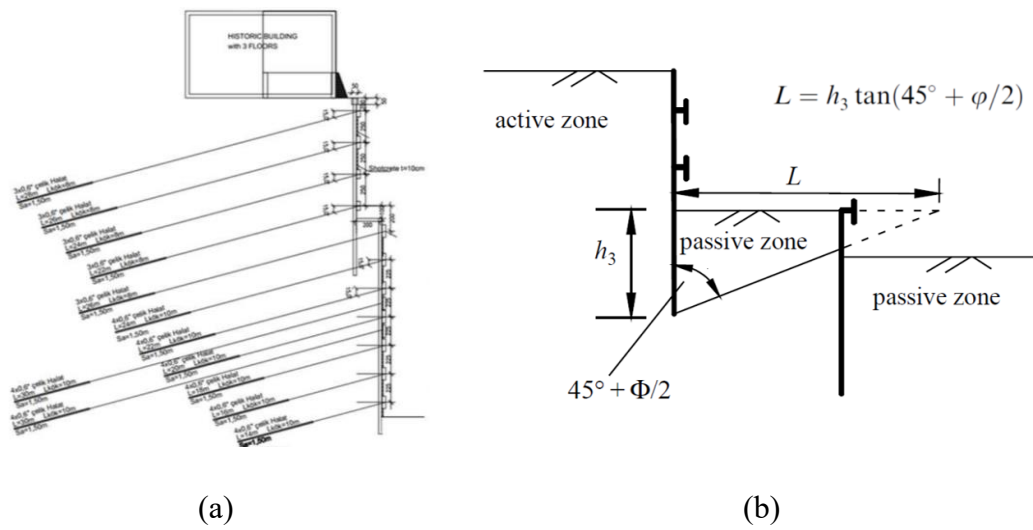


Figure 2.9 (a) Multi-tier pile wall with anchors for an excavation in Istanbul (Aktan, 2014), (b) Double-row excavation support system in China by Fang et al. (2013).

To define the interaction between two walls in a multi-tier wall system, there is also “Method for Step Walls” as described by CivilTech Software company (<https://civiltech.com/downloads/stepwall.pdf>) (Figure 2.10). According to CivilTech Software company, if the horizontal distance between two walls is greater than the value of “ $X_c$ ” shown in Figure 2.10, then the two walls do not have an impact on each other, i.e. they do not interact. It is also mentioned that “overall stability of the complete wall system should be checked”, and that “tiebacks are recommended to reduce the embedment of upper walls, therefore reducing the impact on the lower walls”.

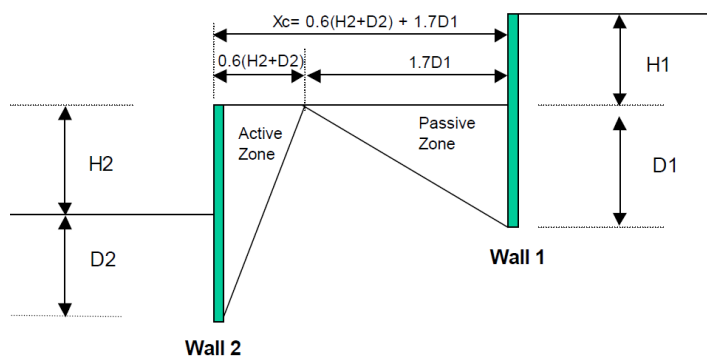


Figure 2.10 Description of the interaction between two walls

## **2.6. Finite Element Method and Plaxis 2D Analysis**

Finite element method (FEM) is one of the most commonly used approaches for designing of geotechnical structures. Process of modeling geometry of the problem with finite element method includes simplifications and approximations. Defined geometry is divided into a number of “finite elements” (which could be triangular or quadrilateral in shape), each consisting of a number of nodes. Each node has a number of degrees of freedom that implies to the unknowns in the boundary value problem. When the geotechnical parameters of the soils are evaluated properly, via extensive site investigations, laboratory and in-situ tests; this method can produce highly realistic results that can be applied to practical problems.

Any type of soil condition could be simulated by using the finite element method. For given geometry; applied loads, displacement boundary conditions, and material stress-strain law (i.e. constitutive model). Many geotechnical problems contain soil-structure interaction when applying finite element analysis to such problems it is necessary to include structural components. Simulation of excavation or construction with 2D continuum elements by using finite element method is a complex process.

### **2.6.1. Plaxis 2D**

Plaxis 2D is a two-dimensional finite element software used for analysis of any geotechnical problem. Identifying the problem is the key point at the beginning of analysis. In this case, the problem is anchored multi-tier pile wall shoring system. A brief summary of the features of Plaxis 2D is given below for anchored pile wall shoring system.

#### **2.6.1.1. Graphical Model Input**

The input of soil layers, structures, condition stages, load, and boundary conditions are based on convenient CAD drawing procedures, that allows for detailed modeling of the geometry cross-section. 2D finite element mesh can be easily generated from this geometry model.

#### **2.6.1.2. Define Idealized Soil Profile**

Appropriate geotechnical parameters which give compatible results with in-situ and lab tests must be determined before creating a model. Soil layers with different thickness can be formed by soil polygon in Plaxis 2D.

#### **2.6.1.3. Plate**

Plates behave as one-dimensional beams defined as linear elastic material that structures with a flexural rigidity. Bored piles in shoring system are defined as plates.

#### **2.6.1.4. Interface**

Joint elements are available for soil-structure interaction modeling. Interface elements can be used to simulate the thin area of intensely shearing material at the contact between the pile and surrounding soil.

#### **2.6.1.5. Ground Anchor**

Springs can be defined as elastic or elastoplastic material with their normal stiffness and maximum force values. Pre-stress values can be also defined in excavation support systems. Anchors are defined as elastoplastic material in all analysis in this study.

#### **2.6.1.6. Embedded Beam Row**

Grout part of an anchor is defined as embedded beam row to describe the interaction between soil and grout. Embedded beam row is defined as elastoplastic material by taking into consideration of elastic stiffness properties. Grout body of anchors are defined as elastoplastic material in all analysis in this study.

#### **2.6.1.7. Loads**

Various types of loads can be identified in the scope of the program which are line loads, point loads and distributed loads. In each stage of construction, load parts and load levels can be activated or deactivated independently.

#### **2.6.1.8. Auto Mesh Establishment**

After completing the geometry of the model and assigning related materials, finite element mesh generation can be generated automatically in Plaxis 2D. There are 5 alternatives for global coarseness which vary from very fine to very coarse. Geometry mesh can be regenerated by using lower coarseness, global or local refinement can be done if needed. In this study, in the case study and in the parametric studies, “fine” mesh type was used to obtain more accurate results.

#### **2.6.1.9. Staged Construction**

This feature enables realistic simulation of construction and excavation processes. Bored pile and anchor systems are constructed by stages. Firstly, construction of bored piles is completed in the field. Subsequently, soil is excavated to the lower elevation of the first row of anchor cross-beam. After the excavation is completed, construction of anchorage is made. Prestressing is given and anchorages are locked to the pre-stress load. The anchors are locked, the next excavation phase starts. The same process continues up to the lower level of the excavation.

In the Plaxis 2D, the same system can be modeled. The bored piles are activated first. Then the soil layer, identified the first excavation, is deactivated. The grout body and free length forming the anchor are activated and the pre-stressing load is given to the free length part. After applying the prestress load, the next soil layer defined the excavation will be deactivated and continue up to the lower elevation of the excavation. This procedure allows for a realistic assessment of stresses and displacements as caused by soil excavation during an underground construction project.



## CHAPTER 3

### CASE STUDY

#### 3.1. Introduction

A building was planning to be constructed in Çukurambar, ANKARA. It was necessary to make excavation up to a depth of 30.00 m in order to construct foundation and basements of buildings. However, due to the lack of sufficient distance for slope excavations; it was necessary to build shoring system, in order to ensure safety of construction, surrounding structures and roads. The shoring system was constructed as multi-tier pile wall which were supported by temporary pre-stressed soil anchors. In this study, the cross section of shoring system, which is the deepest excavated section, was analyzed by two-dimensional finite element method with different material models and compared with the measurements taken at the site. Diameter of bored piles was 80 cm and horizontal distance between the centers of bored piles was 100 cm. For this project, information about the soil exploration results, geological structure of the site was all taken from the geological report prepared by IKSA Engineering Co. (2016).

#### 3.2. Project Information

Construction area is situated on an approximate 2-hectare area in the rapidly developing Çukurambar District of Ankara, Turkey. Some data related to the project are as follows:

- ✓ Project consists of 2 separate blocks: A Blok includes residential and exclusive residence, B Blok is comprised by office and hotel rooms.
- ✓ Total number of floors: 33
- ✓ There are 10 floors basement, ground floor and 33 typical floors

- ✓ The building length: ~130 m from the ground surface
- ✓ Maximum bottom of excavation: ~30 m from the ground surface

The foundation formwork plan is presented in Figure 3.1.

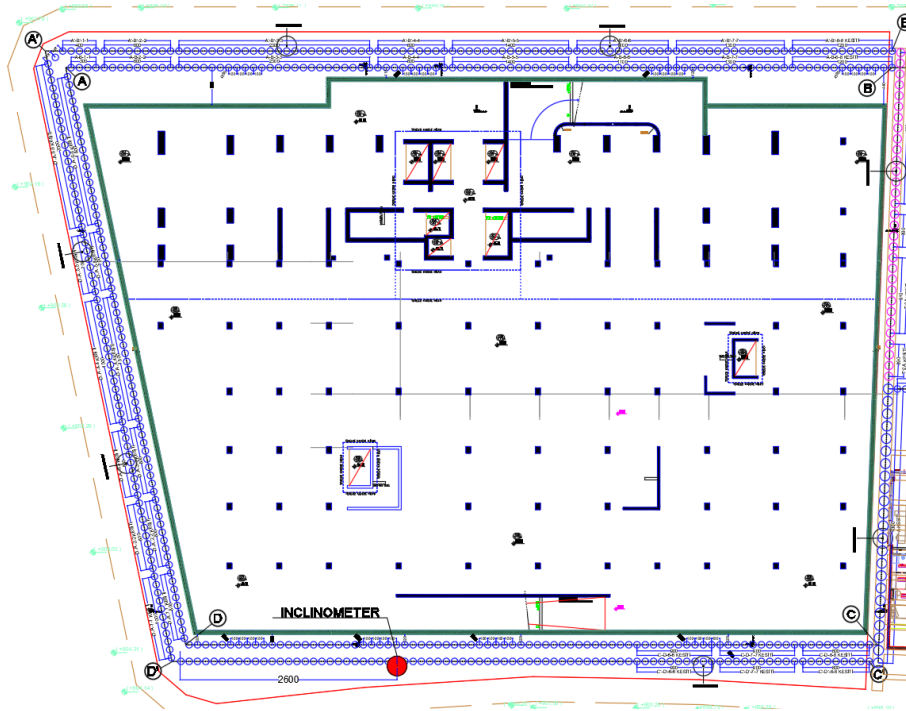


Figure 3.1 Foundation formwork plan and pile layout plan

### 3.3. General Geology and Soil Properties

IKSA Engineering Co. drilled 9 boreholes and performed field and laboratory tests between April and May 2016. The locations of boreholes are shown in Figure 3.2.



Figure 3.2 Locations of boreholes

Ground surface elevations and depths of the boreholes are given in Table 3.1. An example of one of the borehole logs (SK8, which is the borehole closest to the cross section being analyzed) is given in Appendix A.

Table 3.1 Locations and depth of boreholes

Boring Number	Depth (m)	Ground Surface Elevation (m)
SK-1	68	897,54
SK-2	65	894,64
SK-3	60	889,16
SK-4	74	895,09
SK-5	61	890,74
SK-6	69	898,92
SK-7	55	900,94
SK-8	52	898,02
SK-9	49	894,43

The ground formation obtained in all borings was defined as Ankara Clay. Ankara Clay is silt-clay unit which is typically reddish brown, brown colored, comprises of gravel, sand and lime concretions in the region Ankara City and its vicinity (Birand, 1978). In general, the upper level is brownish, the lower levels are reddish brown and/or reddish color. There is water-bearing, semi-round, small-medium-sized gravel and medium-dense sand layer within the Ankara Clay. Consistency of the soil is generally medium plasticity and locally low or high plasticity. The details of field and laboratory tests are described below.

Groundwater level was observed between 35.0 and 40.0m in drilling wells, which does not affect the shoring system due to being below the foundation level.

### 3.3.1. Field Tests

Within the scope of field works, standard penetration test (SPT) and pressuremeter test (PMT) were carried out. The details of field tests are given below.

### 3.3.1.1. Standard Penetration Test (SPT)

The most commonly used in-situ tests, worldwide, is the Standard Penetration Test (SPT). The experiment is based on the principle of sliding the dynamic slit tube with standard dimensions to the dynamic energy applied by dropping a ram of 63.5 kg weight from 76 cm height. For drilling in the field an automatic hammer with energy efficiency,  $E_m = 0.60$  was used. The change of SPT-N values with depth is shown in Figure 3.3. It is observed that SPT-N values are increasing with depth. Because of this, it is decided to divide the soil profile into four sublayers, where, in each sublayer, soil properties will be assumed to be uniform. The bottom of excavation and four sublayers of clay is shown in the same figure.

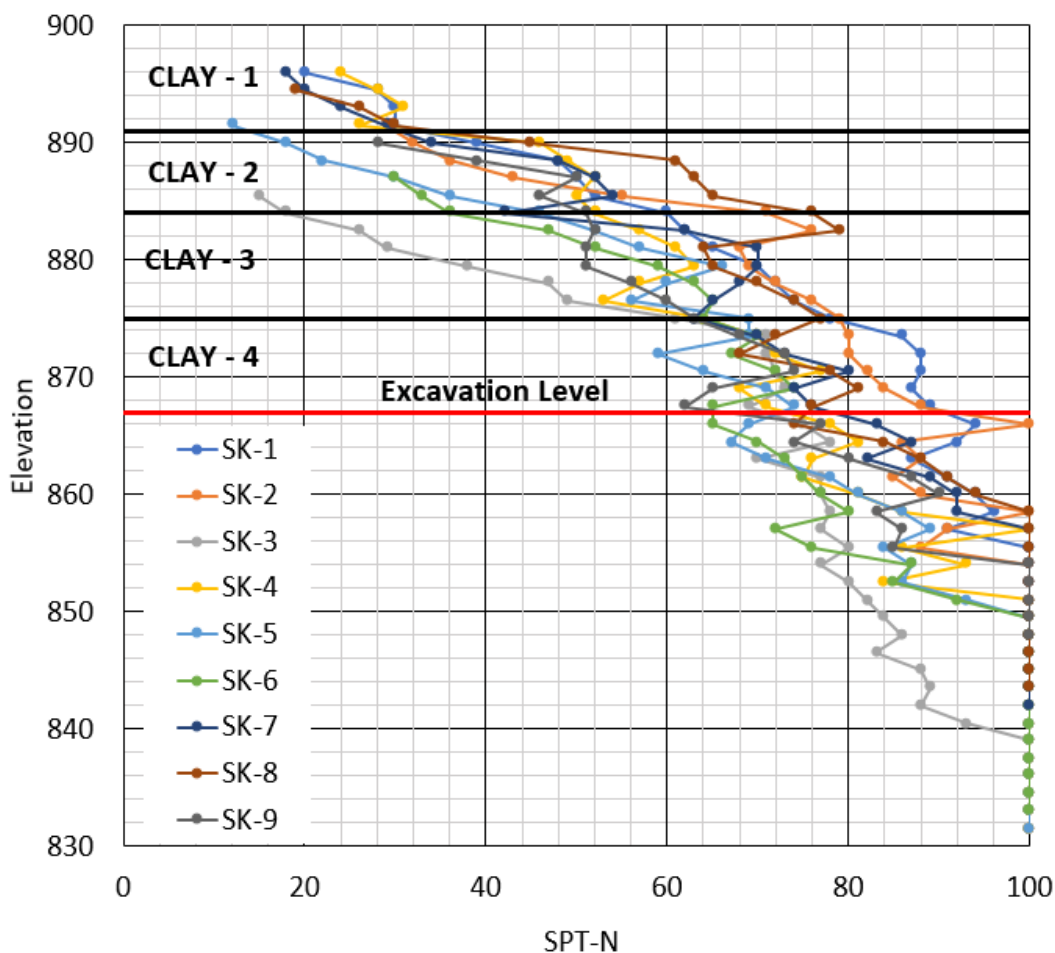


Figure 3.3 Change in SPT-N values with depth

### 3.3.1.2. Pressuremeter Test (PMT)

The pressuremeter test is an in-situ experiment in which the load / deformation parameters of the ground are determined. The basic mechanical properties of the ground from the load / deformation graphs obtained at each experimental level by Menard pressuremeter experiment; deformation modulus,  $E$ , and limit pressure value  $P_L$ . The limit pressure value is determined from the last measurement in the experiment, and the pressure modulus is determined from the pressure / volumetric change measurements recorded during the test. The Net Limit Pressure ( $P_L$ ) and the Pressuremeter Modulus ( $E_M$ ) values obtained from the pressuremeter experiments are given in Figure 3.4. and Figure 3.5.

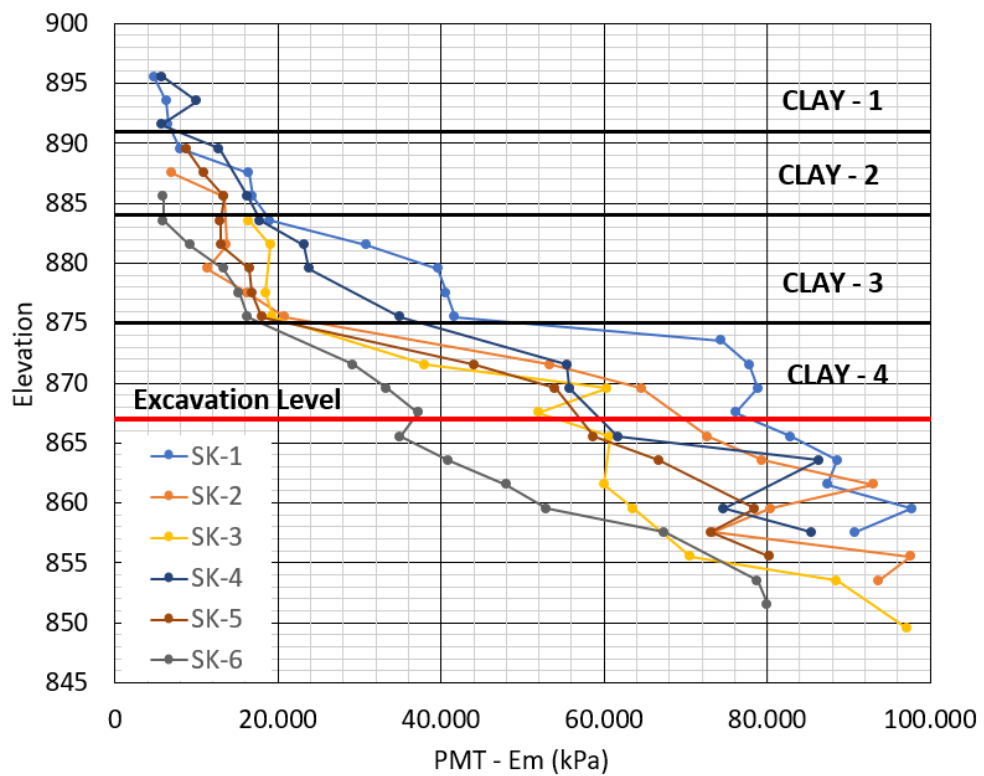


Figure 3.4 Pressuremeter modulus ( $E_M$ ) values with depth

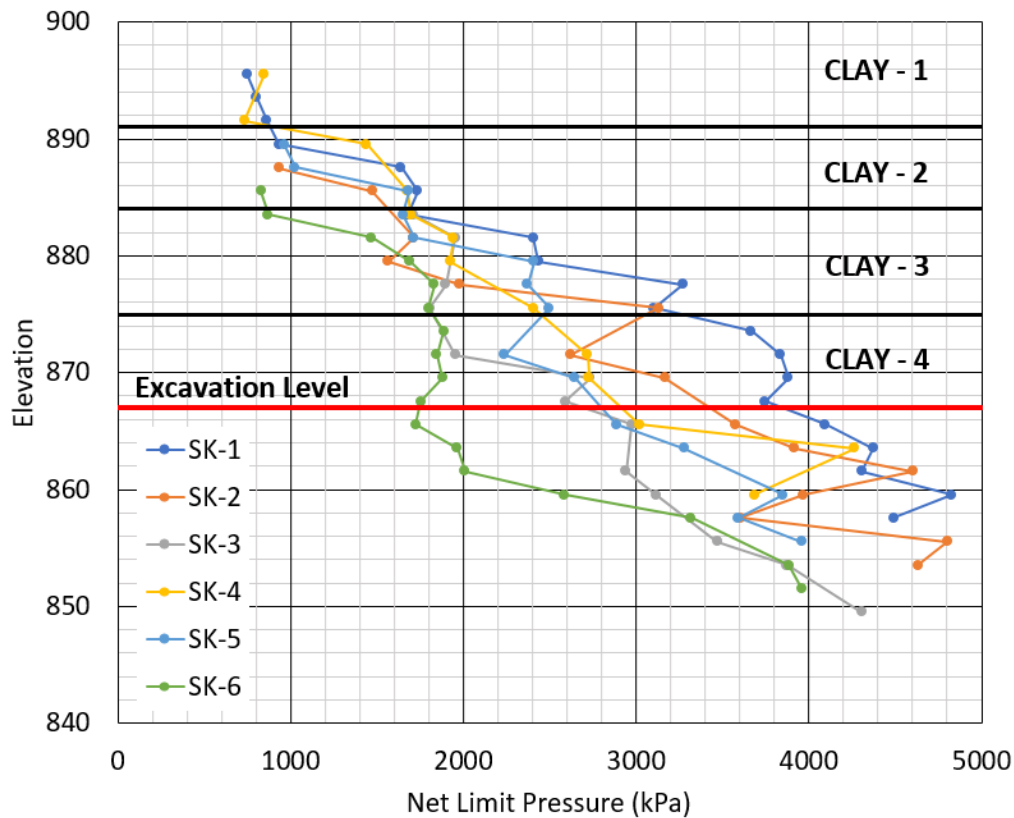


Figure 3.5 Net limit pressure ( $P_{LN}$ ) values with depth

### 3.3.2. Laboratory Tests

Laboratory experiments were carried out on disturbed and undisturbed samples taken from the investigated area. Sieve analysis, Atterberg limits, natural water content and unit weight were determined to help identify the engineering properties of soils. In addition, triaxial experiments were carried out on the cohesive specimens to determine shear strength parameters. Atterberg limits are summarized in Figure 3.6, Figure 3.7 and Figure 3.8.

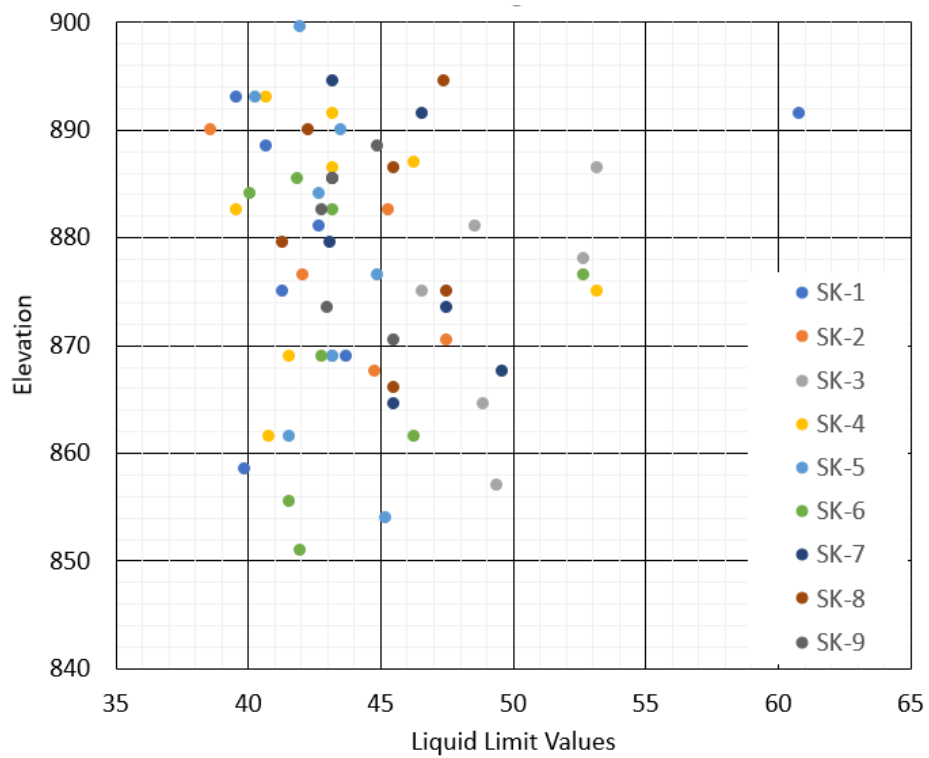


Figure 3.6 Laboratory test results (liquid limit, %, with depth)

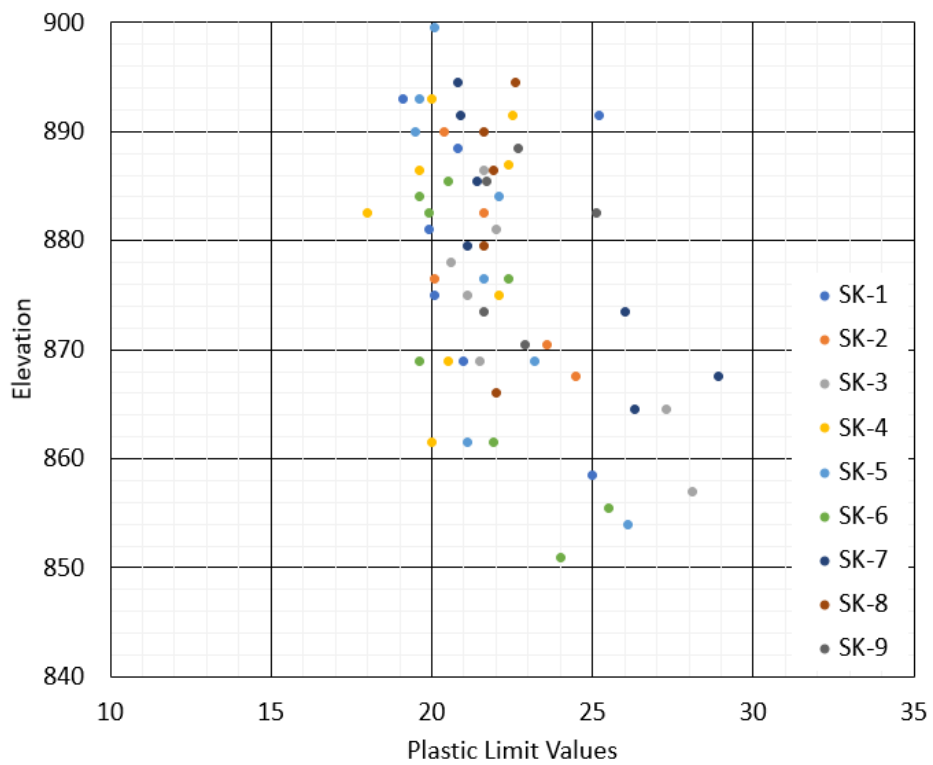


Figure 3.7 Laboratory test results (liquid limit, %, with depth)

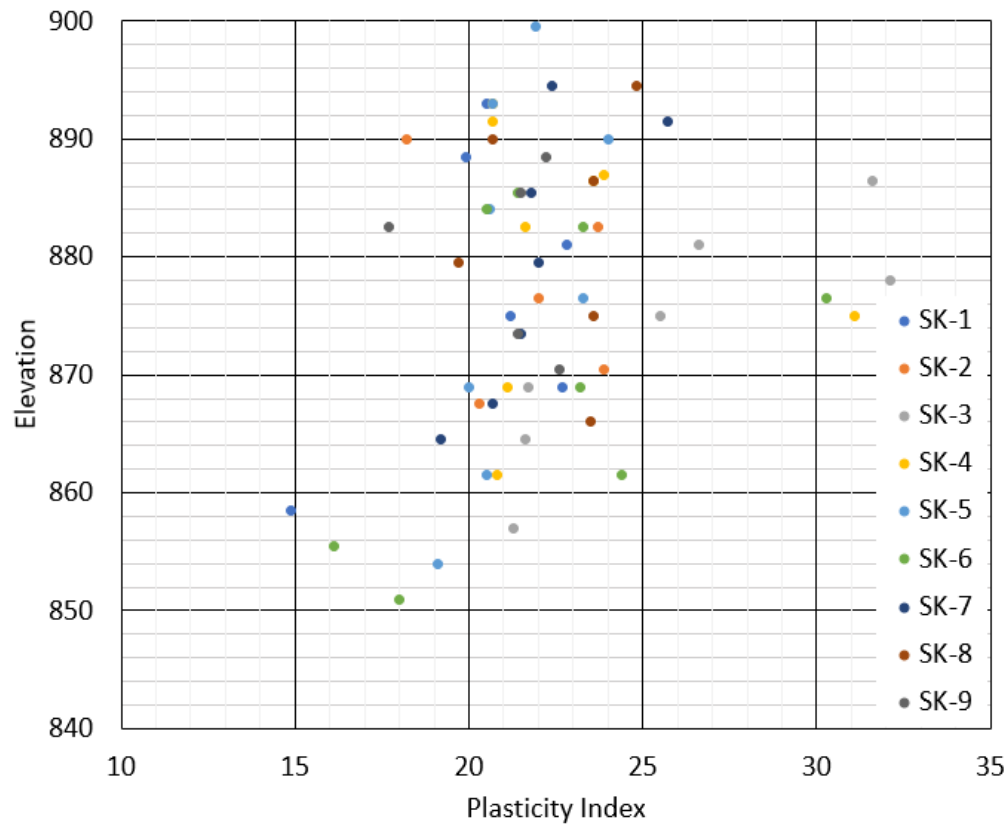


Figure 3.8 Laboratory test results (plasticity index, %, with depth)

### 3.3.3. Determination of Undrained (Short Term) Parameters

#### 3.3.3.1. Undrained Shear Strength

Undrained shear strength ( $c_u$ ) values of the Ankara Clay were determined according to SPT-N values and pressuremeter data.

Undrained shear strength values were calculated for different depths using the Stroud (1974) correlation given in Figure 3.9. According to Stroud (1974):

$$c_u = f_1 \times N_{60} \quad (3.2)$$

$f_1$  can be found in Figure 3.9 using the Plasticity Index

$N_{60}$ : Corrected SPT-N value corresponding to 60% of the maximum theoretical energy

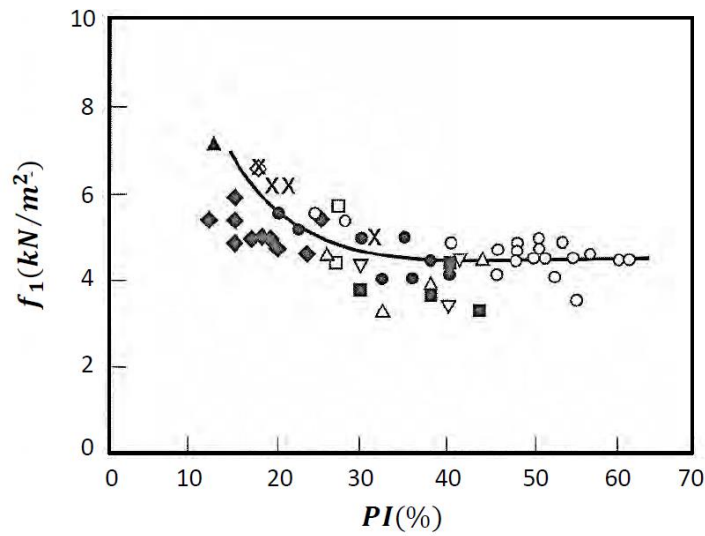


Figure 3.9 SPT- $N_{60}$  –  $C_u$  ( $C_u = f_1 \times \text{SPT-}N_{60}$ ) –  $PI$  Correlations (Stroud 1974)

Majority of the plasticity index values of clay were between 20% – 25% (Figure 3.8). Considering the best fit line and also the variation of data used by Stroud (1974) in Figure 3.9, the value of  $f_1$  was obtained as 4.5 and undrained shear strength values are plotted in Figure 3.10.

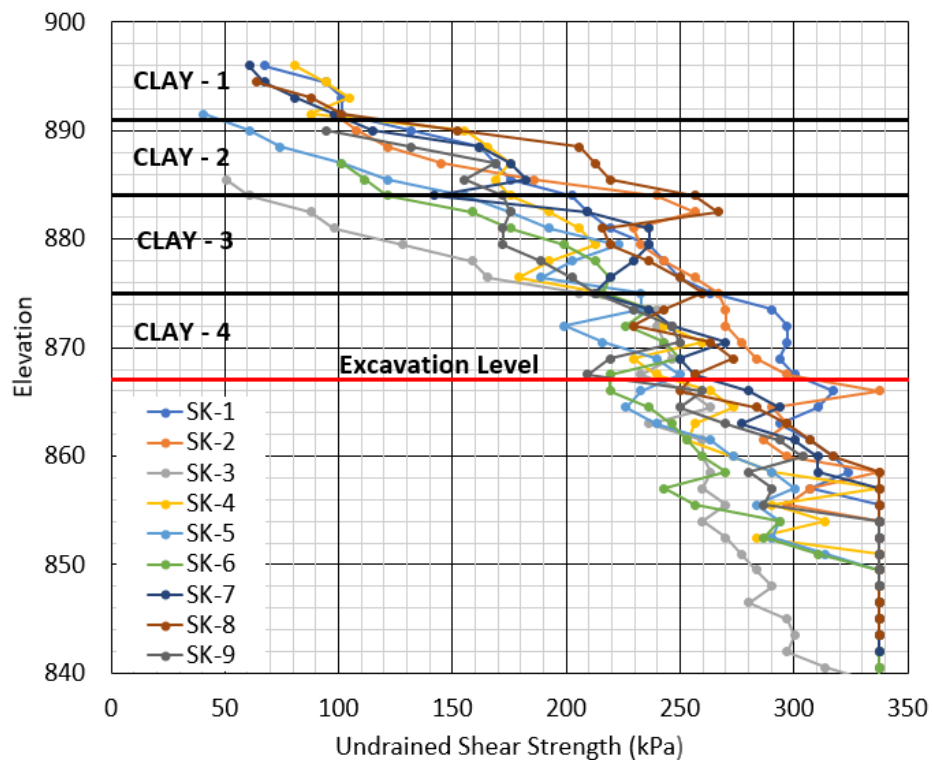


Figure 3.10 Undrained shear strength values using Stroud (1974) correlation with SPT- $N_{60}$

Using the values of the net limit pressures ( $P_L$ ) from the pressuremeter test, the values of undrained shear strength for different depths were calculated using the following relation (Briaud, 1992) and are given in Figure 3.11.

$$c_u = 0.67 \times (P_L) \times 0.75 \quad (3.3)$$

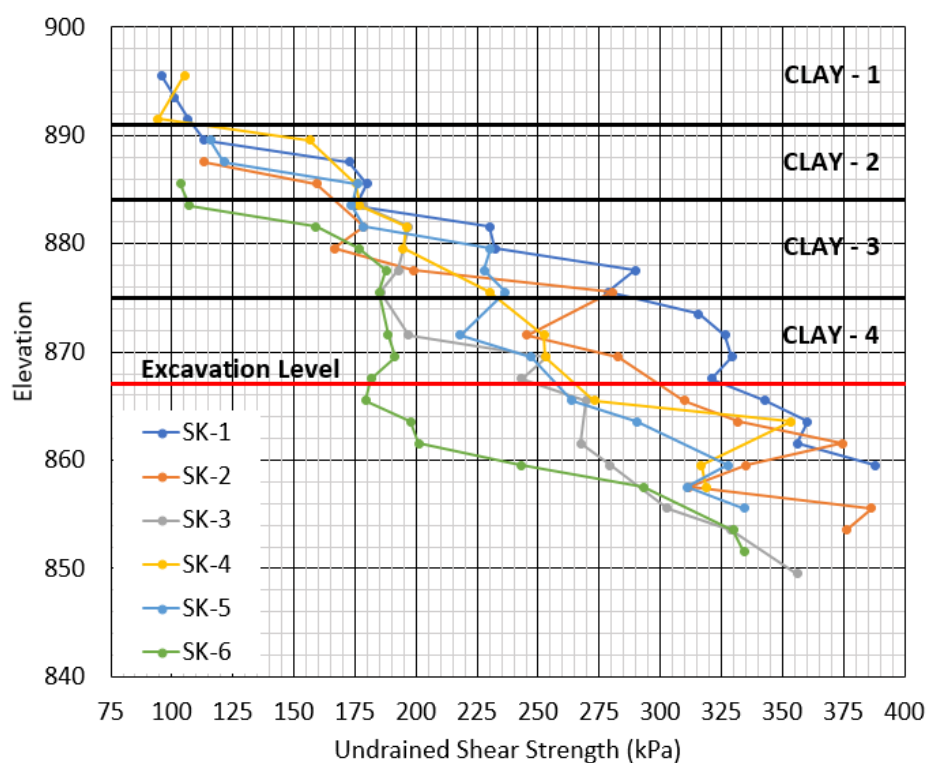


Figure 3.11 Undrained shear strength values from pressuremeter test (Briaud, 1992)

Undrained shear strength values are obtained according to the both SPT-N results and pressuremeter results, and idealized soil profile (which is divided into 4 segments: Clay-1 through Clay-4) and their properties are given in Table 3.2.

Table 3.2 Idealized soil profile and their properties, including  $c_u$  (kPa) values

Soil Layer	SPT- $N_{(ave)}$	SPT- $N_{60}$	PI (%)	Stroud 1974	Briaud 1992	Design $c_u$ (kPa)
				$C_u = f_1 \times N_{60}$	$c_u = 0.67 \times (P_L)^{0.75}$	
Clay-1	24	18.00	25	81	100	80
Clay-2	42	31.50	22	142	150	145
Clay-3	60	45.00	23	203	210	200
Clay-4	78	58.50	20	263	290	275

### 3.3.3.2. Undrained Friction Angle

Undrained friction angle in clay is considered as zero in design of shoring system.

### 3.3.3.3. Undrained Elastic Modulus

Undrained elastic modulus ( $E_u$ ) values for the Ankara Clay were calculated according to following correlations:

Butler (1975) noted that, in consideration of results obtained from many case studies, the relationship between the undrained deformation modulus,  $E_u$  (in units of MPa) and SPT-N can be expressed by the ratio given following relation:

$$E_u = \sim 1.2 \times N_{60} \quad (3.4)$$

Undrained elastic modulus ( $E_u$ ) can be also estimated with undrained shear strength, plasticity index and overconsolidation ratio (OCR). Variation of undrained modulus with OCR (Jamiolkowski et al, 1979) is given in Table 3.3.

Table 3.3 Variation of undrained elastic modulus with OCR (Jamiolkowski et al. 1979)

OCR	Soil Plasticity	$E_u/c_u$
< 2	PI < 30%	600 - 1500
2 - 4	PI < 30%	400 - 1400
4 - 6	PI < 30%	300 - 1000
6 - 10	PI < 30%	200 - 600
< 2	PI = 30 - 50%	300 - 600
2 - 4	PI = 30 - 50%	200 - 500
4 - 10	PI = 30 - 50%	100 - 400
< 2	PI > 50%	100 - 300
2 - 10	PI > 50%	50 - 250

Birand (1977) data shows that OCR values of a sample of Ankara clay ranges from 8 near the ground surface to a value of 2 at a depth of 9 m, and further decreases with depth toward 1, indicating that after about 15 m depth Ankara clay is normally consolidated at a site. Birand (1977) also states that in Ankara soils, the natural water

content values are near the plastic limit values, which supports the existence of preloading.

İspir (2011) reports that OCR of Ankara clay ranges from 1.1 – 1.8, for undisturbed samples taken from 4 sites along Konya Road in Ankara. Samples had liquid limit values of 50%-68%, plasticity index values between 27% and 40%, and their sampling depths and OCR values were as follow: depth of 4 m OCR = 1.81, depth of 15 m OCR=1.44, depth of 16 m OCR=1.45 and depth of 21 m OCR=1.0-1.1.

Ordemir et al. (1965) noted that Ankara clay is an overconsolidated clay due to desiccation, and its natural water content is close to its plastic limit.

The overconsolidation ratio of the Ankara clay (OCR) was also checked by Ladd et al (1977). From SPT-N values, undrained shear strength values are estimated and  $c_u/\sigma'_v$  ratios are calculated and compared with data in Table 3.4. Therefore, OCR value of Ankara clay in the field is estimated to be between 1.1 - 4 considering the undrained shear strength obtained from the empirical equations and the effective vertical pressure ratio in the field.

Table 3.4 Overconsolidation and undrained shear strength ratio (after Ladd et al. 1977)

Overconsolidation Ratio	$c_u/\sigma'_v$
1	0.2 to 0.3
2	0.4 to 0.5
4	0.7 to 0.8
8	0.9 to 1.2
10	1.3 to 1.5

Mayne et al. (2001) express the overconsolidation ratio for clay according to undrained strength ratio and friction angle which is given in Table 3.5.

Table 3.5 Over consolidation from undrained strength ratio (after Mayne et al., 2001).

$C_u/\sigma'_v$	0.2	0.22	0.3	0.4	0.5	0.7	1.0	1.25	1.50	2.0
Friction Angle	Overconsolidation Ratio									
20	1.5	1.7	2.3	3.1	3.8	5.0	8.0	10.0	11.0	15.0
30	1.0	1.0	1.4	1.9	2.4	3.3	5.0	6.0	7.0	10.0
40	1.0	1.0	1.0	1.4	1.7	2.4	3.5	4.0	5.0	7.0

Mesri (1989) described the undrained shear strength as given formula in Eq 3.5;

$$C_u = 0.22 \times \sigma'_0 \quad (3.5)$$

$$OCR = \sigma'_c / \sigma'_0 \quad (3.6)$$

Undrained shear strength of clay is known from field test results. For clay layers,  $\sigma'_0$  can be calculate by Eq 3.5 and OCR values can be obtained from Eq 3.6.

With the help of information and formulas given above about OCR values of clay, obtained values are summarized in Table 3.6.

Table 3.6 Over consolidation from undrained strength ratio (after Mayne et al., 2001).

Soil Layer	SPT- $N_{(ave)}$	SPT- $N_{60}$	$C_u$ (kPa)	OCR (Mesri 1989)	OCR (Mayne et al.,2001)	OCR (Ladd Et al.,1977)	OCR (İspir, 2011)	OCR (Design)
Clay-1	24	18.00	80	4.50	5.0	4.0	1.80	4.0
Clay-2	42	31.50	145	2.88	2.9	2.0	1.44	2.0
Clay-3	60	45.00	200	2.36	2.4	2.0	1.45	1.5
Clay-4	78	58.50	275	2.58	2.2	1.0	1.10	1.1

While determining the undrained elastic modulus values, the following relationship (Jamiołkowski et al. 1979) was used

$$E_u = \sim 500 \times c_u \text{ (for clay-1)} \quad (3.7a)$$

$$E_u = \sim 700 \times c_u \text{ (for clay-2, clay-3, clay-4)} \quad (3.7b)$$

According to Poulos and Small (2000), undrained elastic modulus values as a function of SPT-N and plasticity index (PI) is shown in Figure 3.12.

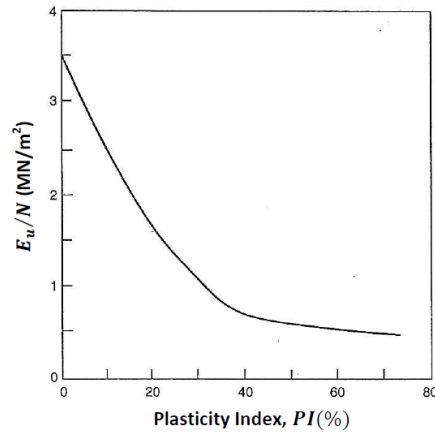


Figure 3.12 Plasticity index and  $E_u / N$  correlations (Poulos and Small, 2000)

In the study area; plasticity index of Ankara Clay is mainly between ~20 to 25%. Therefore, the coefficient of SPT N value was chosen as around 1.5, according to Poulos and Small (2000).

$$E_u = \sim 1.5 \times \text{SPT-N} \quad (3.8)$$

According to the above formulas undrained elastic modulus were calculated for clay layers are given in Table 3.7.

Table 3.7 Undrained Elastic Modulus,  $E_u$  (kPa) Values

Soil Layer	SPT- $N_{(ave)}$	SPT- $N_{60}$	PI (%)	Eq 3.4 (MPa)	Eq 3.5a-b (MPa)	Eq 3.6 (MPa)	$E_u$ -ave (MPa)	Design $E_u$ (MPa)
Clay-1	24	18.00	25	21.6	40.0	36.0	32.5	32.5
Clay-2	42	31.50	22	37.8	101.5	63.0	67.4	67.0
Clay-3	60	45.00	23	54.0	140.0	90.0	94.6	95.0
Clay-4	78	58.50	20	70.2	171.5	117.4	119.7	120.0

### 3.3.4. Determination of Drained (Long Term) Parameters

#### 3.3.4.1. Drained Friction Angle

Figure 3.14 shows collected data from the literature in a plot of drained friction angle  $\phi'_{nc}$  vs.  $I_p$  for primarily normally consolidated clays ( $I_p$  range 5- 240%).  $\phi'_{nc}$  symbolize a peak secant value with the assumption that  $c'_{nc}$  is zero. The data values vary widely,

for example, at  $I_p=20\%$  the value of  $\phi'_{nc}$  varies between  $25^0$  and  $35^0$ . However, despite the significant dispersion, a trend is seen to decreasing  $\phi'$  with increasing  $I_p$ . The data also suggest the lower bound value for  $\phi'_{nc}$  at a given value of  $I_p$ .

Drained friction angle values for the Ankara Clay were calculated according to following relations suggested by Figure 3.13:

$$\phi' = 43-10 \times \log(I_p) \quad (\text{Mean}) \quad (3.9)$$

$$\phi' = 39-11 \times \log(I_p) \quad (\text{Lower bound}) \quad (3.10)$$

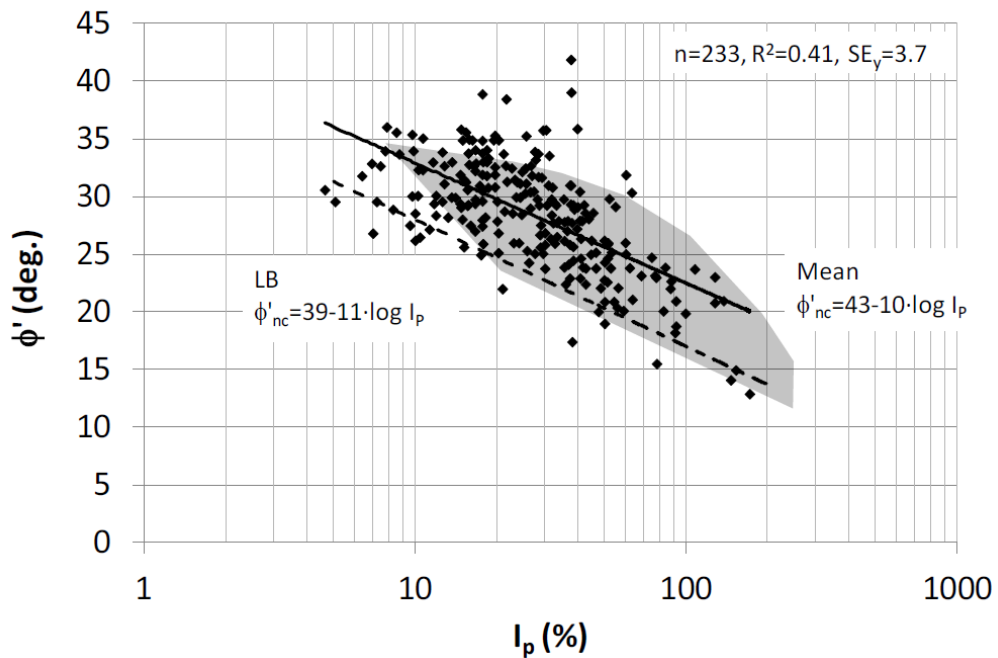


Figure 3.13  $\phi'_{nc}$  vs.  $I_p$  for primarily normally consolidated reconstituted and undisturbed clays (Sorensen and Okkels, 2013)

Figure 3.14 shows the variation of effective stress friction angle,  $\phi'$ , for several normally consolidated clays (Bjerrum and Simons, 1960; Kenney, 1959). It can be seen from the figure that; the friction angle decreases with the increase in plasticity index.

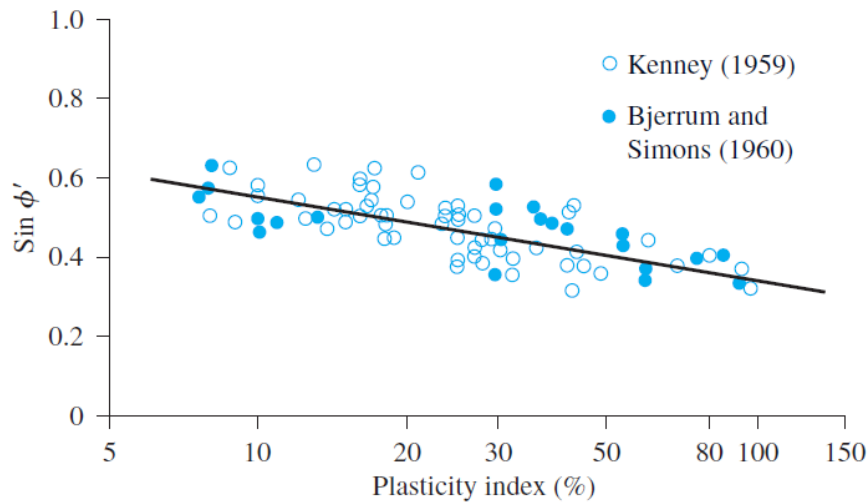


Figure 3.14 Variation of  $\sin \phi'$  with plasticity index for normally consolidated clays (Das 2007)

Drained friction angle was computed for idealized soil profile according to the both mean and lower values of suggested by Sorensen and Okkels (2013), Bjerrum and Simons (1960); Kenney (1959). Mean values of effective friction suggested by Sorensen and Okkels (2013) are very close to the values which were obtained from Figure 3.14. Drained friction angle of idealized soil profile is given in Table 3.8.

Table 3.8 Drained friction angle  $\phi'$  values

Soil Layer	PI (%)	Lower Value	Mean Value	Bjerrum and Simons	Design $\Phi'$
		$\Phi' = 39 - 11 * \log(\text{PI})$	$\Phi' = 43 - 10 * \log(\text{PI})$	$\Phi'$	
Clay-1	25	23.6	29.0	28.0	28
Clay-2	22	24.2	29.6	29.0	29
Clay-3	23	24.0	29.4	29.0	29
Clay-4	20	24.7	30.0	30.0	30

### 3.3.4.2. Drained Cohesion

Based on a comparison of the drained and undrained bearing capacity in connection to plate loading tests on clay, the Danish code of practice for foundations suggests the following equation for a cautious estimate of  $c'_{oc}$  on the basis of  $c_u$ :

$$c' = 0.1 \times c_u \text{ (kPa)} \quad (3.11)$$

Figure 3.15 shows the relationship between  $c'_{oc}$  and  $c_u$  based on data from triaxial compression tests that were performed by The Danish Geotechnical Institute over the past decades on undisturbed overconsolidated clays; ranging from clay till of low plasticity to extremely high plasticity marine Tertiary clays (Sorensen and Okkels, 2013).

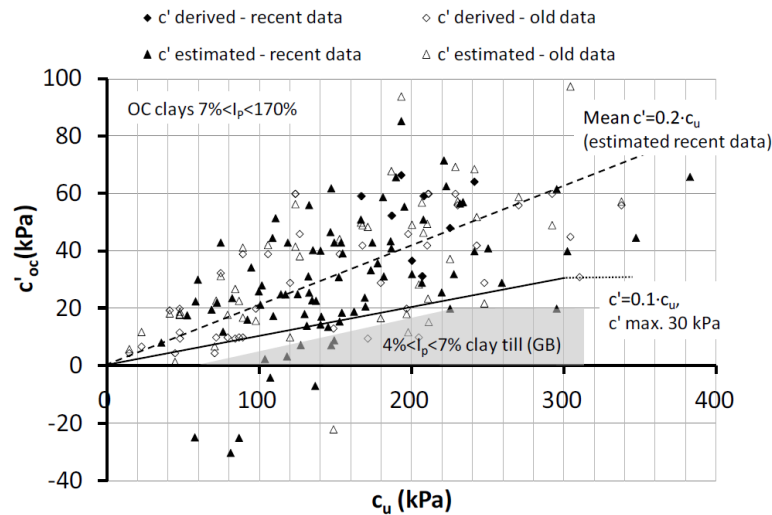


Figure 3.15 Relation between  $c'_{oc}$  and  $c_u$  for overconsolidated clays (Sorensen and Okkels, 2013)

Lunne et al. (1997) suggested that the effective cohesion value can be found by  $c' = a \times \tan \phi'$  correlation, and that the  $\alpha$  value can be obtained from Table 3.9.

Table 3.9 Possible values of  $\alpha$  factor in different soil types (Lunne et al. 1997)

Soil Type	$\alpha$	$\tan \phi'$
Soft clay	5-10	0.35-0.45
Medium Stiff Clay	10-20	0.40-0.55
Stiff Clay	20-50	0.50-0.60
Soft Silt	0-5	0.50-0.60
Medium Stiff Silt	5-15	0.55-0.65
Stiff Silt	15-30	0.60-0.70

Drained shear strength values were calculated for idealized soil profile according to the design parameters of undrained shear strength and drained friction angle, and are given in Table 3.10.

Table 3.10 Drained Shear Strength,  $c'$  (kPa) Values

Soil Layer	PI (%)	Design $C_u$ (kPa)	Design $\Phi'$	$c' = 0.1 \times C_u$	$c' = a \times \tan \Phi'$	$c'_{ave}$	Design $c'$ (kPa)
Clay-1	25	80	28	8.0	5.3	6.66	6
Clay-2	22	145	29	14.5	11.1	12.79	12
Clay-3	23	200	29	20.0	19.4	19.70	19
Clay-4	20	275	30	27.5	28.9	28.18	28

### 3.3.4.3. Drained Elastic Modulus

Drained elastic modulus ( $E'$ ) values for the Ankara clay were calculated according to following correlations:

$$E' \text{ (kPa)} = c_u \text{ (kPa)} \times 270 \quad (\text{Stroud et al. 1975}) \quad (3.12)$$

$$E' \text{ (MPa)} = 0.9 \times \text{SPT-N} \quad (\text{CIRIA, 1995}) \quad (3.13)$$

Poulos and Small (2000) suggested that the relationship between the long-term/drained deformation modulus  $E'$ , and short-term/ undrained modulus  $E_u$  on cohesive soils was given below:

$$E' \text{ (kPa)} = 0.6 \times E_u \text{ (kPa)} \quad (\text{Poulos and Small 2000}) \quad (3.14)$$

Drained elastic modulus values were calculated for idealized soil profile in accordance with the design parameters of undrained shear strength and undrained elastic modulus. Furthermore, drained elastic modulus was obtained from pressuremeter results. Drained shear strength values of idealized soil profile values are given in Table 3.11.

Table 3.11 Drained Elastic Modulus,  $E'$  (MPa) Values

Soil Layer	SPT- $N_{(ave)}$	Design $C_u$	Design $E_u$	Eq 3.10	Eq 3.11	Eq 3.12	$E'_{ave}$ (MPa)	Design $E'$ (MPa)
Clay-1	24	80	32.5	21.6	21.6	19.5	20.9	20.0
Clay-2	42	145	67	39.2	37.8	40.2	39.1	39.0
Clay-3	60	200	95	54.0	54.0	57.0	55.0	55.0
Clay-4	78	275	120	74.3	70.2	72.0	72.2	72.0

Geotechnical parameters were obtained based on site investigation studies including boreholes, in-situ tests and laboratory experiments and empirical correlations existing in the literature. Idealized soil profile is given in Figure 3.16. Drained (long term) and undrained (short term) geotechnical parameters are summarized in Table 3.12.

Table 3.12 Drained and Undrained Parameters of Ankara Clay used in this study area

Soil Layer	Thickness (m)	Undraind (Short Term) Parameters			Draind (Long Term) Parameters			OCR
		Cu (kPa)	$\Phi_u$	Eu (MPa)	c' (kPa)	$\Phi'$	E' (MPa)	
Clay-1	9.00	80	0	32.5	6	28	20.0	4.00
Clay-2	7.00	145	0	67.0	12	29	39.0	2.00
Clay-3	9.00	200	0	95.0	19	29	55.0	1.50
Clay-4	-	275	0	120.0	28	30	72.0	1.00

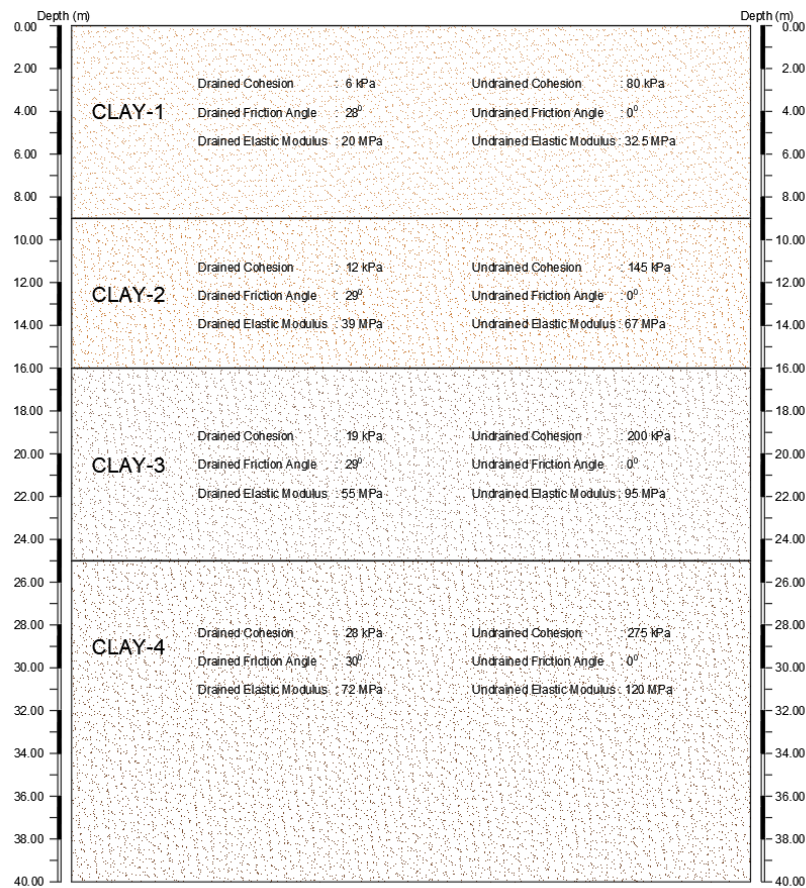


Figure 3.16 Idealized Soil Profile

### 3.4. Soil Models

Constitutive soil models used in the case study analysis, Mohr Coulomb and Hardening Soil are described as follows:

#### 3.4.1. Mohr Coulomb Material Model (MC)

Mohr-Coulomb model is linear elastic perfectly plastic type soil constitutive model, which can be used for first approximation of soil behavior. Linear elastic part of MC model is based on Hooke's Law of elasticity. Perfectly plastic part is based on MC failure criterion. Mohr-Coulomb model is using 5 input parameters. Soil stiffness is characterized by using modulus of elasticity and Poisson's ratio. Strength characteristics are modelled using  $c$  (cohesion),  $\phi$  (friction angle) and  $\psi$  (dilation angle). Mohr-Coulomb model indicates that after stresses reach hexagonal yield surface, strains become plastic and continue to increase without increase in stress.

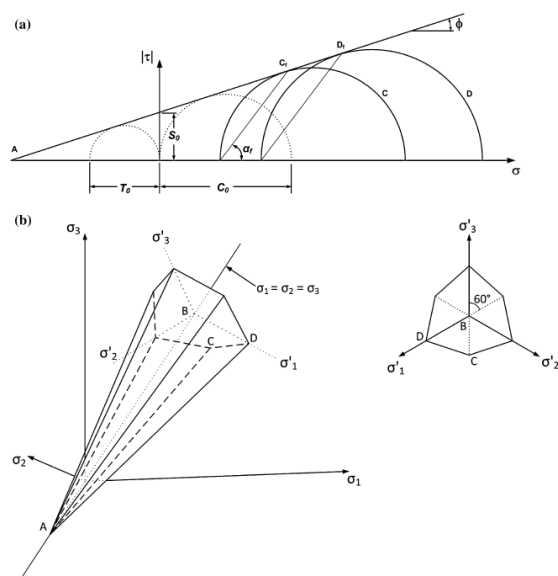


Figure 3.17 Mohr–Coulomb failure criterion: a) linear envelope in the Mohr diagram; b) pyramidal surface in principal stress space and cross-section in the equipressure plane

### 3.4.2. Hardening Soil Material Model (HS)

The Hardening Soil Model is developed based on the Duncan and Chang (1970) hyperbolic model. The hyperbolic soil model based on the assumption of stress-strain curves of soil that are obtained from the triaxial test results are approximately hyperbolic-shaped. The inelastic stress-strain behavior of soil is represented with different modulus of elasticity values for loading and unloading conditions in the hyperbolic model. The Hardening Soil Model is an advanced model for simulation of soil behavior and based on the Mohr-Coulomb failure criterion. Hardening soil model varies from MC model with its approximation of stiffness.

The soil parameters to describe the soil with Hardening Soil Model are listed below:

- ✓  $c_{ref}$  : effective cohesion
- ✓  $\Phi$  : effective angle of internal friction
- ✓  $E_{50ref}$  : secant stiffness at 50% stress level in standard drained triaxial test
- ✓  $E_{oedref}$  : tangent stiffness for primary oedometer loading
- ✓  $m$  : power for stress-level dependency of stiffness
- ✓  $E_{urref}$  : unloading /reloading stiffness (default  $E_{urref}=3E_{50ref}$ )
- ✓  $\nu_{ur}$  : poisson's ratio for unloading-reloading (default  $\nu_{ur}=0.2$ )
- ✓  $p_{ref}$  : reference stress for stiffness (default  $p_{ref}=100$  stress units)
- ✓  $K_{oNC}$  :  $K_o$  value for normal consolidation (default  $K_{oNC}=1-\sin\phi$ )
- ✓  $R_f$  : failure ratio  $q_f/q_a$  (default  $R_f = 0.9$ )

In Hardening Soil Model, the stiffness depends on the stress level. The Figure 3.18 demonstrates that the hyperbolic stress-strain relation in primary loading for a standard drained triaxial test. As can be seen in Figure 3.18, the secant modulus parameter  $E_{50}$  is obtained by a triaxial strain curve at 50% of the ultimate shear strength  $q_f$ .  $E_{50}$  is used instead of the initial modulus  $E_0$  for primary loading in Hardening Soil Model.

In Hardening Soil Model, the parameter  $m$  is the power for stress-level dependency of stiffness and it is given in this formula:

$$E_{50} = E_{50}^{ref} \left( \frac{c \cot \varphi - \sigma'_3 \sin \varphi}{c \cos \varphi + p^{ref} \sin \varphi} \right)^m \quad 3.15$$

where  $c$  and  $\varphi$  are cohesion and internal friction angle.  $E_{50}^{ref}$  is a reference stiffness modulus corresponding to the reference stress  $p^{ref}$ .

In Plaxis,  $p^{ref}$  can be taken  $100 \text{ kN/m}^2$ . As can be seen in the formula,  $E_{50}$  depends on effective confining pressure  $\sigma'_3$  in a triaxial test.

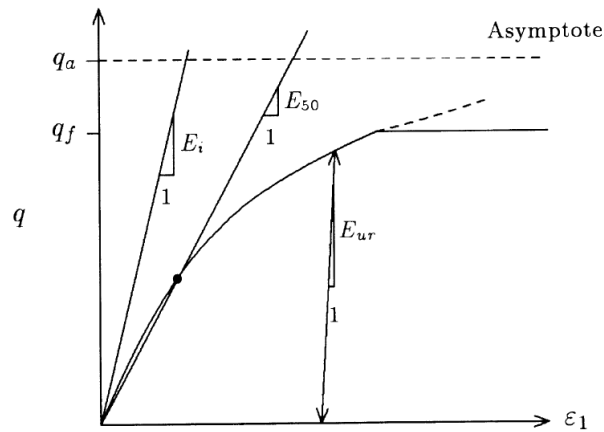


Figure 3.18 Hyperbolic stress-strain relation in primary loading for a standard drained triaxial test (after Schanz et al., 1999).

In Plaxis, the value for  $m$  can be taken as 1.0 for soft soils and for other soils the  $m$  value varies between  $0.5 \sim 1.0$ . Viggiani and Atkinson (1995) reports the exponent numbers  $m$  for different clays at very small strains as a function of plasticity index  $I_p$  Figure 3.19a, whereas Hicker (1996) presents them as a function of the liquid limit which is given in Figure 3.19b.

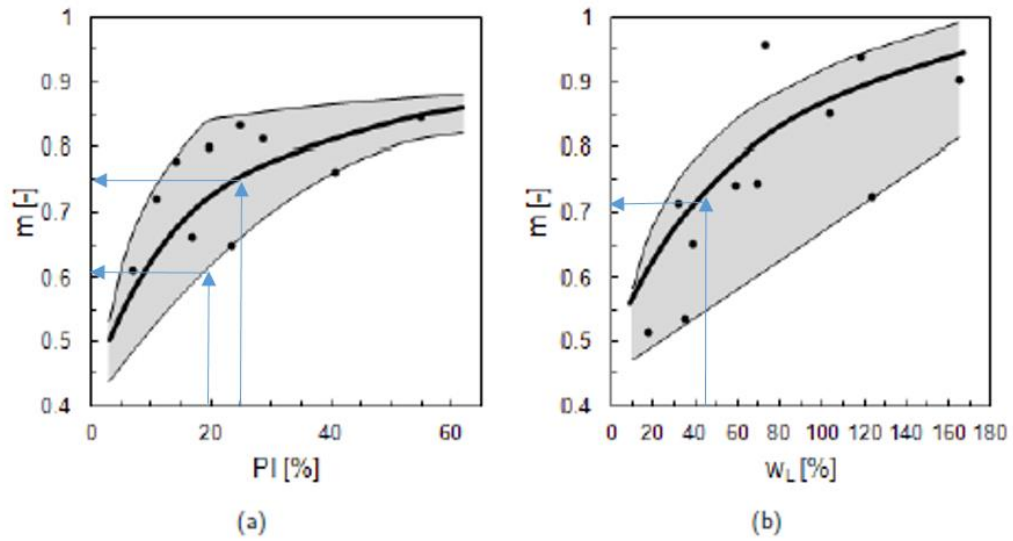


Figure 3.19 Power law exponent  $m$  related to a) Plasticity Index PI (Viggiani and Atkinson, 1995) and b) liquid limit  $w_L$  (Hicker, 1996)

According to the laboratory results for case study (i.e liquid and plastic limit values),  $m$  values are obtained as 0.6 (lower value), 0.70 to 0.75 (mean values) for Ankara clay layers. In all case and parametric study Plaxis 2D analysis,  $m$  value is accepted as 0.70 for all clay layers.

In Hardening Soil Model, oedometer stiffness modulus  $E_{oed}$  is used to define the stiffness for 1D compression and defined for a reference stress  $p_{ref}$ , as:

$$E_{oed} = E_{oed}^{ref} \left( \frac{c \cot \varphi - \sigma'_1 \sin \varphi}{c \cos \varphi + p^{ref} \sin \varphi} \right)^m \quad 3.16$$

The oedometer modulus is used to model the ground behavior at compression. Definition of the tangent stiffness for primary oedometer loading  $E_{oedref}$  at a reference stress  $p_{ref}$  is shown in Figure 3.20.

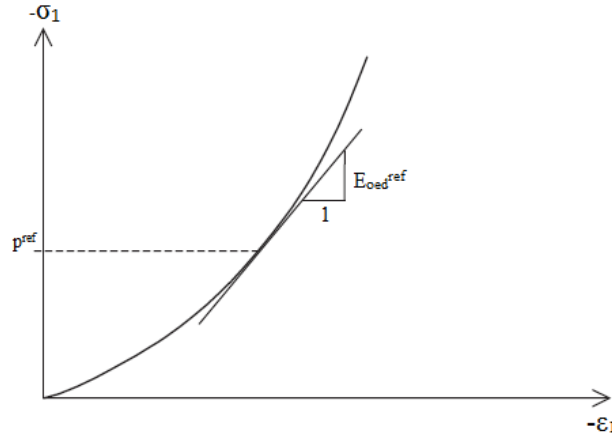


Figure 3.20 Definition of  $E_{oed}^{ref}$  in oedometer test results (Plaxis Material Models Manual, 2011)

For unloading and reloading stress paths, unloading/reloading stiffness modulus  $E_{ur}$  is used and defined for a reference stress  $p_{ref}$ , as:

$$E_{ur} = E_{ur}^{ref} \left( \frac{c \cos\phi - \sigma'_3 \sin\phi}{c \cos\phi + p^{ref} \sin\phi} \right)^m \quad 3.17$$

$E_{ur}^{ref}$  can be accepted as three times  $E_{50}^{ref}$  which is indicated in Plaxis Material Models Manual (2019).

As different modulus of elasticity parameters,  $E_{50}^{ref}$ ,  $E_{ur}^{ref}$  and  $E_{oed}^{ref}$ , the soil stiffness is identified more accurately, therefore, the modelling of the soil deformations are obtained more accurate.

### 3.5. Shoring System

Excavation depth is around 30.00 m which were stated in the architectural and structural projects. As shoring system, the most widely used method in Turkey, bored pile and anchored shoring system was selected. Unlike standard construction, shoring system was designed as multi-tier pile wall supported by temporary pre-stressed soil anchors. Reasons for choosing a multi-tier pile wall as a shoring system for deep excavation were mentioned in the Introduction chapter of this study. The facade view of constructed bored piles was shown in Figure 3.21. Other pictures during and at the end of construction of the shoring system can be seen in Appendix C.



Figure 3.21 Facade view of constructed bored piles

The excavation was around 30 m deep, with a multi-tier reinforced concrete pile wall system supported by pre-stressed ground anchors. This system is modeled by two-dimensional finite element method and the results are interpreted by comparing with the results obtained in the field from inclinometer measurements.

### 3.5.1. Section Details

The bored piles in shoring system, were 80 cm in diameter and had 100 cm center to center spacing (Figure 3.22 and Table 3.13). Bored piles were supported by 4x0.6'' temporary pre-stressed ground anchors with variable horizontal spacings, 4 anchor bars with 8 m grout length (Figure 3.23). Anchor bars had a diameter of 0.60 inch and were conforming to ASTM A-416 requirements. Anchors were inclined at 15° from the horizontal (Figure 3.23). Potential sliding wedge was drawn from ~5 m below from the 30-m-deep excavation bottom level and it was offset as 0.20 x Excavation depth. Free length of anchor had been extended beyond the obtained potential sliding surface. Further details of the general layout and facade view of piles and anchors can be seen in Appendix B.

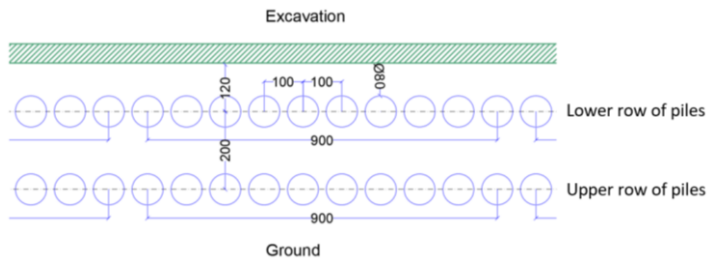


Figure 3.22 Top view of piles

Table 3.13 Pile and Anchor Details of Deep Excavation

	Upper Pile	Lower Pile
Length (m)	19.70	20.50
Diameter (m)	0.80	0.80
Spacing (m)	1.00	1.00

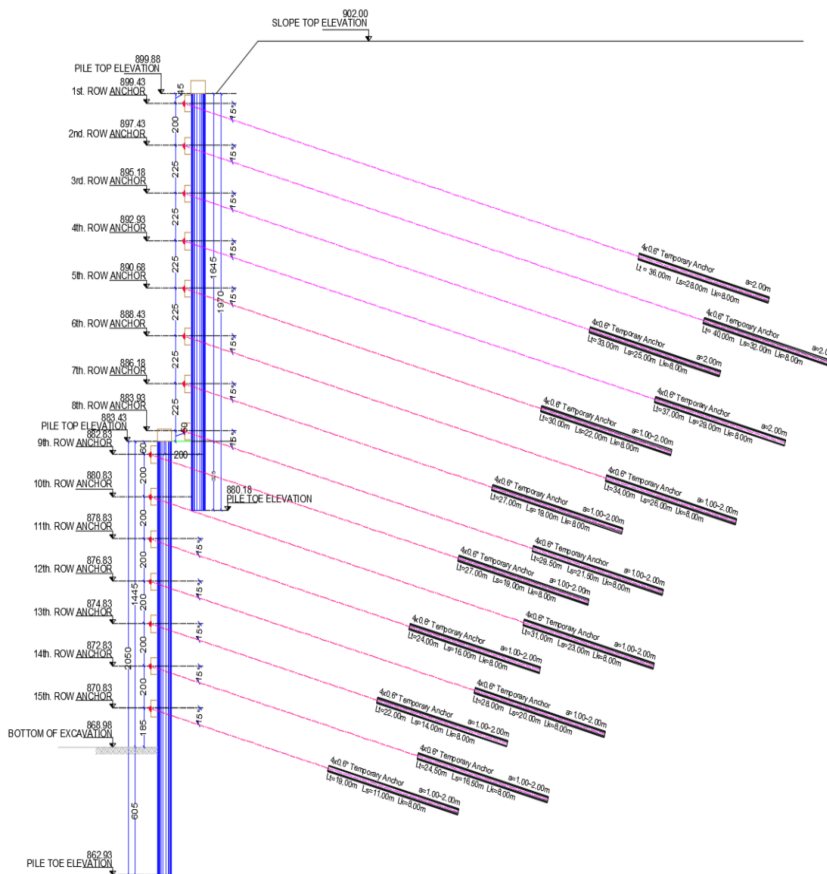


Figure 3.23 Cross section details of the deep excavation

Table 3.14 Anchor details of the deepest excavation section

Anchor Row	Free Length (m)	Bonded Length (m)	Total Length (m)	Horizontal Spacing (m)	Horizontal Angle (°)
1	28.00	8.00	36.00	2.00	15°
2	32.00	8.00	40.00	2.00	15°
3	25.00	8.00	33.00	2.00	15°
4	29.00	8.00	37.00	2.00	15°
5	22.00	8.00	30.00	1.00 - 2.00	15°
6	26.00	8.00	34.00	1.00 - 2.00	15°
7	19.00	8.00	27.00	1.00 - 2.00	15°
8	21.50	8.00	29.50	1.00 - 2.00	15°
9	19.00	8.00	27.00	1.00 - 2.00	15°
10	23.00	8.00	31.00	1.00 - 2.00	15°
11	16.00	8.00	24.00	1.00 - 2.00	15°
12	20.00	8.00	28.00	1.00 - 2.00	15°
13	14.00	8.00	22.00	1.00 - 2.00	15°
14	16.50	8.00	24.50	1.00 - 2.00	15°
15	11.00	8.00	19.00	1.00 - 2.00	15°

### 3.5.2. Anchor Details and Bond Length Capacity

While anchor length was designed; the free length had been extended beyond the possible planes that could create the potential slip surface. Thus, bonded part of the anchors, which provides the actual carrying capacity, was kept out of the sliding surface.

The failure wedge method recommended in BS 8081 (1989) was used while determining the free anchor length. The failure wedge was drawn from around 3 m below the bottom of the excavation to make an angle of  $45+\phi/2$  degrees from the horizontal. The bonded part of anchor was placed starting at a distance  $0.20 \times H$  ( $H$ =total excavation height including the equivalent surcharge height) behind the failure wedge.

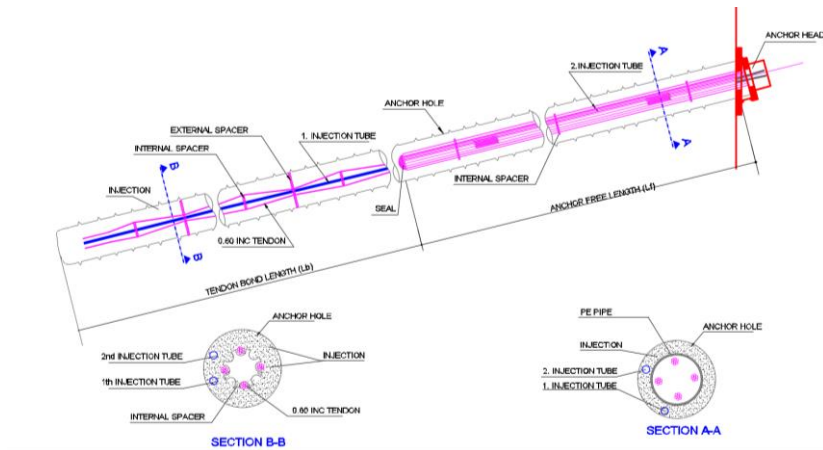


Figure 3.24 4×0,6” Temporary anchor typical cross section

The values proposed in the literature for bond stress for ground/grout interface along anchor bond zone according to lithology is given in Figure 3.25.

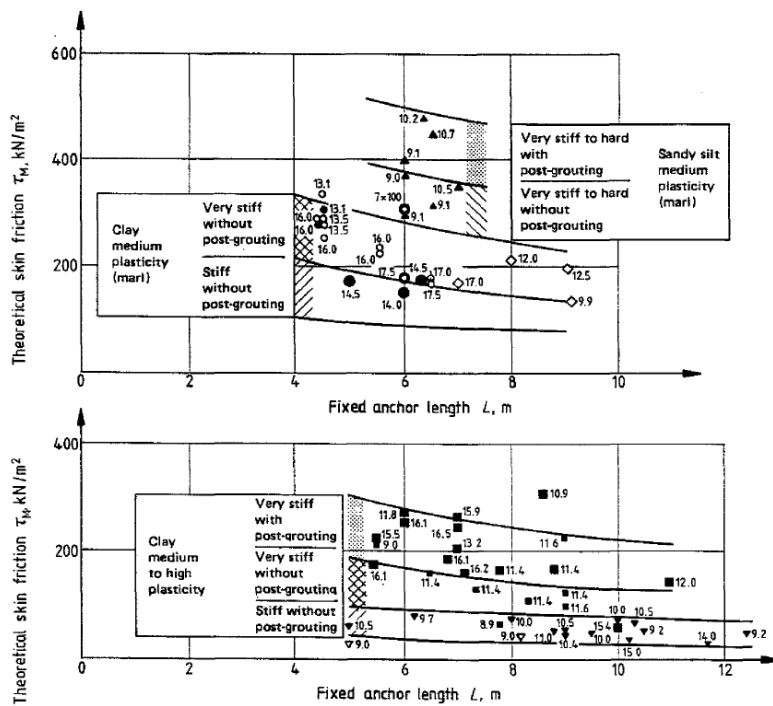


Figure 3.25 Skin friction in cohesive soils for various fixed anchor lengths, with and without post-grouting (after Ostermayer, 1974)

Skin friction ( $f_{sult}$ ) of Ankara Clay was selected as 275.00 kN/m<sup>2</sup> for 8.00 m fixed anchor length based on given literature above. 8.00 m bond length anchorage capacity calculation:

For temporary anchors ground/grout safety factor is recommended as F.S = 2.00 (BS 8081, 1989).

$$\tau_{ult} = \text{Bond length area} \times f_{sult}$$

$$\tau_{ult} = 8.00 \times 275.00 \times \pi \times 0.15 = 1036.7 \text{ kN}$$

$$\tau_{allowable} = \tau_{ult} / 2.00 = 1036.7 / 2.00 = 518.3 \text{ kN}$$

The above limit value was targeted in anchors to be produced in shoring system.

### 3.5.3. Tensile Capacity of Anchorages

The ultimate tensile capacity of 1 strand tendon consist of 7 strands and 0.60'' diameter is 26.58 tons. Allowable load carrying capacity for 1 strand tendon is 156 kN (15.9 ton). Allowable load carrying capacity for 4 anchor cables of temporary anchorages is;

$$P = 4 \times 15.90 = 63.6 \text{ ton}$$

### 3.6. Finite Element Modelling of Multi-Tier Pile Wall

Cross section of shoring system having the deepest part of the excavation is analyzed by finite element method. When the model is created in Plaxis 2D program, analysis is made according to the construction stages performed in the field. Geotechnical parameters obtained from the laboratory and field test results for Ankara Clay are used in the analyzes.

Consistent with construction stages, in Plaxis 2D model, first upper pile is activated. Then excavation is carried out to a maximum of 50 cm below the first-row of anchors. After the excavation is completed, the materials identified as free and bonded parts of the anchor are activated and prestressed to the free part of anchor.

Other excavations and anchorage stages are continued respectively until the excavation of 7th anchor row is completed. After the 7th excavation, lower bored pile is activated, and the excavation and anchor construction continued. Thus, all soil excavated and anchored materials (free and bonded zone) are activated until the bottom of the excavation.

The same system constituted with different material models, both short term and long-term solutions, and the results are compared. The results obtained are also compared with in-situ inclinometer measurements. Results of Plaxis 2D analysis using hardening soil material model and drained geotechnical parameters are given in the following figures. Further details of construction stages, deformed mesh, pile horizontal deformations etc. can be seen in Appendix D. Pile wall is modeled using plate elements and the anchor is modeled using “node-to-node anchors” for free length and “embedded beam row” for bond lengths. For modelling node-to-node anchor and for modelling embedded beam row, elastic and elasto-plastic material model options are possible. In this case study, elasto-plastic material model is used for both free length and bond length, considering their maximum capacity. Material parameters used in Plaxis 2D program, for bored piles and for anchors, are given in Table 4.1, Table 4.2 and Table 4.3 in Chapter 4.

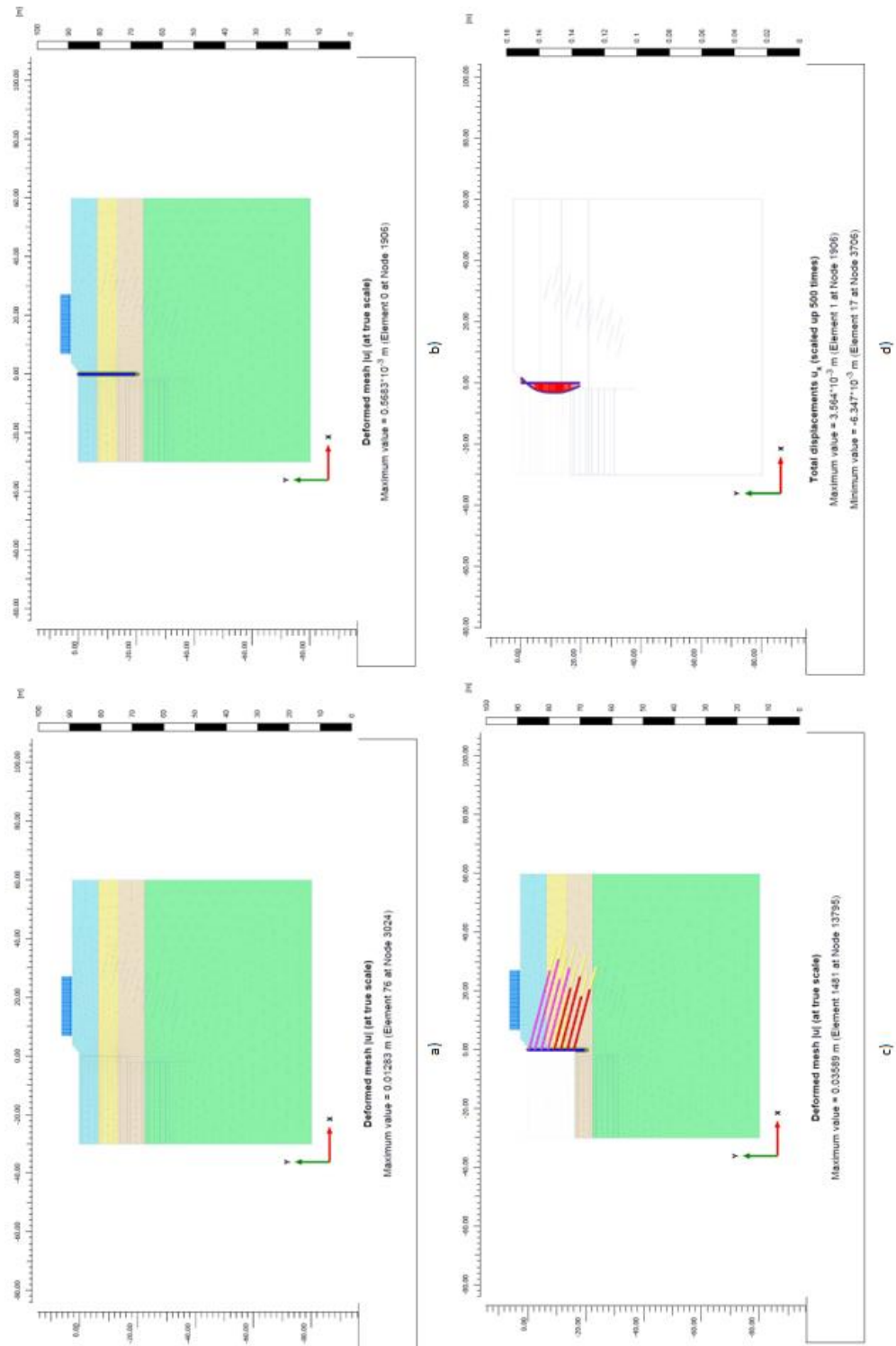


Figure 3.26 a) Initial phase, b) upper pile construction, c) upper part of anchors and excavation works, d) upper pile horizontal displacement.

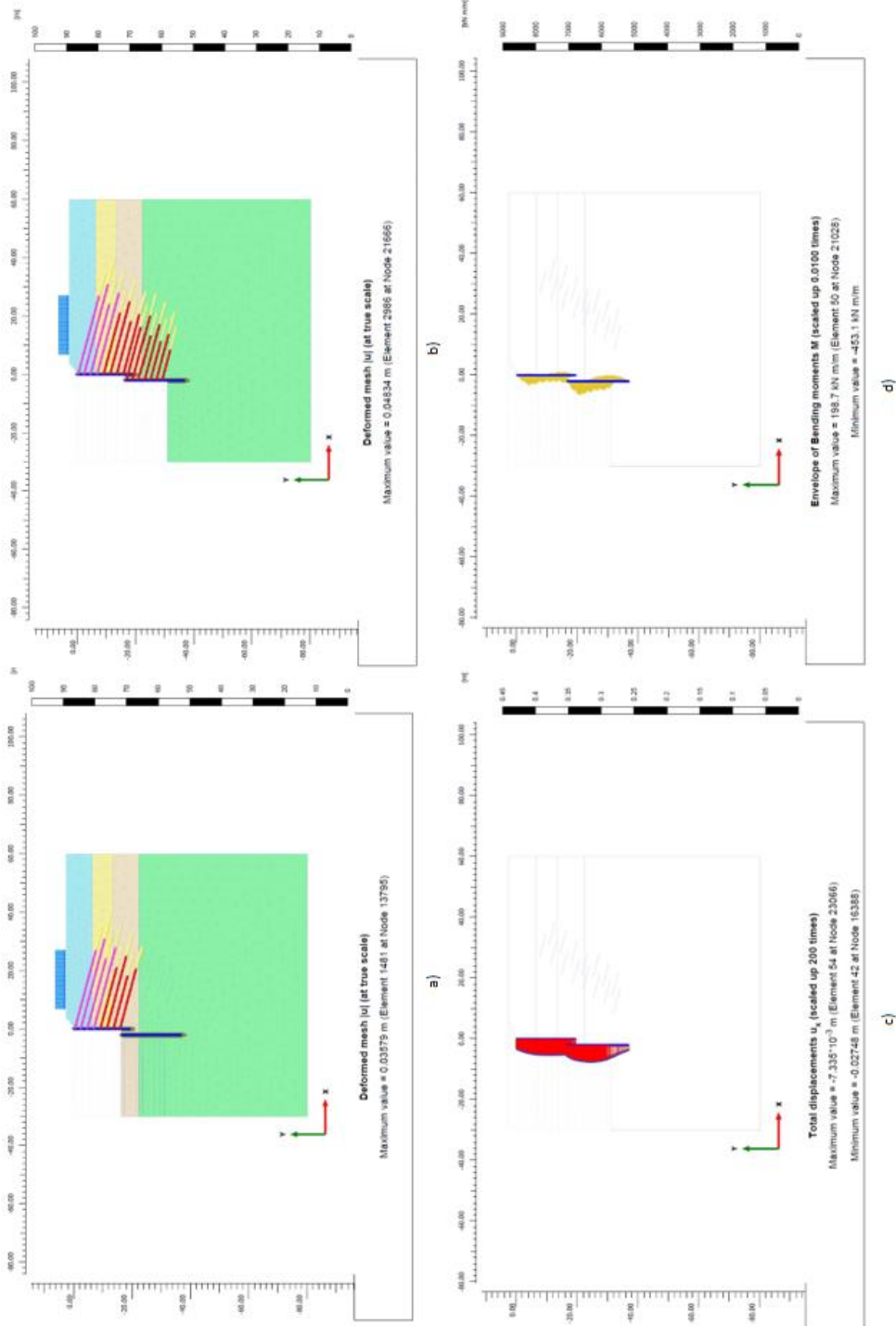


Figure 3.27 Lower pile construction, lower part of anchors and excavation works, horizontal displacement of shoring system, bending moments of piles.

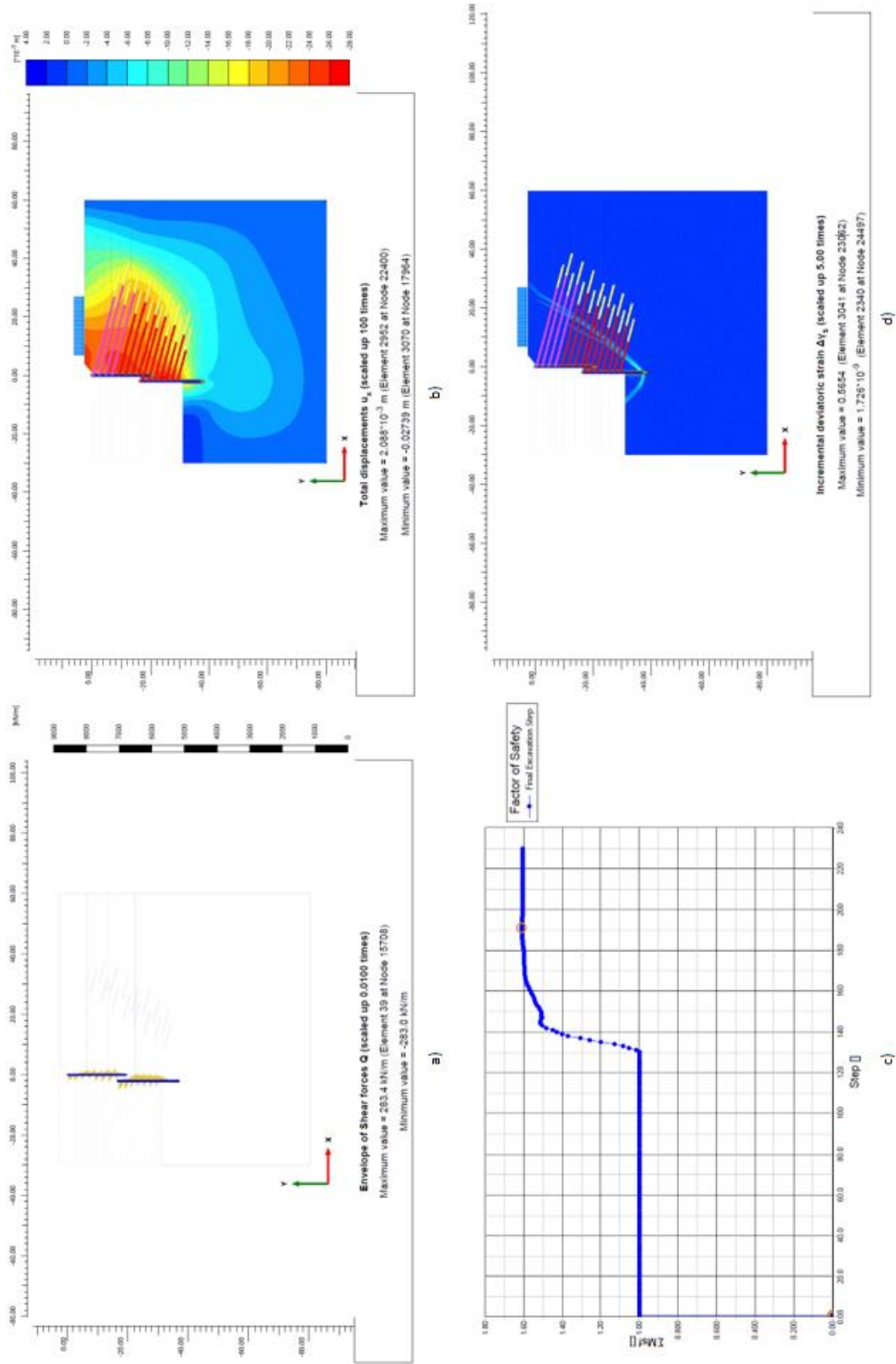


Figure 3.28 Shear forces on piles, horizontal displacement of shoring system, factor of safety, incremental deviatoric strain

In addition to these analysis, Plaxis 2D software has two different solutions for undrained condition which are undrained A and undrained B in hardening soil model.

Undrained A condition is a short-term material behavior in which stiffness and strength are defined in terms of effective properties, undrained B material behavior in which stiffness is defined in terms of effective properties and strength is defined as undrained shear strength.

The same solutions are repeated using Hardening soil model and undrained A and undrained B as the drainage type. In addition to these solutions, analyzes using Mohr Coulomb material model with drained geotechnical parameters are completed. Horizontal deformation on piles are shown in Figure 3.25. Maximum moment and shear forces values of upper and lower piles are given in Figure 3.26 and Figure 3.27 and in Table 3.15 and Table 3.16.

Table 3.15 Obtained results from Plaxis 2D analysis (1-continues)

Analysis Number	Material Model	Drainage Type	Upper Pile Displacement (cm)	Upper Pile Moment (kNm/m)	Upper Pile Shear (kN/m)	Lower Pile Displacement (cm)
1	H.S	Drained	2.61	322	227	2.75
2	H.S	Undrained (A)	3.33	383	228	3.00
3	H.S	Undrained (B )	7.53	316	362	7.86
4	M.C	Drained	2.60	325	242	4.81

Table 3.16 Obtained results from Plaxis 2D analysis (2)

Analysis Number	Material Model	Drainage Type	Lower Pile Moment (kNm/m)	Lower Pile Shear (kN/m)	Max. Anchor Load (kN)	Factor of Safety
1	H.S	Drained	453	283	512	1.61
2	H.S	Undrained (A)	463	285	514	1.59
3	H.S	Undrained (B )	363	360	510	1.66
4	M.C	Drained	412	310	517	1.61

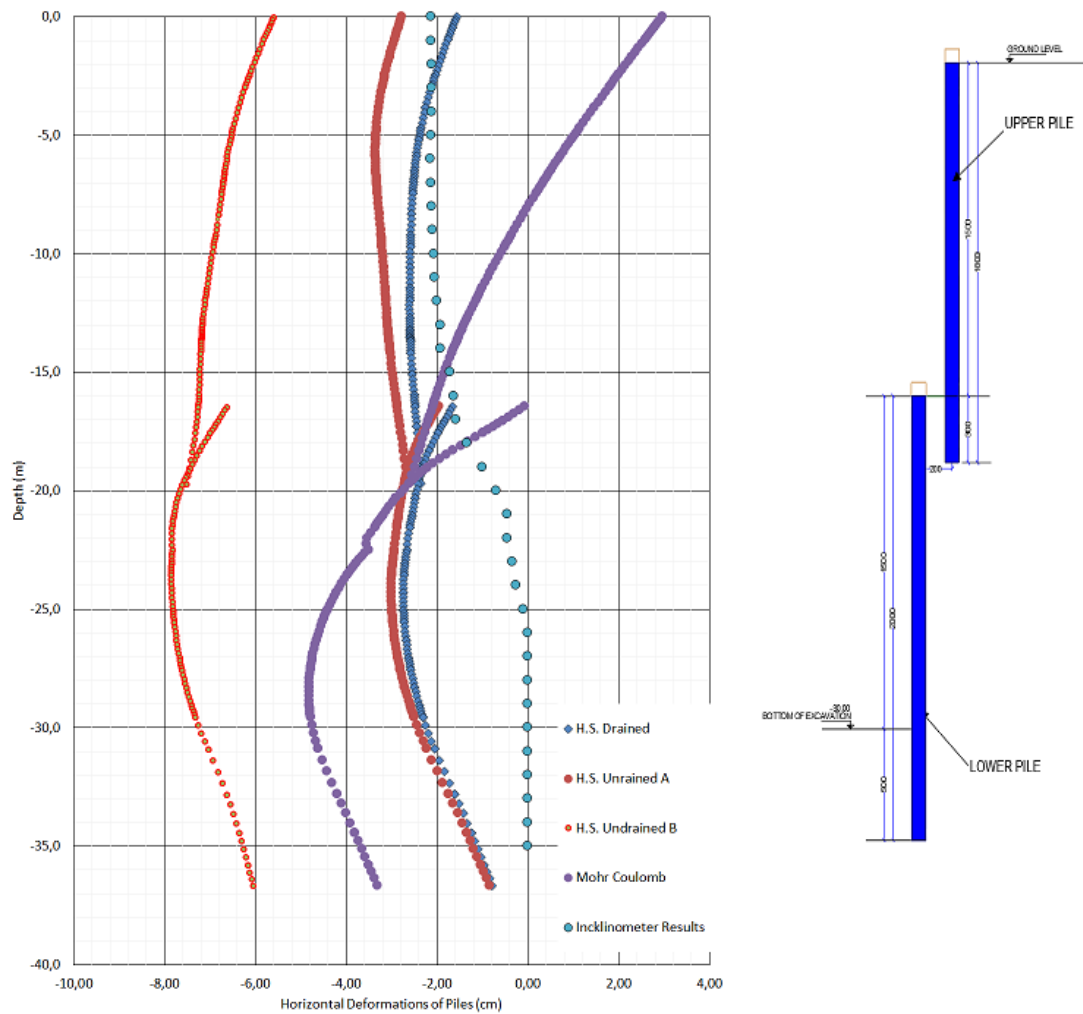


Figure 3.29 Horizontal deformations on piles in Plaxis 2D

### 3.7. Inclinometer Measurements

The cross-section analyzed in the scope of this thesis is the deepest excavation where the inclinometer measurements were taken. The graphic obtained from inclinometer measurements taken on the field between April 2017 to December 2017 is given in Figure 3.30. The maximum horizontal movement measured is about 23 mm and it is observed in the upper pile, whereas the lower pile moved by about 3 mm only.

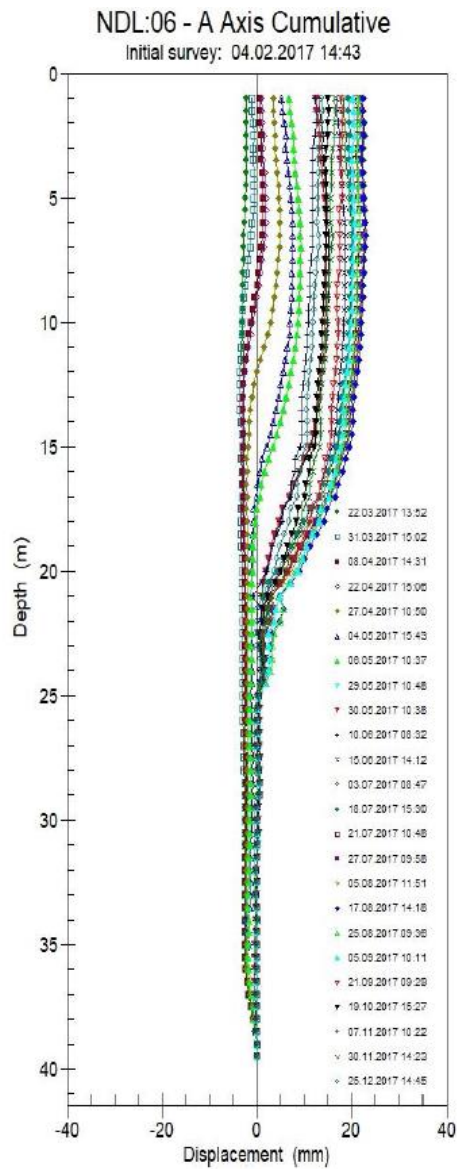


Figure 3.30 Inclinometer measurements

### 3.8. The Effect of Overconsolidation Ratio On the Behavior of Shoring System

The overconsolidation ratio (OCR) values were calculated in previous section by using empirical formulas. In this section, the behavior of the shoring system is investigated by using, the default value of OCR as 1.00 in Plaxis 2D, regardless of the calculated OCR values.

The analysis number 1 given in the Table 3.13 is the same analysis used in the case study. In the same shoring cross section, the OCR value of the clay layers is assumed to be 1.00 given by default value. The results of the analysis are given as analysis number 2 in Table 3.17 and Table 3.18.

Due to the anchor density, the deformations are low. However, when deformation rates are considered, if the OCR value is accepted as 1, horizontal deformation increased as 30% for upper pile, 10% for lower pile. As the OCR value increases, the horizontal active forces to the piles increases.

Therefore, in the case of clay soil units in shoring systems, the OCR value must be calculated and taken into consideration in the analysis. Otherwise, more deformations could be observed in the shoring system than expected values.

Table 3.17 Obtained results from Plaxis 2D analysis (1-continues)

Analysis Number	Material Model	Drainage Type	OCR	Upper Pile Displacement (cm)	Upper Pile Moment (kNm/m)	Upper Pile Shear (kN/m)	Lower Pile Displacement (cm)
1	H.S	Drained	4, 2, 1.5,1.1 (for clay layers respectively)	2.02	287	227	2.53
2	H.S	Drained	1 (For all layers)	2.61	322	227	2.75

Table 3.18 Obtained results from Plaxis 2D analysis (2)

Analysis Number	Material Model	Drainage Type	OCR	Lower Pile Moment (kNm/m)	Lower Pile Shear (kN/m)	Max. Anchor Load (kN)	Factor of Safety
1	H.S	Drained	4, 2, 1.5,1.1 (for clay layers respectively)	372	277	530	1.62
2	H.S	Drained	1 (For all layers)	453	283	512	1.61

### 3.9. Comparison of Results

According to the results of the finite element analyses, it is seen in Figure 3.26 that, the largest deformations are obtained by using Hardening soil constitutive model (Undrained B), where more than 7 cm of maximum horizontal deformations are observed in the lower pile. Mohr-Coulomb (Drained) analysis results do not seem to be realistic, since it indicates a backward movement at the top of the upper pile by more than 3 cm (Figure 3.26). Results obtained by Hardening Soil Model (Drained) and Hardening Soil Model (Undrained A) show a similar trend.

In all of the Plaxis 2D results, the lower end of the lower pile moves (in the range of 1 cm to 5 cm, depending on the selected constitutive model), whereas in inclinometer measurements in Figure 3.30, the lower end of the lower pile does not move.

General deformation behavior measured by inclinometer (in Figure 3.30) could not be captured by any of the constitutive models used in Figure 3.26. The “closest” pile horizontal deformation behavior to inclinometer measurements is obtained by using the Hardening Soil Model and drained geotechnical material parameters.

In contrast to Plaxis 2D results, the inclinometer measurements indicate that deformation of the lower pile was smaller than Plaxis 2D analysis results. Inclinometer measurements show that displacements decrease with increasing depth and reach to zero value at the bottom of the piles. One of the reasons for this situation may be that the accepted soil parameters for the lower layers of Ankara clay is greater than the values used in this study.

Another conclusion is that the OCR values must be calculated for the clay layers and used in Plaxis 2D analysis. As the OCR value increased for the near to the ground surface, horizontal deformations of piles increased.

## CHAPTER 4

### PARAMETRIC STUDIES

#### 4.1. Introduction

There are various parameters that affect the behavior of multi-tier pile wall shoring system. The purpose of this section is to investigate variations in the factors affecting shoring system behavior in series of parametric analyses in a stiff cohesive soil. Numerical models are developed by using the soil parameters given in Chapter 3. Lateral deformation, moment and shear forces on piles, anchor loads and global factor of safety of the shoring system are studied by systematically changing some of the design and geometrical parameters of multi-tier pile wall. These parameters are:

- Embedment length of upper pile
- Embedment length of the lower pile (socket length),
- Effect of having an anchor at the overlap zone between two piles
- The horizontal distance between upper and lower piles
- Interface friction coefficient between pile and soil,
- Higher and lower intensity anchor placement (i.e. anchor per m<sup>2</sup> area of wall)

In all analyses; only the investigated parameter is systematically changed and results are analyzed, while keeping other parameters constant at certain selected values, as described in the following sections.

#### 4.2. Description of Model

Multi-tier pile wall consists of two piles described as “upper pile” and “lower pile”. Piles have different lengths, but all piles have 80 cm diameter and 100 cm pile spacing center to center. Depth of the excavation is selected as 30 m, which is greater than 20-25 m, i.e. a suitable depth for choosing multi-tier pile wall system.

In most deep excavation shoring systems using anchors in Turkey, 0.6 inch strand tendons are being used in order to provide horizontal support. In parametric study; all piles are supported by 4x0.6” pre-stressed, temporary soil anchors.

Horizontal and vertical spacings of anchors is changed according to designs. In the parametric study, finite element analyses using Plaxis 2D software for plane-strain condition are performed with different interval of anchorages (different intensity of anchor per m<sup>2</sup> area of wall).

The length of the anchors is determined according to the sliding wedge method. (BS8081, 1989). Sliding wedge is determined by drawing a line which is 45+  $\phi/2$  degree with horizontal. To design length of the soil anchor, sliding wedge is offset by 0.2 x H (Depth of excavation).

The geometry of the simplified multi-tier pile wall shoring system, which is almost similar to case study in the previous chapter, is given in Figure 4.1.

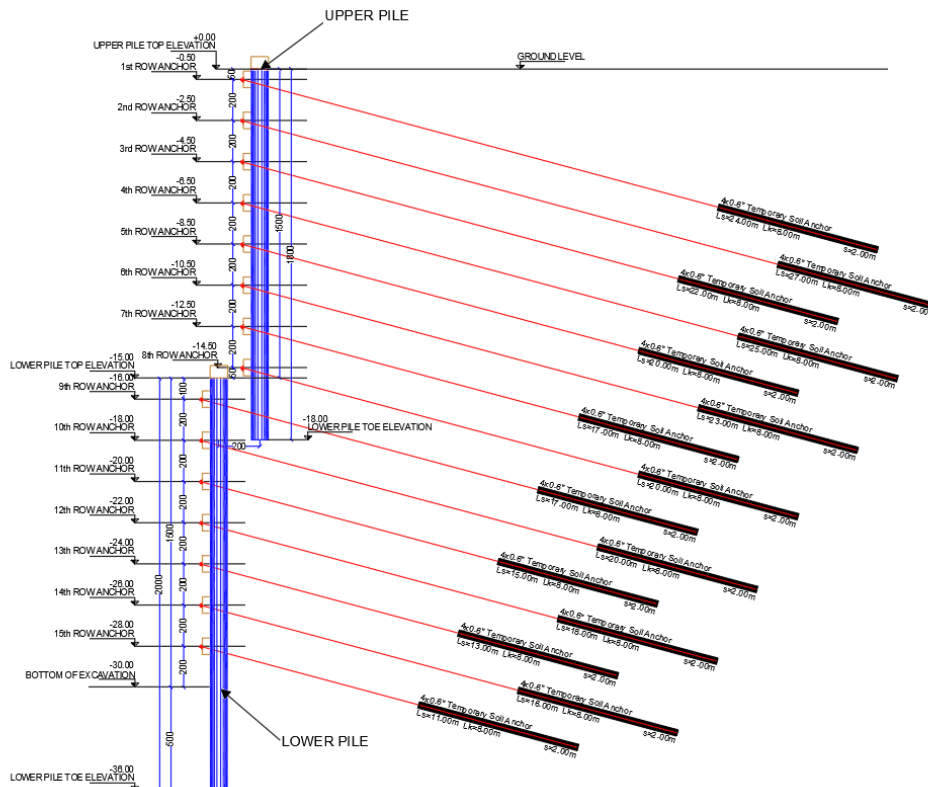


Figure 4.1 Geometry of multi-Tier pile wall shoring system that is used in parametric study

In the first parametric study, socket size of lower pile is fixed and length of the upper pile is changed to determine optimum socket size of the upper pile. Then, socket size of the upper pile is kept constant, and the variation of socket length of lower pile is examined.

Intensity of anchors is also an important factor that may affect the behavior of the system. To investigate the effect of the anchor intensity level, different analyses are conducted using two different intensity levels, however both intensity levels should provide a stable wall system. Therefore, in order to select socket sizes of upper and lower piles, analyzes are made according to different intensity of anchor per m<sup>2</sup> area of wall. According to these analyzes, socket lengths and optimum intensity of anchors in shoring system are determined.

After, socket length of both piles are determined, the effect of having an anchor at the overlap zone of both piles and soil-pile interface friction coefficient are investigated. Final step of the parametric study is to study the effect of the horizontal distance between upper and lower piles, and observe if there is a certain horizontal distance after which two pile walls should be designed as “two separate pile walls”, rather than one single wall for a 30-m deep excavation.

### **4.3. Soil Properties**

Within the scope of the parametric study, idealized soil profile obtained from field and laboratory experiments performed in case study in Ankara clay was used. Therefore; the parametric study is carried out in a stiff clay soil profile. Hardening soil model is used as material constitutive model and drained soil parameters are used in finite element analyses which were given in the previous chapter. Overconsolidation ratio of clay is taken as 4.0, 2.0, 1.5 and 1.1, for clay-1 to clay-4, respectively.

### **4.4. Material Properties**

Material parameters used in Plaxis 2D program, for bored piles and for anchors, are given in Table 4.1, Table 4.2 and Table 4.3.

Table 4.1 PLAXIS 2D input parameters of bored piles

Material	Diameter (m)	Spacing (m)	Elastic Modulus (MPa)	EA (kN/m)	EI (kN/m <sup>2</sup> /m)
Upper / Lower Pile	0.80	1.00	30.000	15.08E6	603.2

Table 4.2 PLAXIS 2D input parameters of anchors free length

Material	Pieces	Steel Diameter (inch)	Horizontal Spacing (m)	Elastic Modulus (kPa)	EA (kN)
Anchors	4	0.6	2.00	2.1E8	117.600

Table 4.3 PLAXIS 2D input parameters of anchors bonded length

Material	Diameter (m)	Horizontal Spacing (m)	Elastic Modulus (MPa)
Embedded Beam Row	0.15	2.00	28.000

## 4.5. Parametric Analysis

According to the geotechnical parameters obtained from the case study, 5 different parametric studies affecting the shoring system are carried out. Content of parametric analyzes are listed below:

1. Determination of Upper Pile Socket Length (overlap length of two piles)
2. Determination of Lower Pile Socket Length
3. Effect of having an anchor at the overlap zone between two piles
4. Effect of intensity of anchors per m<sup>2</sup> of wall area
5. Effect of soil-pile interface friction
6. Effect of horizontal distance between upper and lower piles

### 4.5.1. Determination of Upper Pile Socket Length

Firstly, parametric analyzes are performed to determine socket length (embedment length) of upper pile. To clearly describe the “socket length of upper pile”, it is shown in the general geometry in Figure 4.2. In these analyzes, socket length of lower pile is kept constant at 5.00 m (actually, different socket lengths of lower pile is used, and it

will be seen in details in the following section that the lower pile socket length of 5 m is suitable). Since excavation depth of 30.00 m is constant, entire anchorage length is kept constant in all multi-tier pile wall systems. Upper pile socket length, without any other changes in the shoring system, is changed between 1.00 m and 5.00 m and finite element analyzes are performed. Table 4.4 gives a summary of the variables and their values used in the analyses in this section. The vertical spacing of anchors is changed in order to see the effect of anchor intensity per m<sup>2</sup> of wall area. Accordingly, the analyzes are performed with anchorage at two different intensities (Table 4.4), the first one “higher intensity (1 anchor per 4 m<sup>2</sup> area of wall)” with a vertical spacing of 2.00 m and horizontal spacing of 2.00 m and the second one “lower intensity (1 anchor per 4.5 m<sup>2</sup> area of wall)” with a vertical spacing of 2.25 m, and horizontal spacing of 2.00 m. Although, the two levels of intensities may not seem to be too different from each other to observe the difference in the results, further lowering the intensity (i.e. 1 anchor per 5 m<sup>2</sup> area of wall etc.) resulted in unstable shoring system, and/or the anchor loads approach the limit values of the steel ropes and bonded lengths, and some of the analyses could not be conducted, therefore comparisons could not be made. Hence, they are selected as: 1 anchor per 4.0 m<sup>2</sup> and 4.5 m<sup>2</sup> area of wall (total anchorage intensity is decreased by 12.5%).

Table 4.4 Summary table of parametric studies for socket length of upper pile

Analysis Number	Constant Parameters	Variables (Upper Pile Socket Length)	Intensity of Anchors
1	- Lower Pile Socket Length: 5.00 m  - Horizontal Distance Between Two Piles: 2.00 m  - Anchor Lengths	1.00 m	Lower Intensity
2		1.00 m	Higher Intensity
3		2.00 m	Lower Intensity
4		2.00 m	Higher Intensity
5		3.00 m	Lower Intensity
6		3.00 m	Higher Intensity
7		4.00 m	Lower Intensity
8		4.00 m	Higher Intensity
9		5.00 m	Lower Intensity
10		5.00 m	Higher Intensity

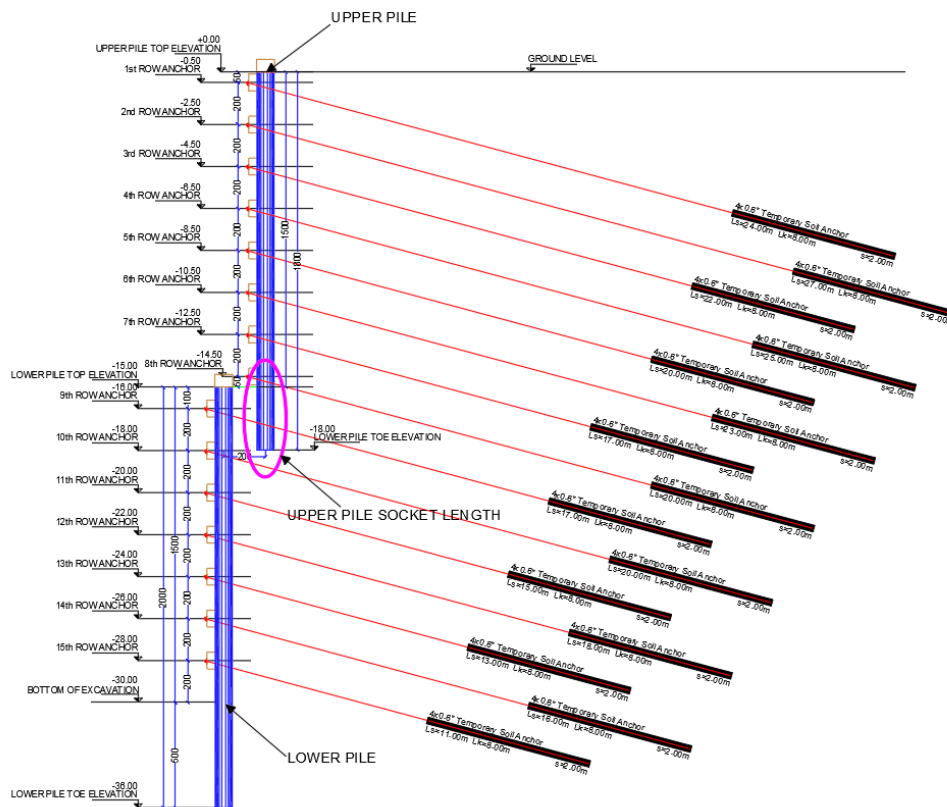


Figure 4.2 Cross section of shoring system (Upper pile socket length)

The results including horizontal deformation, moment and shear forces, maximum anchor loads and factor of safety obtained from finite element analyses are given in following tables below. Table 4.5 and Table 4.6 show that finite element analysis results of when higher intensity anchors is used in shoring system (i.e. 2.00 m x 2.00 m anchor pattern).

Table 4.5 Plaxis 2D analyses results with higher intensity anchors (1-continues)

Upper Pile Socket Length (m)	Upper Pile Horiz. Displacement (cm)	Upper Pile Moment (kN.m/m)	Upper Pile Shear (kN/m)	Lower Pile Horiz. Displacement (cm)
1.00	3.93	404	196	3.61
2.00	3.70	404	196	3.60
3.00	3.54	404	196	3.59
4.00	3.52	404	196	3.59
5.00	3.48	404	197	3.59

Table 4.6 Plaxis 2D analyses results with higher intensity anchors (2)

Upper Pile Socket Length (m)	Lower Pile Moment (kN.m/m)	Lower Pile Shear (kN/m)	Max. Anchor Load (kN)	F.S.
1.00	436	236	509	1.46
2.00	428	272	508	1.47
3.00	427	273	501	1.50
4.00	426	272	499	1.51
5.00	428	272	498	1.51

Table 4.7 and Table 4.8 show results for the case when lower intensity anchors are used in shoring system (i.e. 2.25 m x 2.00 m anchor pattern).

Table 4.7 PLAXIS analyses results with lower intensity anchors (1-continues)

Upper Pile Socket Length (m)	Upper Pile Horiz. Displacement (cm)	Upper Pile Moment (kN.m/m)	Upper Pile Shear (kN/m)	Lower Pile Horiz. Displacement (cm)
1.00	4.30	416	199	4.38
2.00	4.15	415	201	4.22
3.00	3.86	416	200	4.02
4.00	3.84	415	200	4.02
5.00	3.76	415	201	3.98

Table 4.8 PLAXIS analyses results with lower intensity anchors (2)

Upper Pile Socket Length (m)	Lower Pile Moment (kN.m/m)	Lower Pile Shear (kN/m)	Max. Anchor Load (kN)	F.S.
1.00	437	275	518	1.46
2.00	428	272	514	1.47
3.00	427	272	514	1.50
4.00	426	272	514	1.51
5.00	429	272	517	1.51

PLAXIS analyses results are also given as graphics to see the differences more clearly in the following figures. In these graphics, in the legend of the figures, (1) correspond to higher intensity anchor per m<sup>2</sup> area of wall (2.00 m x 2.00 m), (2) correspond to lower intensity anchor per m<sup>2</sup> (2.25 m x 2.00 m).

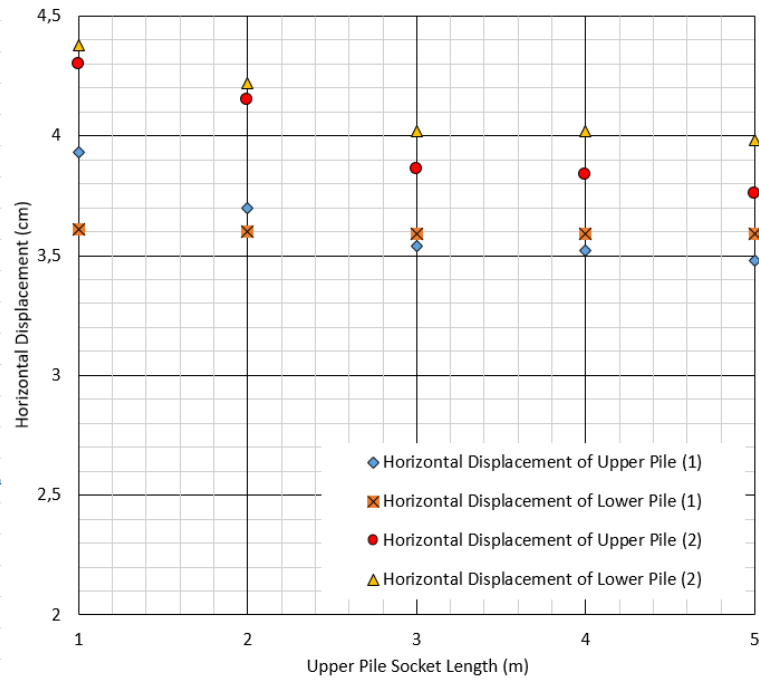


Figure 4.3 Horizontal displacement results ((1) indicates higher intensity anchor per m<sup>2</sup> area)

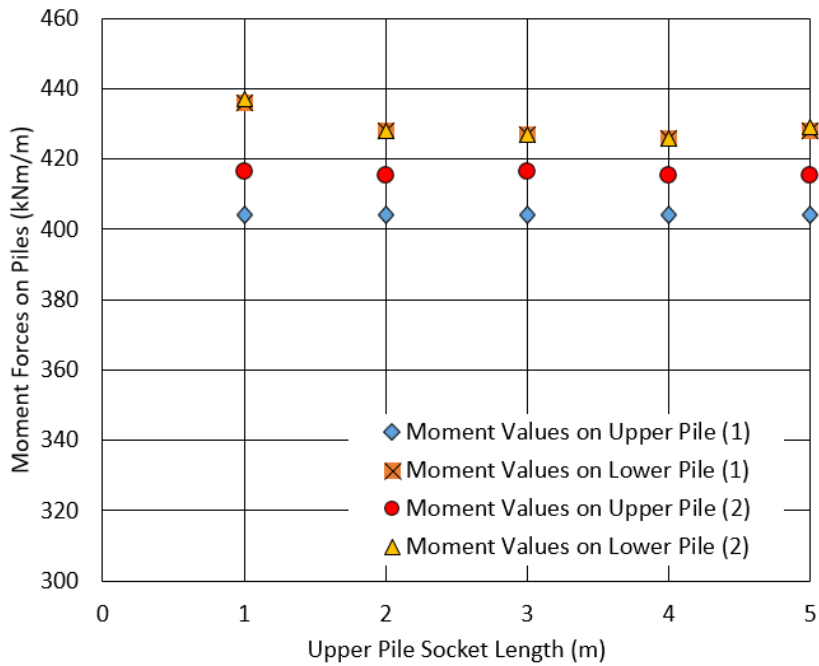


Figure 4.4 Moment values on piles ((1) indicates higher intensity anchor per m<sup>2</sup> area)

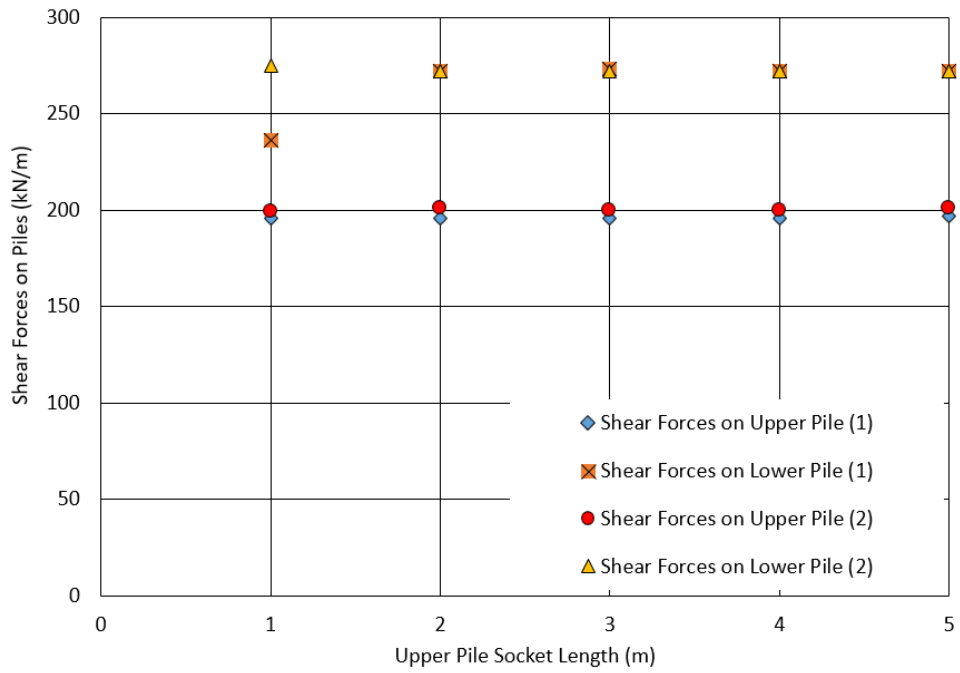


Figure 4.5 Shear forces on piles ((1) indicates higher intensity anchor per m<sup>2</sup> area)

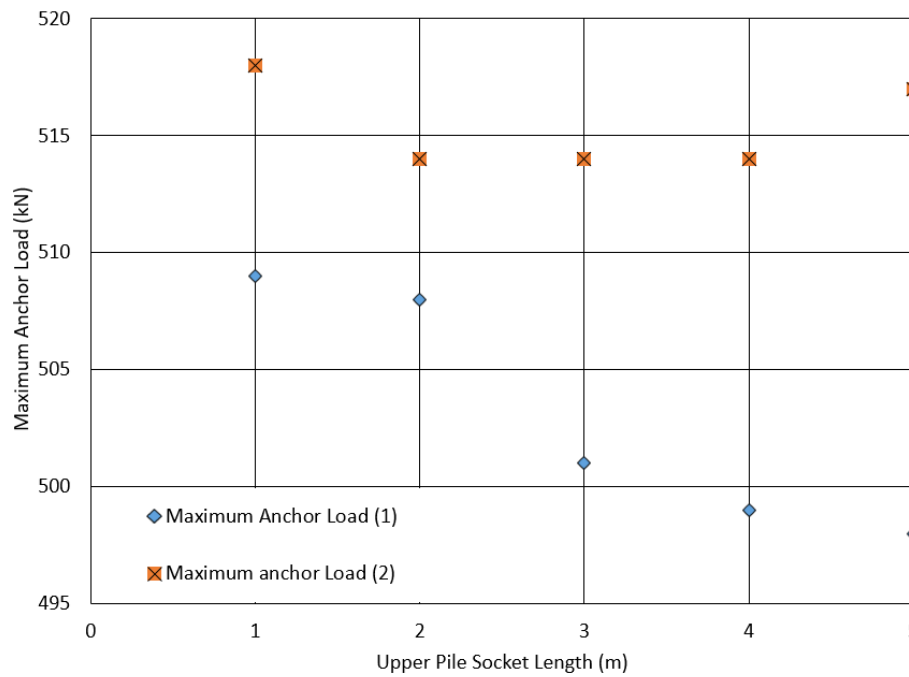


Figure 4.6 Maximum Anchor Load ((1) indicates higher intensity anchor per m<sup>2</sup> area)

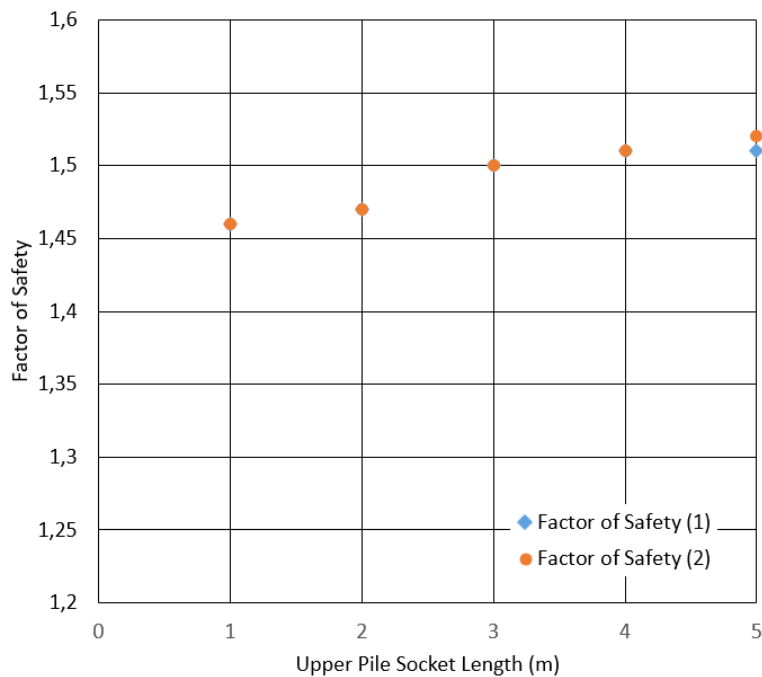


Figure 4.7 Factor of Safety Values ((1) indicates higher intensity anchor per m<sup>2</sup> area)

When higher anchor intensity (2.00 m x 2.00 m) is used and upper pile socket length is changed between 1.00 to 5.00 m:

- Horizontal displacement values of upper pile are obtained between 3.93 and 3.48 cm (Figure 4.3). There is a %11 decrease in horizontal displacements while socket length increases from 1.00 m to 5.00 m. In case socket length increases from 1.00 m to 3.00 m, horizontal displacement of upper pile decreases by ~ 10% and there is a slight difference afterwards. There is no change in the moment and shear forces of upper pile (Figures 4.4 and 4.5).
- Horizontal deformation, moment and shear forces of the lower pile did not change when upper pile socket length is changed from 1 m to 5 m.
- Maximum anchor load is 505 kN and factor of safety value is obtained as 1.46. It is seen that changing socket length of upper pile does not affect maximum anchor loads and factor of safety values (Figures 4.6 and 4.7).

When lower anchor intensity (2.25 m x 2.00 m) is used and upper pile socket length is changed between 1.00 to 5.00 m:

- It is observed that horizontal deformations of the upper pile ranged from 4.30 cm to 3.76 cm (Figure 4.3). If socket length increases from 1.00 m to 3.00 m, a 10% reduction is observed in horizontal deformation of upper pile. Also; there is a slight difference between the moment and shear forces of upper pile (Figures 4.4 and 4.5).
- Horizontal deformation of both upper and lower pile increases by ~10% compared to higher anchor intensity (Figure 4.3).
- There are very small differences in the moment and shear forces of lower piles.
- Although; total anchorage intensity is decreased by 12.5%, anchor loads increased only from 501 kN to 514 kN which is around 2%.
- Factor of safety values did not change in these analyses (Figure 4.7).

As a result of these results, it is found that upper pile embedment length does not affect shoring system if socket length of upper pile is more than 3.00 m and therefore it can be used as 3.00 m in further analyzes.

#### **4.5.2. Determination of Lower Pile Socket Length**

Parametric analyzes are performed to determine socket length of the lower pile. What is meant by the socket length of lower pile is shown in the general geometry in Figure 4.8. In these analyzes, the socket length of the upper pile is kept constant as 3.00 m. Since the excavation depth 30 m is fixed, the entire anchorage length is kept constant in all the multi-tier pile wall systems. Finite element analyses are performed by changing the lower pile socket length between 4.00 m and 10.00 m, without any further changes in the shoring system. Analyses are again performed with two different anchor intensities: higher intensity (1 anchor per 4 m<sup>2</sup>) and lower intensity (1 anchor per 4.5 m<sup>2</sup>). A summary table of parameters in analyzes carried out to determine socket length of lower pile is given in Table 4.9.

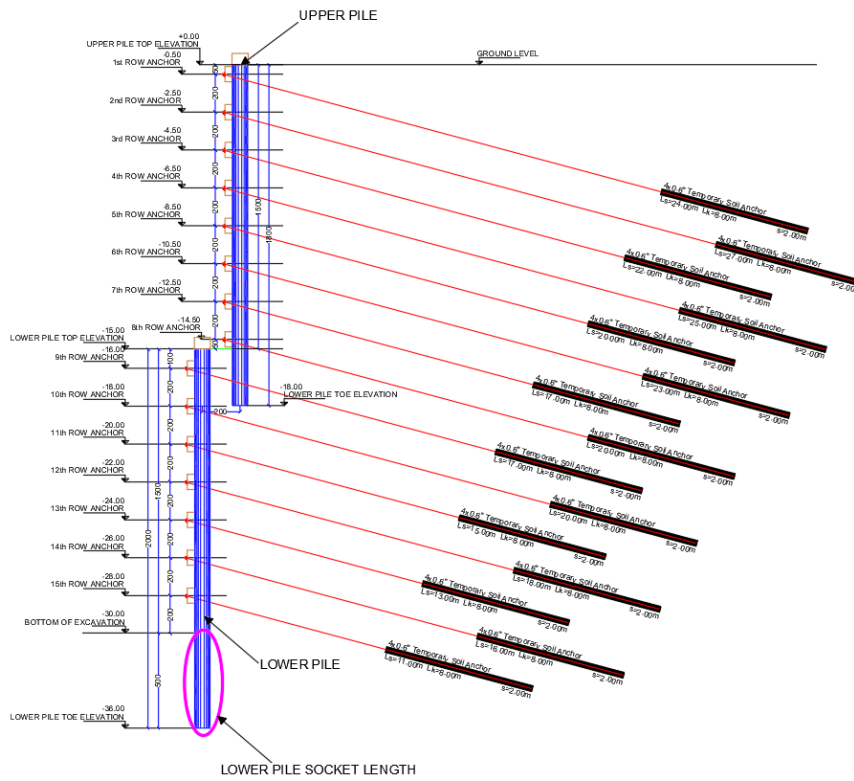


Figure 4.8 Cross section of shoring system (lower pile socket length)

Table 4.9 Summary table of parametric studies for socket length of lower pile

Analysis Number	Constant Parameters	Variables (Lower Pile Socket Length)	Intensity of Anchors
1	- Upper Pile Socket Length: 3.00 m - Horizontal Distance Between Two Piles: 2.00 m - Anchor Lengths	4.00 m	Lower Intensity
2		4.00 m	Higher Intensity
3		5.00 m	Lower Intensity
4		5.00 m	Higher Intensity
5		6.00 m	Lower Intensity
6		6.00 m	Higher Intensity
7		7.00 m	Lower Intensity
8		7.00 m	Higher Intensity
9		8.00 m	Lower Intensity
10		8.00 m	Higher Intensity
11		9.00 m	Lower Intensity
12		9.00 m	Higher Intensity
13		10.00 m	Lower Intensity
14		10.00 m	Higher Intensity

The results including horizontal deformation, moment and shear forces, maximum anchor loads and safety numbers obtained from Plaxis 2D analyzes are given in following tables. Table 4.10 and Table 4.11 show the results for higher intensity anchors (2.00 m x 2.00 m Anchor Pattern).

Table 4.10 PLAXIS analyses results with higher intensity anchors (1-continues)

Lower Pile Socket Length (m)	Upper Pile Horiz. Displacement (cm)	Upper Pile Moment (kNm/m)	Upper Pile Shear (kN/m)	Lower Pile Horiz. Displacement (cm)
4.00	3.93	404	196	3.64
5.00	3.54	404	196	3.59
6.00	3.52	404	196	3.59
7.00	3.49	404	196	3.50
8.00	3.41	404	196	3.46
9.00	3.38	404	196	3.45
10.00	3.32	404	196	3.39

Table 4.11 Plaxis 2D analyses results with higher intensity anchors (2)

Lower Pile Socket Length (m)	Lower Pile Moment (kNm/m)	Lower Pile Shear (kN/m)	Max. Anchor Load (kN)	F.S.
4.00	425	271	505	1.46
5.00	427	273	501	1.50
6.00	427	272	499	1.53
7.00	429	273	498	1.54
8.00	432	275	498	1.57
9.00	433	275	497	1.59
10.00	435	275	497	1.59

Table 4.12 and Table 4.13 show the results for when lower intensity anchor used in shoring system (2.25 m x 2.00 m Anchor Pattern).

Table 4.12 Plaxis 2D analyses results with lower intensity anchors (1-continues)

Lower Pile Socket Length (m)	Upper Pile Horiz. Displacement (cm)	Upper Pile Moment (kNm/m)	Upper Pile Shear (kN/m)	Lower Pile Horiz. Displacement (cm)
4.00	4.40	416	200	4.46
5.00	3.86	416	200	4.02
6.00	3.82	415	200	3.98
7.00	3.80	415	200	3.92
8.00	3.76	415	200	3.87
9.00	3.75	415	200	3.80
10.00	3.70	415	200	3.71

Table 4.13 PLAXIS analyses results with lower intensity anchors (2)

Lower Pile Socket Length (m)	Lower Pile Moment (kNm/m)	Lower Pile Shear (kN/m)	Max. Anchor Load (kN)	F.S.
4.00	425	271	525	1.46
5.00	427	272	514	1.50
6.00	429	274	515	1.53
7.00	430	274	514	1.57
8.00	432	275	514	1.57
9.00	433	275	513	1.59
10.00	435	275	513	1.59

Results are also given as graphics to see differences more clearly in the following figures. In these graphics (1) correspond as higher intensity anchor per m<sup>2</sup> (2.00 m x 2.00 m), (2) correspond as lower intensity anchor per m<sup>2</sup> (2.25 m x 2.00 m).

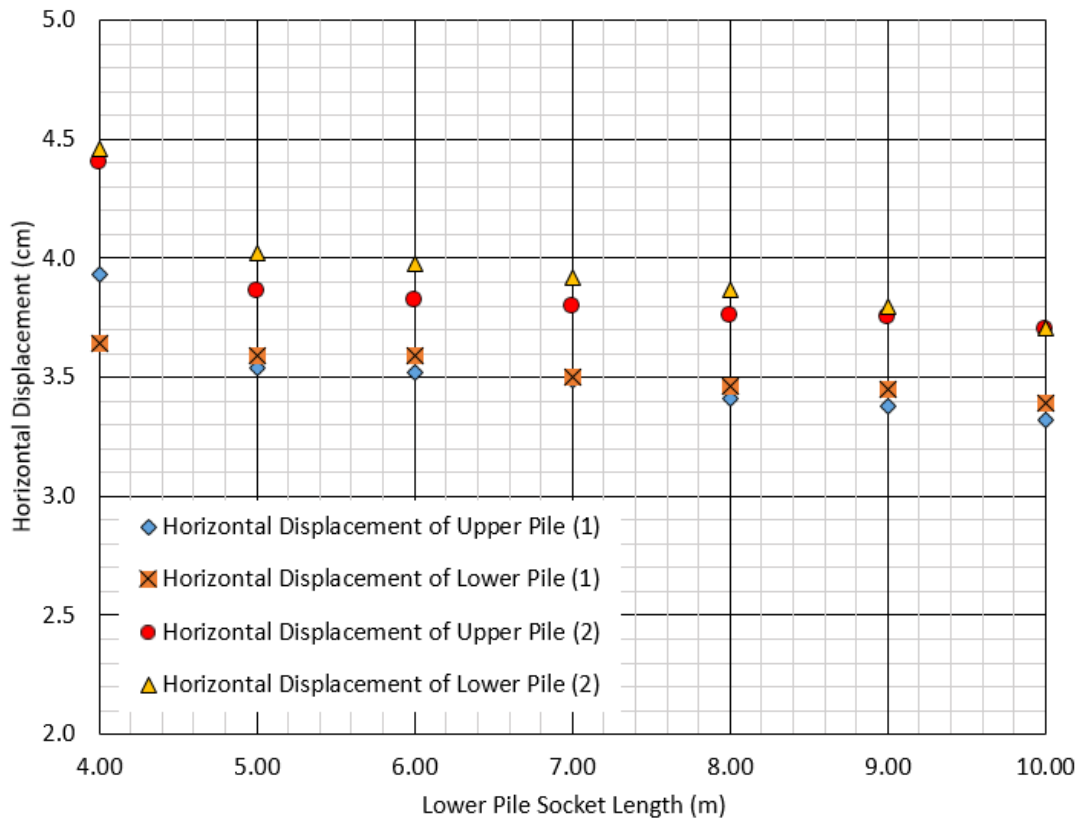


Figure 4.9 Horizontal displacement results ((1) indicates higher intensity anchor per m<sup>2</sup> area)

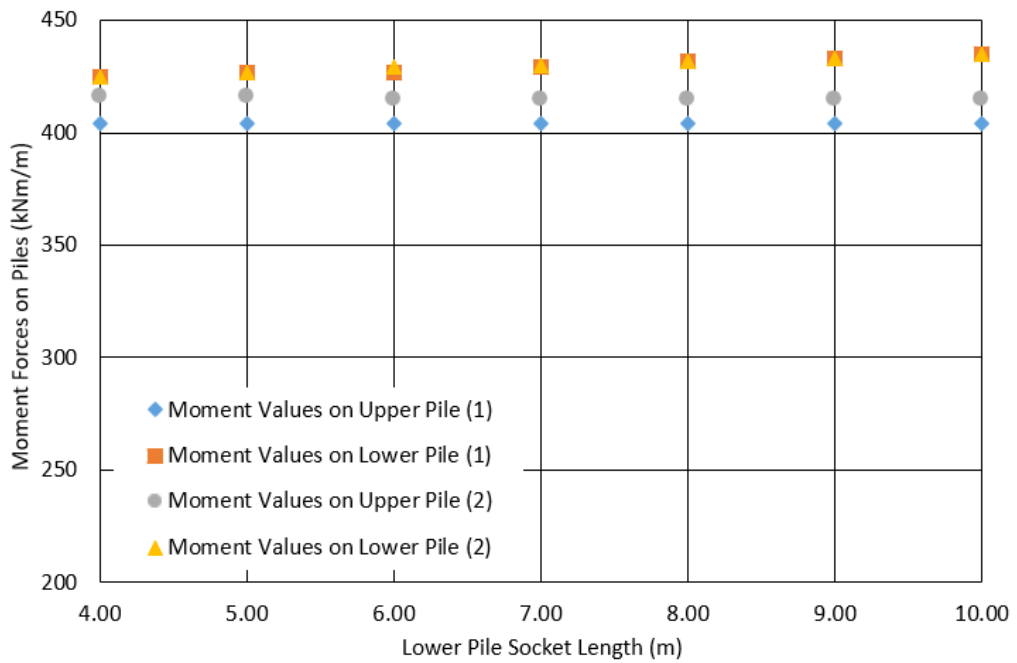


Figure 4.10 Moment forces on piles ((1) indicates higher intensity anchor per m<sup>2</sup> area)

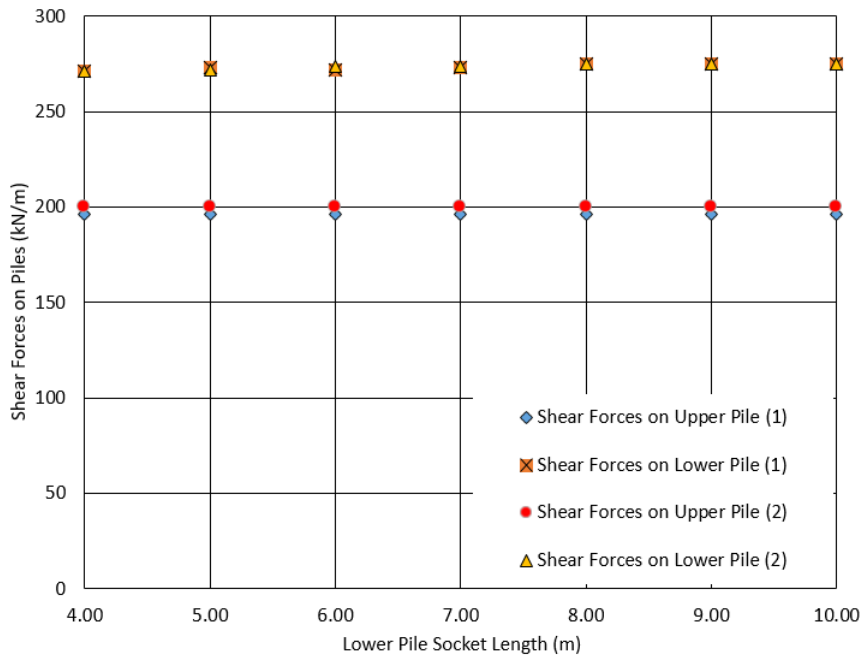


Figure 4.11 Shear forces on piles ((1) indicates higher intensity anchor per m<sup>2</sup> area)

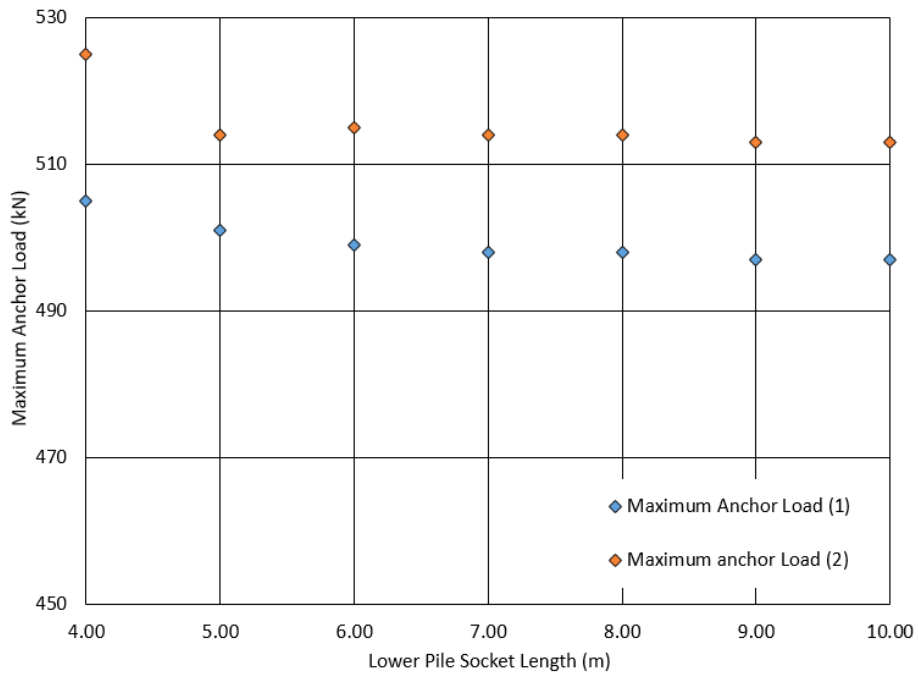


Figure 4.12 Maximum Anchor Load ((1) indicates higher intensity anchor per m<sup>2</sup> area)

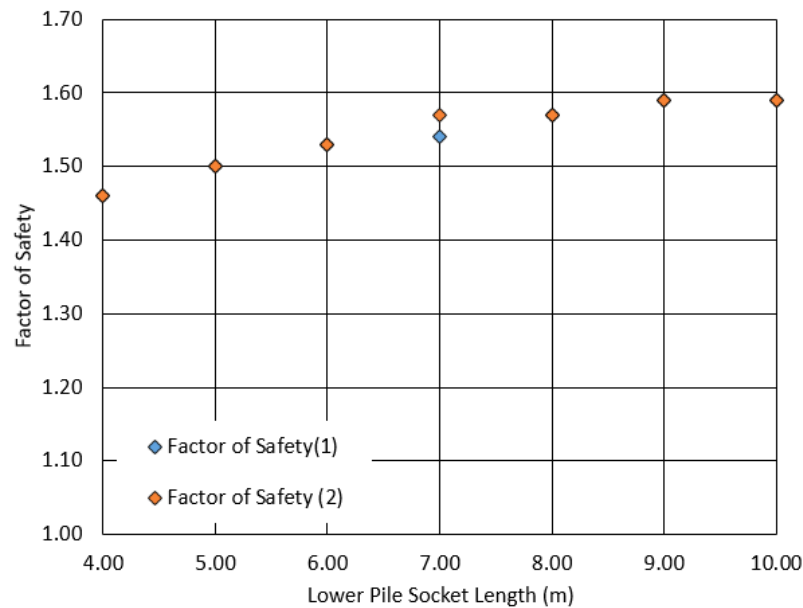


Figure 4.13 Factor of Safety Values ((1) indicates higher intensity anchor per m<sup>2</sup> area)

When higher anchor intensity (2.00 m x 2.00 m) is used and socket length of lower pile is changed between 4.00 m to 10.00 m:

- The displacement values of upper pile have been observed to increase by ~ 15%, which are between 3.32 and 3.93 cm (Figure 4.9). However, there is no change in moment and shear forces on upper pile (Figures 4.10 and 4.11).
- As a result of these analyzes, deformation of lower pile varies between 3.39 cm and 3.64 cm (Figure 4.9), and no significant change in moment and shear forces is determined.
- Maximum anchor load was in order of 500 kN, factor of safety values is 1.50 and it is seen that increase in socket length of lower pile does not affect anchor loads and increase factor of safety values (Figures 4.12 and 4.13).

When lower anchor intensity (2.25 m x 2.00 m) is used and socket length of lower pile is changed between 4.00 m to 10.00 m:

- The horizontal deformations of upper pile vary between 4.40 cm and 3.7 cm (Figure 4.9). There is a slight difference between moment and shear forces on upper pile (Figures 4.10 and 4.11).

- As compared to the higher anchor intensity, moment values on upper piles increase did not change.
- Both upper and lower pile deformations increased by 15% - 20% compared to the higher anchor intensity.
- It can be said that there are small differences in moment and shear forces on lower piles and there is no change that will affect the shoring system.
- Although total anchorage intensity is decreased by 12.5%, anchorage loads increased from 501 kN to 514 kN, which is ~ 3% .
- The factor of safety values increase as the socket length of piles increase.
- However, if the anchor intensity is decreased (i.e. 1 anchor per larger than 4.5 m<sup>2</sup> area of wall), the anchor loads approach the limit values of the steel ropes and bonded lengths.

As a result, it is found that if the socket length is more than 5.00 m it affects the system very little and therefore it should be used as 5.00 m in other analyses. Moreover, displacement values are well below the limit values for a 30.00 m deep excavation.

Accordingly, in order to examine the effect of other variables in parametric analysis, it is considered appropriate and sufficient to use 13 row anchors in total, 3.00 m socket length of upper pile, 5.00 m socket length of lower pile and 2.25 m in vertical and 2.00 m in horizontal anchor intensity.

#### **4.5.3. Effect of pile-soil interface friction**

In order to study the effect of pile-soil friction in modelling the interaction between ground and structural element, interface elements are used in Plaxis 2D, which is symbolized by  $R_{inter}$ .  $R_{inter}$  relates to interface strength which expresses wall friction and soil/wall adhesion and soil strength parameters indicating cohesion and internal friction angle. The interface coefficient of the clay is assumed to be 1.0 analyses for socket length.

$$\tan\phi_i = R_{inter} \times \tan\phi_{soil} \quad (4.1)$$

$$c_i = R_{inter} \times c_{soil} \quad (4.2)$$

Interface coefficients of clay units are commonly used between 0.7 - 1.0. In this section, the effect of the interface coefficient on the shoring system is investigated. Interface coefficient values are taken as 0.70 - 0.85 and 1.00 respectively, for all soil units. The results including horizontal deformation, moment and shear forces, maximum anchor loads and safety numbers obtained from finite element analyzes are given in Table 4.14 and Table 4.15.

Table 4.14 Plaxis 2D analyses results of interface effect (1-continues)

Interface Coefficient	Upper Pile Displacement (cm)	Upper Pile Moment (kNm/m)	Upper Pile Shear (kN/m)	Lower Pile Displacement (cm)
0.70	4.99	412	214	4.46
0.85	4.63	400	213	4.21
1.00	3.86	416	200	4.02

Table 4.15 PLAXIS 2D analyses results of interface effect (2)

Interface Coefficient	Lower Pile Moment (kNm/m)	Lower Pile Shear (kN/m)	Max. Anchor Load (kN)	F.S.
0.70	421	287	580	1.34
0.85	418	298	550	1.41
1.00	427	272	514	1.50

When analysis results are examined, it is already known that the deformations increase as the interface coefficient decreases.

- Moment and shear forces have small variations on both upper and lower piles.
- One of the most important issues to be considered in the design stage is axial loads of anchor. As the interface coefficient decreases, maximum anchor loads increase. If interface coefficient is taken 0.70, it is seen that maximum anchor

load approaches limit values of steel capacity. For this reason, when designing anchored shoring systems, geotechnical parameters should be determined in detail and correctly with interface coefficient and it should be confirmed that capacity of the steel ropes in anchors does not exceed.

#### 4.5.4. Effect of having an anchor on the overlap zone of two piles

In this section, whether or not having an anchor on the overlap zone between upper and lower piles is investigated. The position of the anchor in cross section is indicated in the geometry in Figure 4.14.

In the multi-tier pile wall retaining system for 30.00 m deep excavation, upper pile is designed as 18.00 m and lower pile is designed as 20.00 m in length. The reason for the investigation of the anchors in the two pile overlap zones is the possibility of continuing lower pile construction without the anchoring here, when excavation level is around -15.00 m. Therefore, whether or not placing an anchor on overlap zone between upper and lower piles is investigated. To see the effect of anchor on overlap zone, anchor at level -15.00 m was canceled (7<sup>th</sup> row anchor in Figure 4.14) in PLAXIS and analyzed again. The results obtained are given in table 4.16.

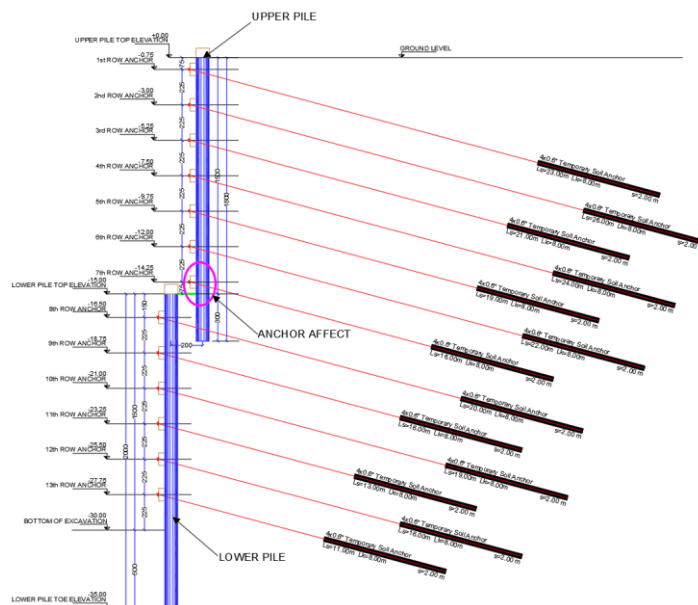


Figure 4.14 Cross section of shoring system (7th Row Anchor)

Table 4.16 Plaxis 2D analyses result of with and without anchor on overlap zone (1-continues)

Condition	Upper Pile Horiz. Displacement (cm)	Upper Pile Moment (kNm/m)	Upper Pile Shear (kN/m)	Lower Pile Horiz. Displacement (cm)
Without anchor in overlap zone	5.11	301	214	4.43
Original (with anchor in overlap zone)	3.86	416	200	4.02

Table 4.17 Plaxis 2D analyses result of with and without anchor on overlap zone (2)

Condition	Lower Pile Moment (kN.m/m)	Lower Pile Shear (kN/m)	Max. Anchor Load (kN)	F.S.
Without anchor in overlap zone	363	295	565	1.34
Original (with anchor in overlap zone)	427	272	514	1.50

When the analysis results are examined; in the case of canceling the anchor on the overlap zone of two piles;

- Deformation and moment values of upper row piles increase by ~ 25%, deformation of lower piles increase by ~ 10%.
- It can be seen that maximum anchor loads exceed the limit values i.e. unsafe.
- Displacements have increased significantly in the socket zone of upper pile and in top of lower pile. While drilling lower pile construction, there is a possibility to have more displacement on socket area of upper pile.

Therefore, in the multi-tier pile wall shoring system, construction of the last row anchors of upper pile must be completed before starting to the forage of the lower pile. Moreover; it is necessary to complete cross beam construction and pre-stress of the last level of anchors of the upper pile. As a result of the analysis, the last anchor of upper pile should be close to the intermediate excavation level (-15.00 m in this case) in the multi-tier pile wall retaining system.

#### 4.5.5. Effect of Horizontal Distance Between Upper and Lower Pile

In this section, the effect of the horizontal distance between upper and lower piles is investigated. Horizontal distance in cross section is indicated in Figure 4.15. Horizontal distance between upper and lower piles should be at least 2.00 m from the center to center of piles for field constructability purposes. Within the scope of the parametric analyses, horizontal distance between piles is started from 2.00 m and gradually increased to determine the distance at which upper and lower pile walls should be designed individually as separate walls with their own anchor lengths, rather than two-walls together designed as a shoring system for a total of 30 m deep excavation.

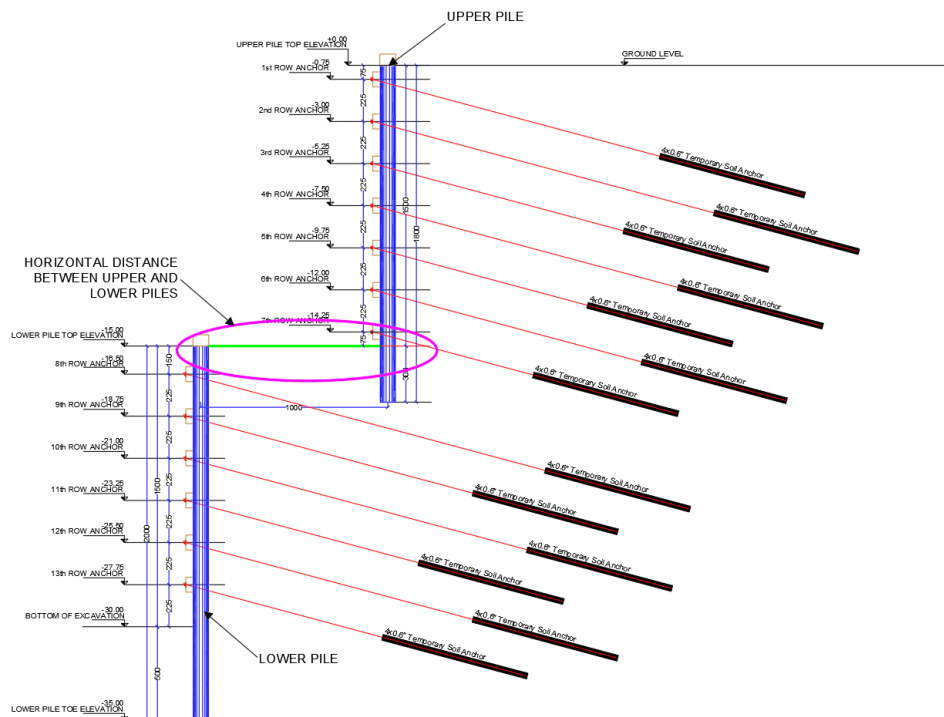


Figure 4.15 Cross section of shoring system (Horizontal Distance)

There are two variables in this parametric study; which are anchor lengths and lateral distance between upper and lower piles.

As horizontal distance increases; failure surface also varies. Accordingly, two different anchor length designs are considered.

- (1) Anchor lengths are re-determined with respect to each slip surface, considering the whole 30-m deep excavation and its failure surface. The length of anchors is determined according to the sliding wedge method (BS8081, 1989). Sliding wedge is determined by drawing a line which is  $45+\phi/2$  degree with horizontal. To determine the length of the soil anchor, sliding wedge is offset by  $0.2 \times H$ . Finite element analyses results are given in Table 4.18 and Table 4.19 and in Figure 4.16 through Figure 4.20.
- (2) In the second stage of parametric analysis on horizontal distance, the anchor design for the two piles is made separately. In other words, the excavation depth was assumed as 15.00 m (intermediate level of two piles) and anchor lengths are re-defined according to the sliding wedge method, and individual failure planes and anchor lengths of each wall are determined separately (Figure 4.21). Finite element analyses results are given in Table 4.20 and Table 4.21 and in Figure 4.23 through Figure 4.26.

Table 4.18 PLAXIS analyses results of effect of horizontal distance (when the failure wedge of the whole 30-m deep excavation is considered) (1-continues)

Horizontal Distance (m)	Upper Pile Horiz. Displacement (cm)	Upper Pile Moment (kNm/m)	Upper Pile Shear (kN/m)	Lower Pile Horiz. Displacement (cm)
2.00	3.86	416	200	4.02
5.00	3.79	391	212	3.98
10.00	3.01	392	212	3.13
15.00	2.96	395	212	3.03
20.00	2.87	398	215	2.90

Table 4.19 PLAXIS analyses results of effect of horizontal distance (when the failure wedge of the whole 30-m deep excavation is considered) (2)

Horizontal Distance (m)	Lower Pile Moment (kNm/m)	Lower Pile Shear (kN/m)	Max. Anchor Load (kN)	F.S.
2.00	427	272	514	1.50
5.00	425	280	510	1.51
10.00	301	245	508	1.56
15.00	249	218	506	1.59
20.00	222	217	501	1.59

The graphics of the results obtained from Plaxis vs horizontal distance between the two piles are given in the following figures (Figure 4.16 ~ Figure 4.20), for the case when the failure wedge of the whole 30-m deep excavation (H) is considered.

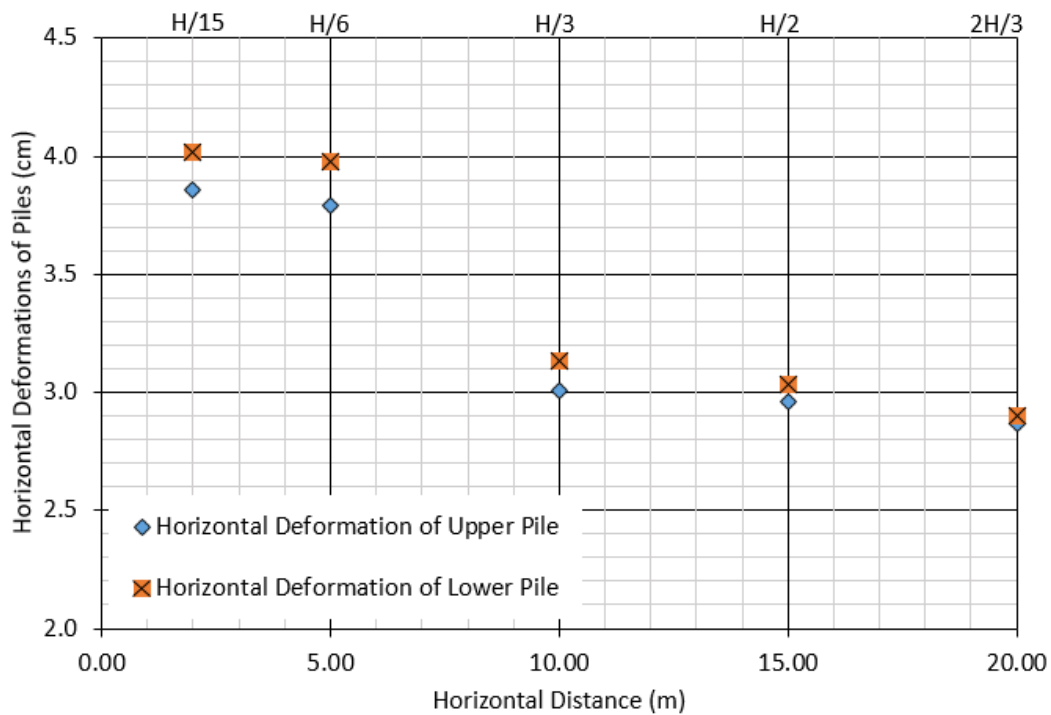


Figure 4.16 Horizontal displacement results (when the failure wedge of the whole 30-m deep excavation is considered)

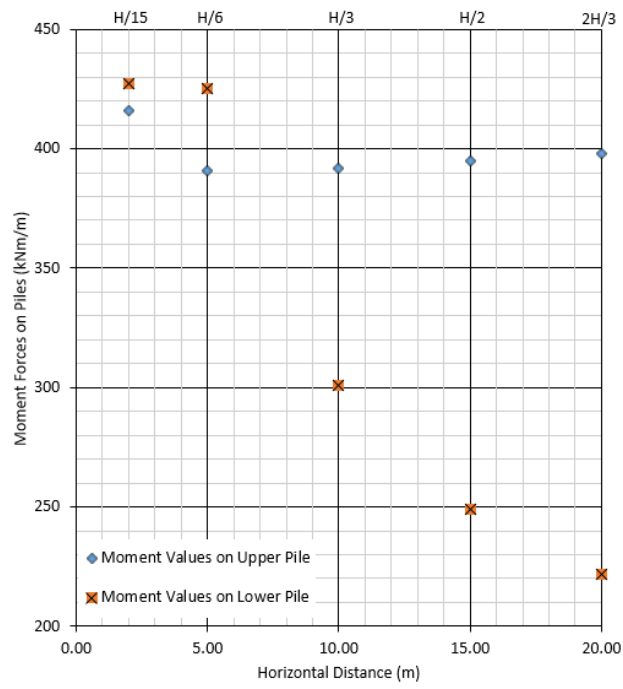


Figure 4.17 Moment values on piles (when the failure wedge of the whole 30-m deep excavation is considered)

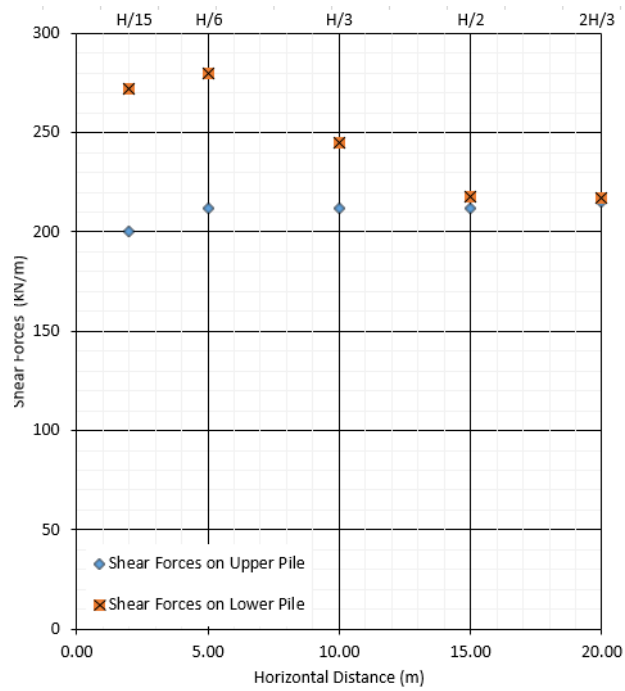


Figure 4.18 Shear forces on piles (when the failure wedge of the whole 30-m deep excavation is considered)

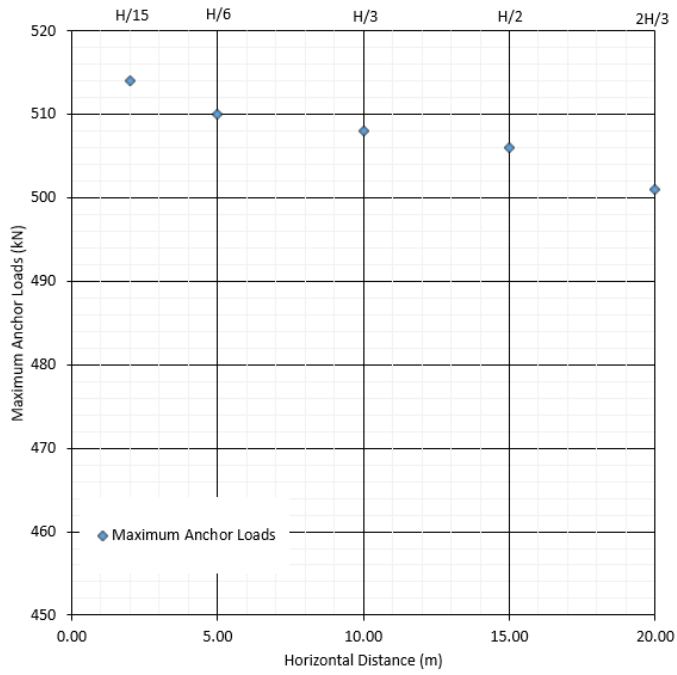


Figure 4.19 Maximum anchor loads (when the failure wedge of the whole 30-m deep excavation is considered)

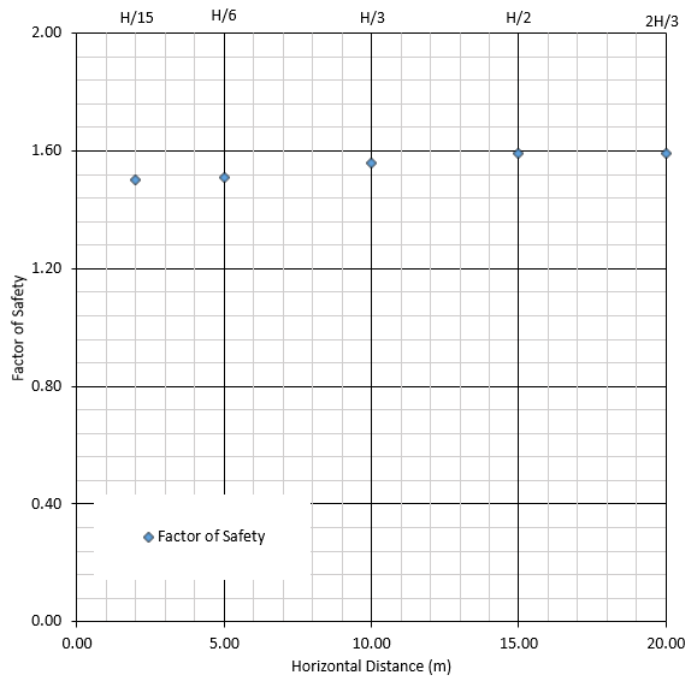


Figure 4.20 Factor of safety values (when the failure wedge of the whole 30-m deep excavation is considered)

When analysis results are examined;

- Horizontal displacement values are maximum in the case where two piles are closest to each other (horizontal distance: 2.00 m (H / 15) in Figure 4.16).
- The horizontal displacement decreases significantly as horizontal distance between two piles increases (Figure 4.16).
- In upper pile, as the horizontal distance between two piles increases, horizontal displacement decreases from 3.86 cm to 2.87 cm (~ 25% reduction). However, since anchor design of upper piles does not change, moment and shear forces do not significantly change in all conditions.
- In lower piles, horizontal displacement value decreases from 4.02 to 2.90 cm. It can be said that displacement value decreases by ~27% as horizontal distance increases up to 20.00 m. Also, there is a reduction in moment and shear forces around 25% -50%.
- If horizontal distance is 15 m and 20 m, it is seen that results of PLAXIS analyses give very close values.
- If horizontal distance between two piles exceeds 10.00 m, the rate of decrease in the horizontal displacements and moment values of piles decreases considerably.

In the second stage of parametric analyses on horizontal distance, the anchor design for the two piles was made separately. In other words, the excavation depth was assumed 15.00 m (intermediate level of two piles) and anchor lengths were redefined according to the sliding wedge method, and individual failure planes of each wall are determined separately (Figure 4.21). For the upper and lower piles, the length of anchors are changed and analyzed again according to the failure surfaces separately drawn for each wall. Results are given in Table 4.20 and Table 4.21.

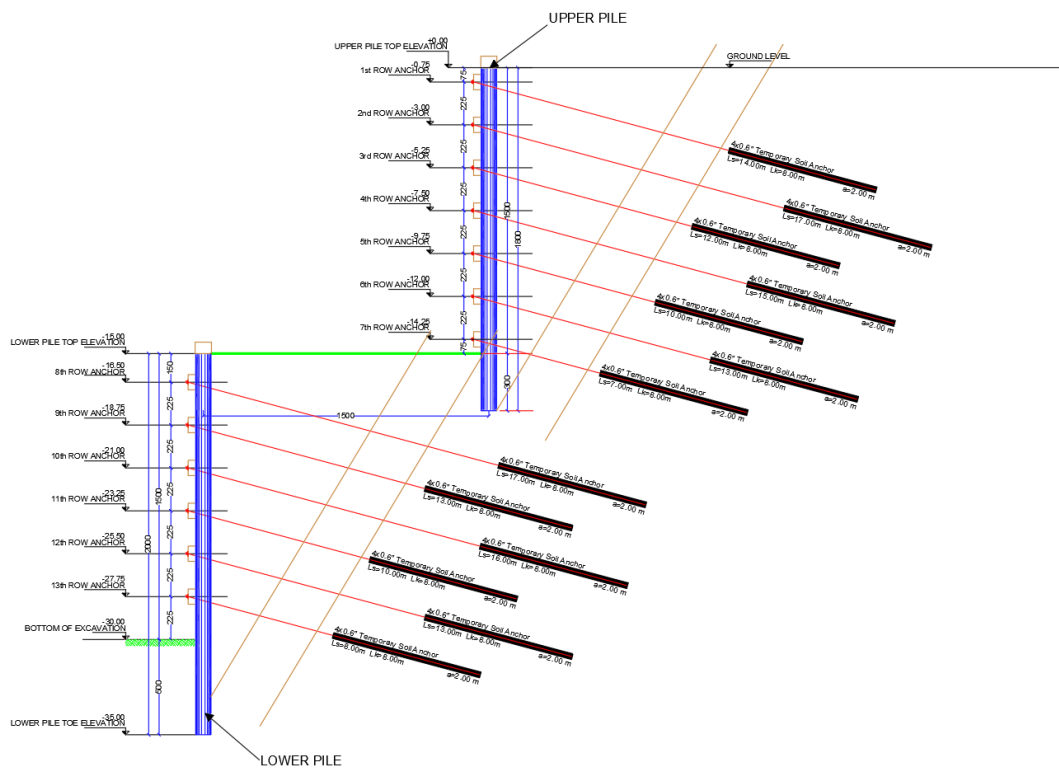


Figure 4.21 Cross section of shoring system (Horizontal Distance) (when the failure wedge of the individual, two separate walls, is considered)

Table 4.20 Plaxis 2D analyses results of effect of horizontal distance (when the failure wedge of the individual, two separate walls, is considered) (1-continues)

Horizontal Distance (m)	Upper Pile Horiz. Displacement (cm)	Upper Pile Moment (kNm/m)	Upper Pile Shear (kN/m)	Lower Pile Horiz. Displacement (cm)
2.00	6.15	400	215	5.61
5.00	4.74	400	217	4.27
10.00	3.59	400	216	3.10
15.00	2.97	400	216	3.00
20.00	2.73	400	216	2.95

Table 4.21 PLAXIS analyses results of effect of horizontal distance (when the failure wedge of the individual, two separate walls, is considered) (2)

Horizontal Distance (m)	Lower Pile Moment (kNm/m)	Lower Pile Shear (kN/m)	Max. Anchor Load (kN)	F.S.
2.00	474	321	551	1.25
5.00	417	294	542	1.29
10.00	324	245	516	1.42
15.00	264	226	512	1.46
20.00	223	220	506	1.49

Results are also given in the following figures (Figure 4.23 ~ Figure 4.26).

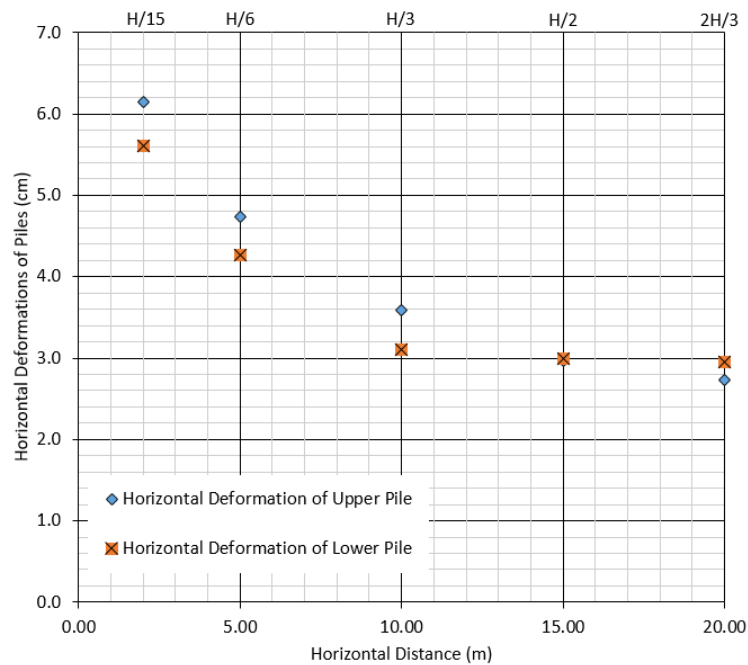


Figure 4.22 Horizontal displacement results (when the failure wedge of the individual, two separate walls, is considered)

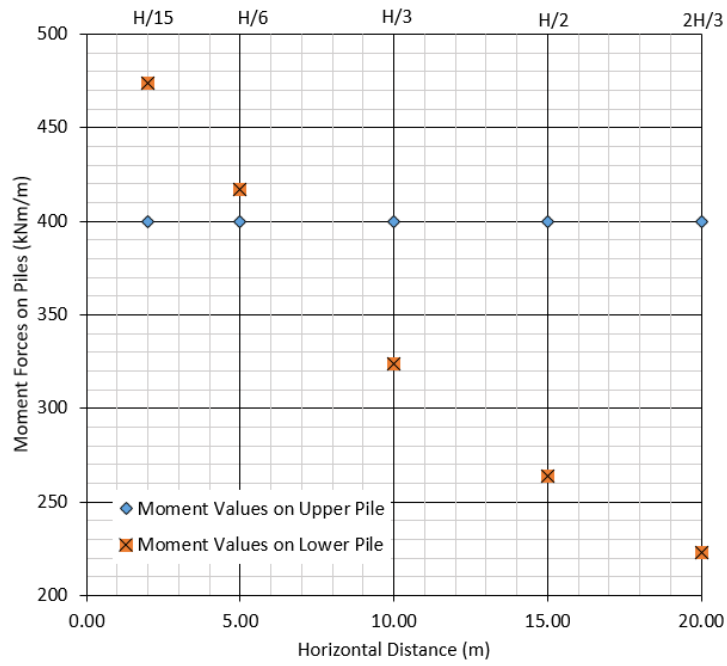


Figure 4.23 Moment values on piles (when the failure wedge of the individual, two separate walls, is considered)

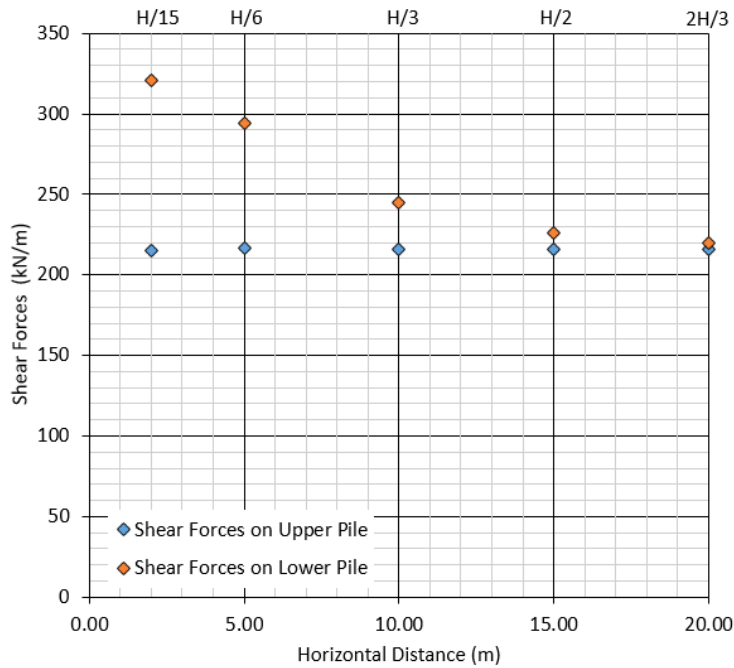


Figure 4.24 Shear forces on piles (when the failure wedge of the individual, two separate walls, is considered)

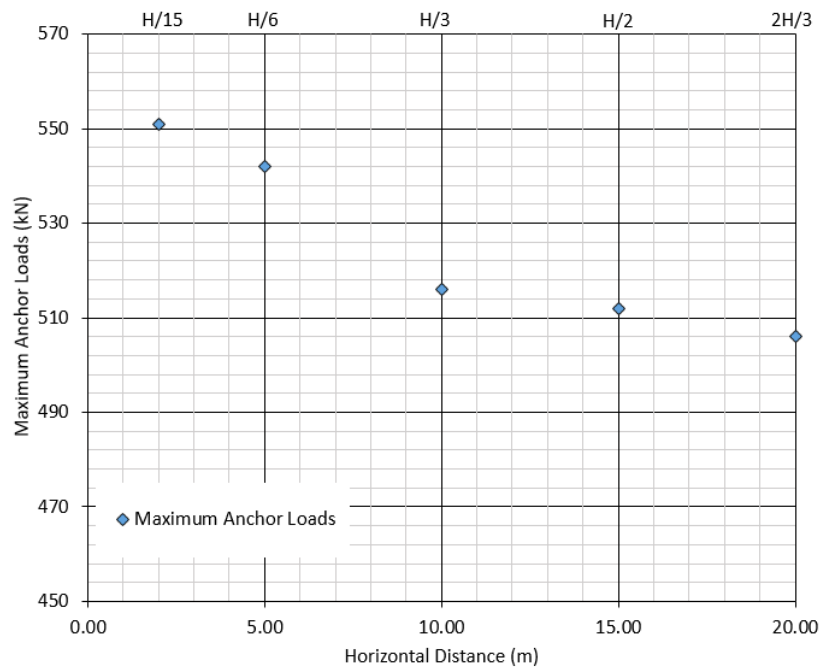


Figure 4.25 Maximum anchor loads (when the failure wedge of the individual, two separate walls, is considered)

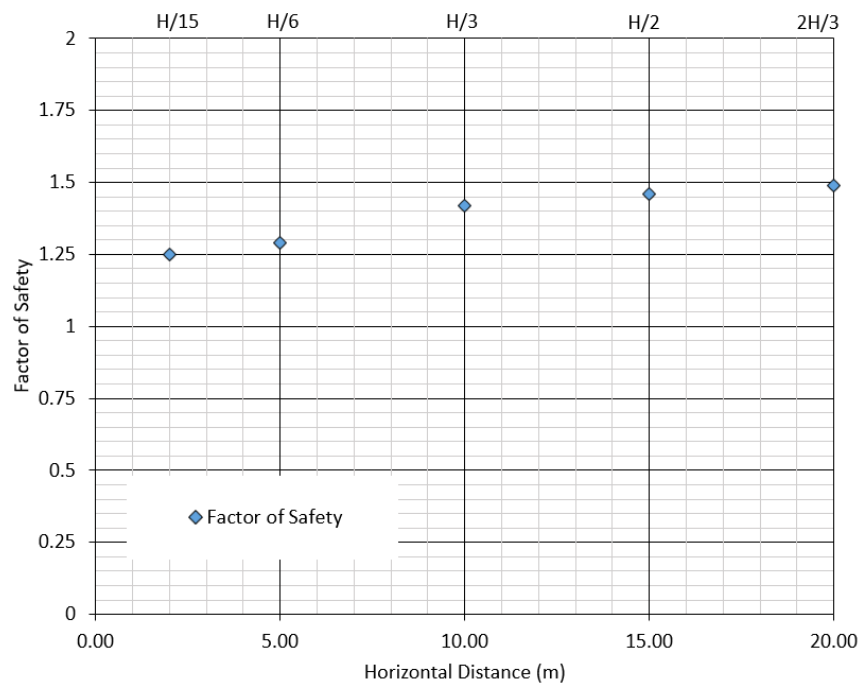


Figure 4.26 Factor of safety values (when the failure wedge of the individual, two separate walls, is considered)

If anchor lengths are designed for two piles that are thought to be completely independent of each other (i.e. two separate walls and their own anchor lengths);

- When horizontal distance is closest ( $H / 15 = 2.00$  m), horizontal displacement of upper piles increased by 60% and horizontal displacement of lower piles increased by 40% compared to case when the design is done combined one wall.
- When maximum displacement values in Table 4.18 and Table 4.20 are compared, for the upper pile as an example, it is seen that for horizontal distances greater than or equal to  $H/3$ , anchor lengths of two walls can be designed separately. It is seen in Table 4.21 factor of safety of global stability is less than 1.30 for horizontal distance less than  $H/3$ . Therefore, for distances less  $H/3$ , a combined failure wedge for whole excavation depth should be considered when determining anchor lengths. However, there is no change in moment and shear forces of upper piles.
- It is seen that maximum loads of anchors reaches to limit values and factor of safety decreases from 1.50 in “dependent case”, to 1.25 in “independent walls case”.
- If the horizontal distance is  $H / 15 = 2$  m and  $H / 6 = 5$  m, factor of safety values are below the acceptable limits and anchor loads exceed the bonded length capacity.
- In the comparison of the “dependent” and “independent walls” cases, the results obtained when the horizontal distance between the two piles is  $H / 3 = 10$  m are closest to each other and within acceptable limits for anchor loads and factor of safety. Therefore, sliding surface of both piles can be separated from each other, and anchor lengths of each wall can be designed separately, for the horizontal distance of  $H / 3 = 10$  m.

For horizontal distance of 2.00 m and 10.00 m horizontal displacement and incremental shear strain plots for “dependent” and “independent” anchor length designs can be seen in Appendix E.

Fang et al. (2013) defined “interaction coefficient” (between 0 and 1) to evaluate the interaction between two walls in multi-tier pile walls with struts. When coefficient is zero there is no interaction, and when it is 1 there is maximum interaction. According to their definition, interaction coefficient is calculated and plotted with horizontal distance between two walls (Figure 4.27). It is seen that as the horizontal distance increases interaction between two walls decrease nonlinearly. The decrease is not linear, as opposed to what was reported by Fang et al. (2013) (Fang et al. (2013) had stated that the interaction coefficient decreases linearly with increasing spacing between the two walls). Furthermore, they described horizontal distance according to passive failure wedge geometry in front of the upper pile. According to this calculation for a vertical overlap length 3.00 m between two piles, the horizontal distance of passive wedge is calculated as 5.1 m and shown in Figure 4.27. Fang et al. (2013) stated that if the horizontal distance between the two walls is greater than this “influence distance” (shown in Figure 2.9(b) and it is 5.1 m in this study), it can be assumed that the interaction is negligible. As seen in Figure 4.27 and Table 4.22, for horizontal distances greater than 5.1 m interaction coefficient is less than 0.5 (i.e. 50%), and for horizontal distances greater than 10 m it is less than 0.056 (i.e. 5.6%).

Table 4.22 Interaction coefficient vs horizontal distance

Horizontal distance between upper and lower walls (m)	Max. Horizontal displacement in the walls (lower wall) $\Delta x$ (cm)	Interaction coefficient $(\Delta x - \Delta x_{\min}) / (\Delta x_{\max} - \Delta x_{\min})$
2.00	5.61	1.000
5.00	4.27	0.496
10.00	3.10	0.056
15.00	3.00	0.018
20.00	2.95	0.000



Figure 4.27 Interaction coefficient vs horizontal distance

Civiltech software program describe the critical distance as follows;

$$X_c = 0.6 (H_2 + D_2) + 1.7 \times D_1 \quad (4.3)$$

In parametric study;

$D_1 = 3.00$  m (embedded length of upper pile)

$H_2 = 15.00$  m (excavation depth of lower pile)

$D_2 = 5.00$  m (Socket length of lower pile)

Using these values  $X_c$  is calculated as 20.1 m. Therefore, according to the Civiltech software program, two walls act independently if the horizontal distance between two walls is greater than 20.1 m.

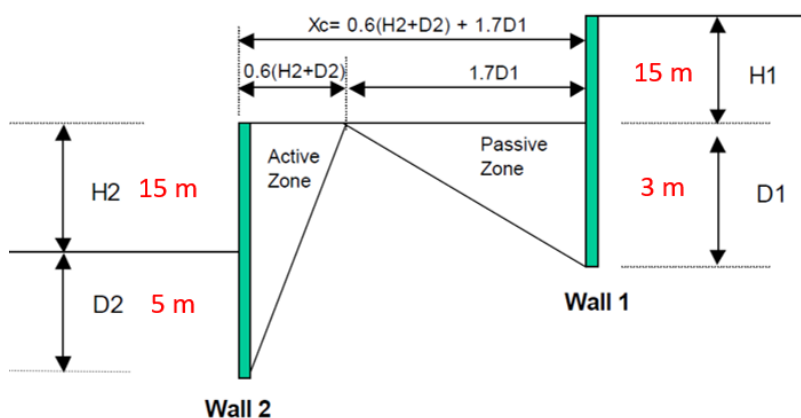


Figure 4.28 Description of the interaction between two walls





## CHAPTER 5

### CONCLUSIONS

The main chapters of this thesis are case study and parametric study.

#### **5.1. Scope of the case study and results**

The study consists of a multi-tier shoring system for a 30-m-deep excavation in a stiff clay. According to SPT and PMT field experiments, geotechnical parameters of soil are determined according to different empirical formulas given in the literature, and long term and short-term design parameters are selected. Multi-tier shoring system is analyzed via finite element method, by using Plaxis 2D software, by selecting different material constitutive models and different drainage types. Four different constitutive models are used in the case study: (1) Hardening soil and drained, (2) Hardening soil and undrained A, (3) Hardening soil and undrained B, (4) Mohr Coulomb and drained type. According to the results of the finite element analyses, the largest deformations are obtained by using Hardening soil constitutive model (Undrained B). Mohr-Coulomb (Drained) analysis results do not seem to be realistic, because of a backward movement at the top of the upper pile. Results obtained by Hardening Soil Model (Drained) and Hardening Soil Model (Undrained A) show a similar behaviour. The “closest” pile horizontal deformation behavior to inclinometer measurements is obtained by using the Hardening Soil Model and drained geotechnical material parameters.

Pile deformation behavior measured by inclinometer could not be obtained by any of the four alternatives. In four of the Plaxis 2D results, the end of the lower pile moves whereas in inclinometer measurements, there is no deformation in the lower pile. In contrast to Plaxis 2D results, the inclinometer measurements indicate that deformation of the lower pile in reality was smaller than Plaxis 2D analysis results. One of the

reasons for this may be accepted soil parameters in the lower layers of Ankara clay is different than the values used in this study. Further investigation of this issue can be conducted.

Another important conclusion is that the OCR values of clay must be taken into account in Plaxis 2D analysis. As the OCR value increased for the near to the ground surface, horizontal deformations of piles increased. Therefore, in Plaxis 2D software, if default value 1 is used for OCR, shoring system may have larger deformation than calculated one.

## **5.2. Scope of the parametric study and results**

There are various parameters that affect the behavior of multi-tier pile wall shoring system. To investigate the variations in the factors affecting shoring system behavior a series of parametric analyses are carried out in a stiff cohesive soil. Lateral deformation, moment and shear forces on piles, anchor loads and global factor of safety of the shoring system are studied by systematically changing some of the design and geometrical parameters of multi-tier pile wall. These parameters are:

- Embedment length of upper pile
- Embedment length of the lower pile (socket length),
- Effect of having an anchor at the overlap zone between two piles
- The horizontal distance between upper and lower piles
- Interface friction coefficient between pile and soil,
- Higher and lower intensity anchor placement (i.e. anchor per  $m^2$  plan area of wall)

In all analyses; only the investigated parameter is systematically changed and results are analyzed, while keeping other parameters constant.

- As the upper pile socket length increases from  $H/30$  to  $H/10$ , horizontal displacement of upper pile decreases by 10% (for 1 anchor per  $4 m^2$  area), and by ~8% (for 1 anchor per  $4.5 m^2$  area).

- There is no, or insignificant, change in the moment and shear forces of upper pile; horizontal deformation, moment and shear forces of the lower pile, and maximum anchor load and factor of safety, when upper pile socket length is changed from  $H/30$  to  $H/6$ , for both anchor intensity levels.
- Horizontal deformation of both upper and lower pile increases by about ~15-20% when anchor intensity is decreased by 12.5%, for a given upper and lower socket lengths.
- Upper pile embedment length does not affect shoring system if socket length of upper pile is more than  $H/10$ , and lower pile socket length does not affect shoring system if socket length is more than  $H/6$ , in both anchor intensities.
- Pile-Soil interface friction coefficient is changed between 0.7 and 1.0 and it is seen that horizontal deformations increase, and maximum anchor load increase as the interface coefficient decreases (moment and shear forces on both piles do not change much).
- If the anchor at the overlap zone of both piles is canceled: deformation and moment values of upper row piles increase by ~25%, deformation of lower piles increases by ~ 10%, and maximum anchor loads exceed the limit values (i.e. unsafe). When the anchor in overlap zone is canceled, displacements increase significantly in the socket zone of upper pile and in top of lower pile. While drilling lower pile construction, there is a possibility to have more displacement on socket area of upper pile. Therefore, in the multi-tier pile wall retaining system, construction of the last row anchors of upper pile must be completed before starting to the forage of the lower pile. Moreover; it is necessary to complete cross beam construction and pre-stress of the last level of anchors of the upper pile. As a result of the analysis, the last anchor of upper pile should be close to the intermediate excavation level (overlap zone of upper and lower piles) in the multi-tier pile wall retaining system.
- When the horizontal distance between two piles are considered: the horizontal displacement of both piles decreases significantly (by about 50%) as horizontal distance between two piles increases from  $H/15$  to  $2H/3$ . Although values for

upper piles do not change, there is a reduction in moment and shear forces of lower piles by about 25%-35% when the horizontal distance between two piles increase. If horizontal distance between two piles exceeds  $H/3$ , the rate of decrease in the horizontal displacements and moment values of piles decreases considerably.

- Factor of safety of global stability is less than 1.30 for horizontal distance less than  $H/3$ , and for distances less than  $H/3$ , a combined failure wedge for whole excavation depth should be considered when determining anchor lengths of upper and lower piles. For horizontal distances greater than or equal to  $H/3$ , anchor lengths of two walls can be designed separately.

### **5.3. Limitations of the study and recommendations for future research**

- The results of this study are valid for two-tier pile wall system having an excavation depth greater than 25 m, in a stiff clay, where there is no ground water table. Results should be investigated for excavations in other soil types.
- Effect of OCR of stiff clay on the results could be investigate in detail.
- All 2D analysis could be compared with 3D analysis.

## REFERENCES

- Aktan, E. (2014). Numerical analysis of prestressed anchored pile wall: Shoring system in front of historic building in Hilton Istanbul Bomonti hotel and conference center project, M.S. Thesis, Istanbul Technical University. 207 p.
- Aktaş, T. (2019) Finite Element Analyses of a Deep Excavation: Case Study, M.S. Thesis, Middle East Technical University, 138 p.
- ASTM A416/A416M-02 (2002). Standard Specification for Steel Strand, Uncoated Seven-Wire for Prestressed Concrete, American Society for Testing and Materials, West Conshohocken, Pennsylvania.
- ASSHTO (1996). Standard Specifications for Transportation Materials 16th Edition, American Association of State Highway and Transportation Officials, Washington, DC.
- Birand, A. (1977). Ankara Yöresi Zeminlerde Ön Yükleme İsootropisi. 4. Tubitak Teknik Kongresi, İzmir
- Bjerrum, L. and Simons, N.E. (1960) Comparison of shear strength characteristics of normally consolidated clays. Norwegian Geotechnical Institute. Publ., 35, pp. 13-22.
- Bowles, J.E. (1988). Foundation Analysis and Design, McGraw-Hill, Singapore.
- BS 8081 (1989). British Standard Code of Practice for Ground Anchorages, British Standard Institution, London.
- CIRIA. (1995). The Standard Penetration Test (SPT): Methods and Use, London
- Coduto, D. P. (2006). Geoteknik Mühendisliği İlkeler ve Uygulamalar, Gazi Kitabevi, Ankara.
- Das, B. M. (1987). Theoretical Foundation Engineering, Developments in Geotechnical Engineering Vol 47, Elsevier Science Publishing Co., NY, USA.
- Das, B. M. (2007). Principles of Foundation Engineering 6th Edition, Pws Publishing Co.
- Dayıoğlu, M. (2010). Derin Kazıların İncelenmesi ve Derin Kazı Uygulaması Üzerine Bir Örnek: Harbiye Kongre Merkezi Derin Temel Kazısı, M.Sc. Thesis, Istanbul Technical University, Istanbul.
- EN1537 (2000). Execution of special geotechnical work, European Standard, CEN, Brussels.

- Fang, K., Zhang, Z., Liu, X., Zhang, Q., and Lin, C. (2013) Numerical Analysis of the Behavior of Special Double-Row Support Structure, *Journal of Civil Engineering and Management*, v. 19(2), p.169-176
- FHWA-IF-99-015. (1999). Ground Anchors and Anchored Systems, Geotechnical Engineering Circular No.4, U.S. Department of Transportation, Federal Highway Administration, Washington DC.
- İspir E. (2011) A Laboratory Study of Anisotropy In Engineering Properties of Ankara Clay, M.Sc. Thesis, Middle East Technical University, 94 p.
- Jamiolkowski, M., Lancellota, R., Marchetti, S., Nova, R., and Pasqualini, E. (1979) Design parameters for clays, State of the Art Report, 7th European Conf. On Soil Mechanics, Brighton.
- Kasktaş A.Ş. (2015) Eroğlu Skyland Project Details  
Retrieved from <https://www.kasktas.com.tr/en/portfolio-item/eroglu-skyland-project/>
- Kenney, T.C. (1959) Discussion of Journal of the Soil Mechanics and Foundation Engineering Division; ASCE 85-SM3, 67–79.
- Ladd C.C., Foott R., Ishihara K., Schlosser F., and Poulos H.G., (1977) Stress-Deformation and Strength Characteristics: SOA Report.” Proc., 9th ICSMFE Tokyo, Vol. 2, pp. 421-494. 1977.
- Lunne T., Robertson K.P. and Powell M.J.J. (1997). “Cone Penetration Testing in Geotechnical Practice” Blackie Academic and Professional.
- NAVFAC, DM-7.2. (1982). Foundations and Earth Structures Design Manual 7.2, Department of the Navy, Alexandria, VA.
- Ordemir, I., Alyanak, I., & Birand, A. (1965). Report on Ankara Clay. Ankara: Faculty of Engineering, METU.
- Ou, C. (2006). Deep Excavation: Theory and Practice, Tylor and Francis Group Publishers, London, UK.
- Öncü, G. (2009). Derin Kazılı İksa Sisteminde Oluşan Yer Değiştirmelerin Hesaplanarak Aletsel Gözlemlerle Karşılaştırılması, M.Sc. Thesis, Yıldız Technical University, Istanbul.
- Plaxis Material Models Manual (2019).
- Plaxis 2D Reference Manual (2019).
- Poulos, H.G. and Small, J.C. (2000) Development of Design Charts for Concrete Pavements and Industrial Ground Slabs, In book: Design Applications of Raft Foundations Edition: 1 Chapter: 2 Publisher: Thomas Telford Limited Editors: J.A. Hemsley

- Stroud, M.A. (1974). The Standard Penetration Test in Insensitive Clays and Soft Rocks. Proceedings, First European Conference on Penetration Testing, Stockholm.
- Sincil, K. (2006). Ankrajlı Kazık Duvarların Sayısal Çözümlemesi: Durum Analizi. Yüksek Lisans Tezi, Atılım Üniversitesi Fen Bilimleri Enstitüsü, İnşaat Mühendisliği Anabilim Dalı, Ankara.
- Sorensen, K.K. and Okkels, N. (2013) Correlation between drained shear strength and plasticity index of undisturbed overconsolidated clays, Proc. 18<sup>th</sup> International Conference on Soil Mechanics and Geotechnical Engineering, Paris
- Sütçüoğlu, M. (2009). A Case Study: A Deep Retaining System Construction With Prestressed Anchors, M.S. Thesis, Dokuz Eylül University, Izmir.
- ÜK, M. (2009). Derin Kazılar ve Derin Kazılara Bir Örnek: Flame Towers Projesi İksa Sistemi, M.Sc. Thesis, Istanbul Technical University, Istanbul.
- Xanthakos, P. (1991). Ground Anchors and Anchored Structures, John Wiley & Sons, Inc., Canada.
- Yüksel, F. (1990). Derin Kazılarda İksa Yöntemleri, M.Sc. Thesis, Istanbul Technical University, Istanbul.
- Url-1 <<https://www.kasktas.com.tr/en/portfolio-item/eroglu-skyland-project/>>, date retrieved 01.09.2019
- Url-2 <<https://civiltech.com/downloads/stepwall.pdf>>, date retrieved 01.09.2019



## APPENDICES

### A. BORING LOGS

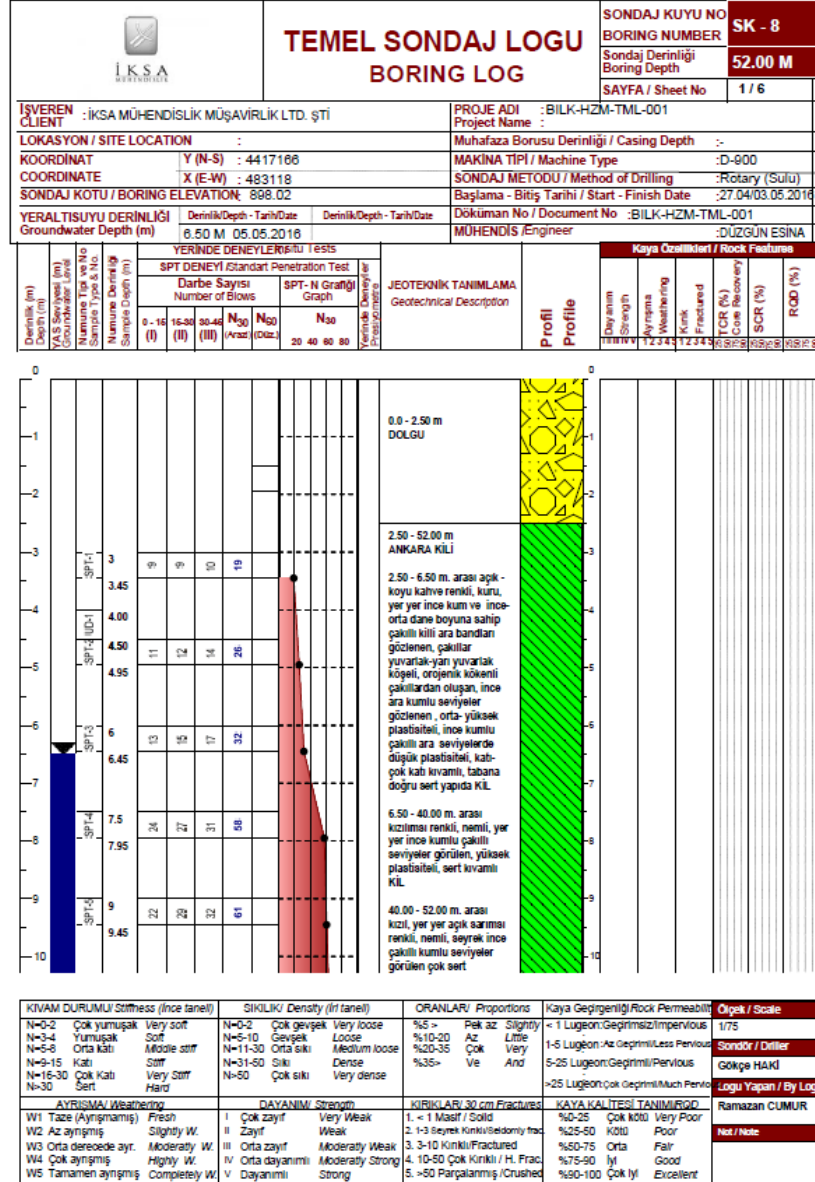
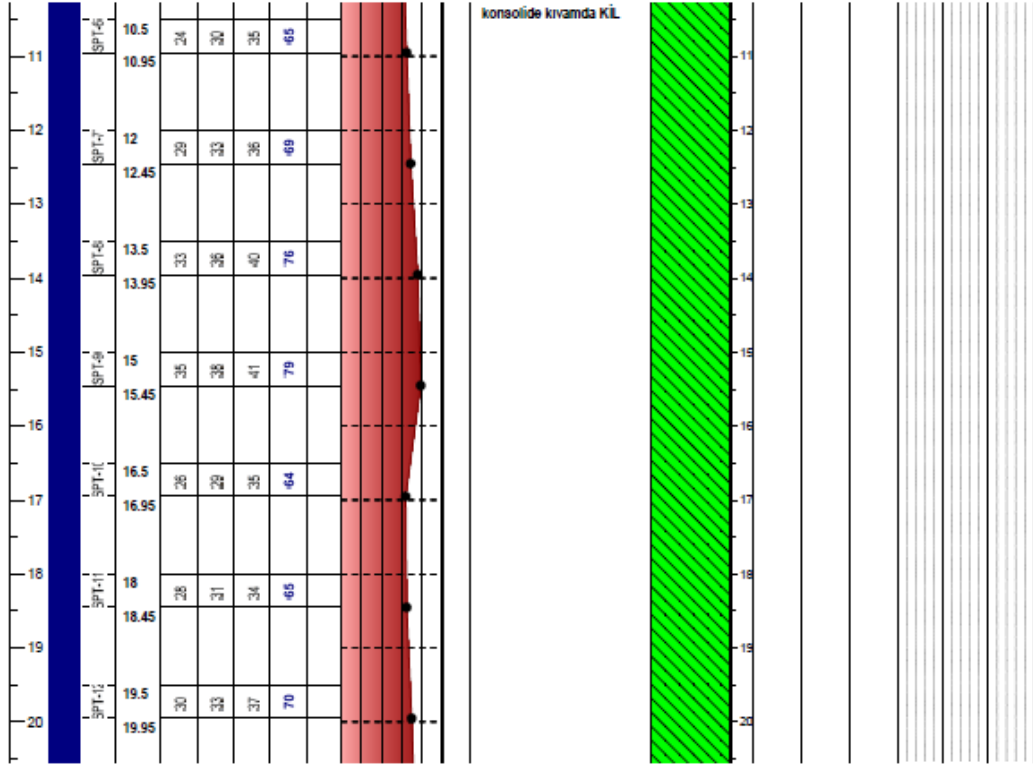


Figure A.1 Boring Log for SK-8



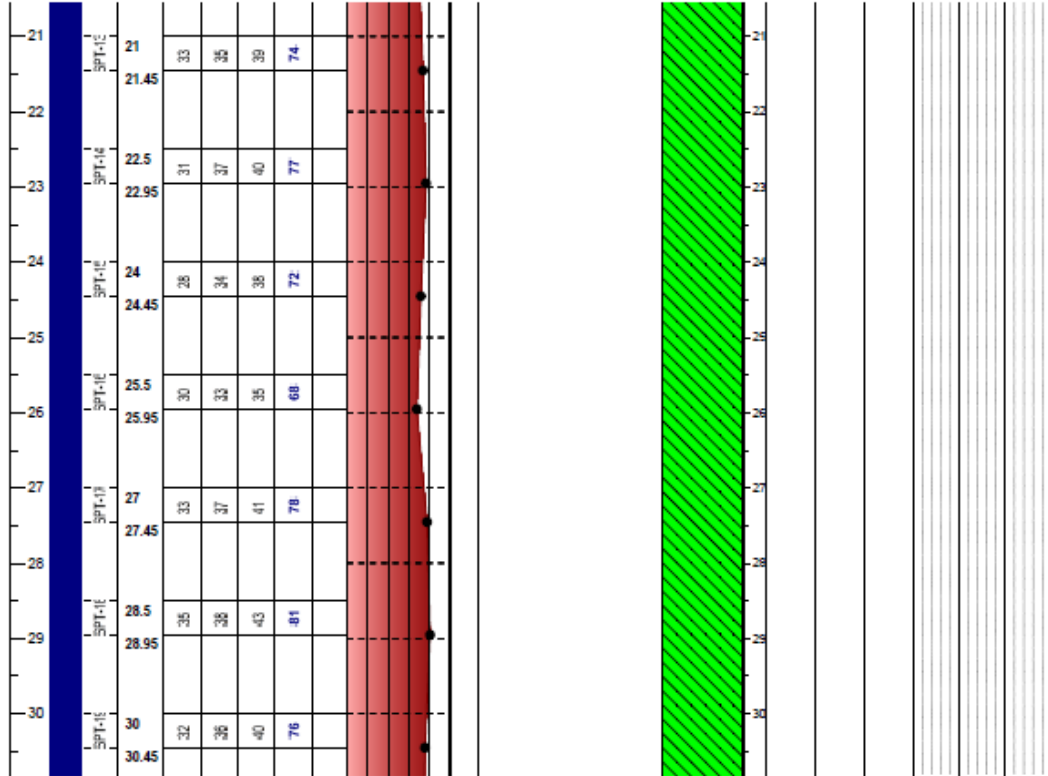
		<b>TEMEL SONDAJ LOGU</b> <b>BORING LOG</b>		SONDAJ KUYU NO BORING NUMBER	SK - 8												
				Sondaj Derinliği Boring Depth	52.00 M												
				SAYFA / Sheet No	2 / 6												
İŞVEREN CLIENT : İKSA MÜHENDİSLİK MÜŞAVİRLİK LTD. ŞTİ			PROJE ADI : BILK-HZM-TML-001 Project Name :														
LOKASYON / SITE LOCATION :			Muhafaza Borusu Derinliği / Casing Depth :-														
KOORDİNAT COORDINATE			Y (N-S) : 4417186 X (E-W) : 483118														
SONDAJ KOTU / BORING ELEVATION: 898.02			MAKİNA TİPİ / Machine Type :D-900 SONDAJ METODU / Method of Drilling :Rotary (Sulu)														
YERALTISUYU DERİNLİĞİ Groundwater Depth (m)			Başlama - Bitiş Tarihi / Start - Finish Date :27.04/03.05.2016														
Derinlik/Depth - Tarih/Date			Döküman No / Document No :BILK-HZM-TML-001														
6.50 M 05.05.2016			MÜHENDİS /Engineer :DUZGUN ESİNA														
Derinlik (m) Depth (m)	Y.A.S Seviyesi (m) Groundwater Level	Numune Tipi ve No Sample Type & No.	Numune Derinliği Sample Depth (m)	YERİNDE DENEYLERİ/In Situ Tests						JEOTEKNİK TANIMLAMA Geotechnical Description	Profil Profile	Kaya Özellikleri / Rock Features					
				SPT DENEYİ/Standart Penetration Test			SPT- N Grafiği Graph					Dayanım Strength	Ayrışma Weathering	Kırık Fractured	TCR (%) Core Recovery	SCR (%)	RQD (%)
Darbe Sayısı Number of Blows			N <sub>60</sub> (Düz.)			N <sub>30</sub> (20 40 80 80)											
				0 - 15 (I)	15-30 (II)	30-45 (III)	N <sub>60</sub> (Arz.)	N <sub>60</sub> (Düz.)	N <sub>30</sub>								



KIVAM DURUMU/ Stiffness (Ince taneli)	SIKLIK/ Density (İri taneli)	ORANLAR/ Proportions	Kaya Geçirgenliği/Rock Permeability	Ölçek / Scale
N=0-2 Çok yumuşak Very soft	N=0-2 Çok gevşek Very loose	%5 > Pek az Slightly	< 1 Lugeon:Gegirimsiz/Impervious	1/75
N=3-4 Yumuşak Soft	N=5-10 Gevşek Loose	%10-20 Az Little	1-5 Lugeon:Az Geçirimli/Less Pervious	Sondaj / Driller
N=5-8 Orta Kati Middle stiff	N=11-30 Orta siki Medium loose	%20-35 Çok Very	5-25 Lugeon:Geçirimli/Pervious	Gökçe HAKI
N=9-15 Kati Stiff	N=31-60 Siki Dense	%35> Ve And	>25 Lugeon:Çok Geçirimli/Much Pervious	Logu Yapan / By Log
N=16-30 Çok Kati Very Stiff	N=60 Çok siki Very dense			Ramazan CUMUR
N=30 Bert Hard				Not / Note
AYRIŞMA/ Weathering	DAYANIM/ Strength	KIRIKLAR/ 30 cm Fractures	KAYA KALİTESİ TANIMI/RQD	
W1 Taze (Ayrışmamış) Fresh	I Çok zayıf Very Weak	1. < 1 Masif / Solid	%0-25 Çok kötü Very Poor	
W2 Az ayrışmış Slightly W.	II Zayıf Weak	2. 1-3 Seyrek Kırıktı/Seldomly frac.	%25-50 Kötü Poor	
W3 Orta derecede ayr. Moderatly W.	III Orta zayıf Moderatly Weak	3. 3-10 Kırıktı/Fractured	%50-75 Orta Fair	
W4 Çok ayrışmış Highly W.	IV Orta dayanımlı Moderatly Strong	4. 10-50 Çok Kırıktı / H. Frac.	%75-90 İyi Good	
W5 Tamamen ayrışmış Completely W.	V Dayanımlı Strong	5. >50 Parçalanmış /Crushed	%90-100 Çok İyi Excellent	

Figure A.2 Boring Log for SK-8

		<h2 style="margin: 0;">TEMEL SONDAJ LOGU</h2> <h3 style="margin: 0;">BORING LOG</h3>		<b>SONDAJ KUYU NO</b> SK - 8 <b>BORING NUMBER</b>								
				<b>Sondaj Derinliği</b> 52.00 M <b>Boring Depth</b>								
<b>İŞVEREN CLIENT</b> : İKSA MÜHENDİSLİK MÜŞAVİRLİK LTD. ŞTİ <b>PROJE ADI</b> : BILK-HZM-TML-001 <b>Project Name</b> :		<b>SAYFA / Sheet No</b> 3 / 6										
<b>LOKASYON / SITE LOCATION</b> :		<b>Muhafaza Borusu Derinliği / Casing Depth</b> :-										
<b>KOORDİNAT</b> Y (N-S) : 4417166 <b>COORDINATE</b> X (E-W) : 483118		<b>MAKİNA TİPİ / Machine Type</b> :D-900										
<b>SONDAJ KOTU / BORING ELEVATION</b> : 898.02		<b>SONDAJ METODU / Method of Drilling</b> :Rotary (Sulu)										
<b>YERALTISUYU DERİNLİĞİ</b> Derinlik/Depth - Tarih/Date : 8.50 M 05.05.2016 <b>Groundwater Depth (m)</b>		<b>Derinlik/Depth - Tarih/Date</b>		<b>Başlama - Bitiş Tarihi / Start - Finish Date</b> :27.04/03.05.2016								
		<b>DERİNİK/DEPTH - TARİH/DATE</b>		<b>Döküman No / Document No</b> :BILK-HZM-TML-001								
		<b>MÜHENDİS /Engineer</b>		<b>:DÜZGÜN ESİNA</b>								
		<b>YERİNDE DENEYLER/İn situ Tests</b>		<b>Kaya Özellikleri / Rock Features</b>								
Derinlik (m) Depth (m)	MAS Sayısı ve No Groundwater Level	SPT DENEYİ /Standart Penetration Test		JEOTEKNİK TANIMLAMA Geotechnical Description	P profil Profile	Dayanım Strength	Ayrışma Weathering	Kırık Fractured	TCR (%) Core Recovery	SCR (%)	ROD (%)	
		Darbe Sayısı Number of Blows	SPT- N Grafiği Graph									
	Numune Tipi ve No Sample Type & No	Numune Derinliği Sample Depth (m)	0 - 15 (I)	15-30 (II)	30-45 (III)	N <sub>30</sub> (Arz)	N <sub>60</sub> (Düz.)	N <sub>90</sub>	20	40	60	80



<b>KIVAM DURUMU / Stiffness (İnce taneli)</b>		<b>SIKLIK / Density (İri taneli)</b>		<b>ORANLAR / Proportions</b>		<b>Kaya Geçirgenliği/Rock Permeability</b>		<b>Ölçek / Scale</b>	
N=0-2 Çok yumuşak N=3-4 Yumuşak N=5-8 Orta kati N=9-15 Kati N=16-30 Çok Kati N>30 Şert	Very soft Soft Middle stiff Stiff Very Stiff Hard	N=0-2 Çok gevşek N=5-10 Gevşek N=11-30 Orta sıkı N=31-50 Sıkı N>50 Çok sıkı	Very loose Loose Medium loose Dense Very dense	%5 > Pek az %10-20 Az %20-35 Çok %35> Ve And	Slightly Little Very And	< 1 Lugeon:Geçirimsiz/Impervious 1-5 Lugeon :Az Geçirimli/Less PerVIOUS 5-25 Lugeon:Geçirimli/PerVIOUS >25 Lugeon:Çok Geçirimli/Much PerVIOUS	1/75 Sondör / Driller Gökçe HAKI Logu Yapan / By Log	Ramazan CUMUR	
<b>AYRISMA/ Weathering</b>		<b>DAYANIM/ Strength</b>		<b>KIRIKLARI/ 30 cm Fractures</b>		<b>KAYA KALİTESİ TANIMI/ROD</b>			
W1 Taze (Ayrılmamış) W2 Az ayrılmış W3 Orta derecede ayr. W4 Çok ayrılmış W5 Tamamen ayrılmış	Fresh Slightly W. Moderately W. Highly W. Completely W.	I Çok zayıf II Zayıf III Orta zayıf IV Orta dayanımlı V Dayanımlı	Very Weak Weak Moderately Weak Moderately Strong Strong	1. < 1 Masif / Solid 2. 1-3 Seyrek kırıklı/Seldomly frac. 3. 3-10 Kırıklı/Fractured 4. 10-50 Çok Kırıklı / H. Frac. 5. >50 Parçalanmış /Crushed	%0-25 Çok kötü %25-50 Kötü %50-75 Orta %75-90 İyi %90-100 Çok İyi	Very Poor Poor Fair Good Excellent	Not / Note		

Figure A.3 Boring Log for SK-8





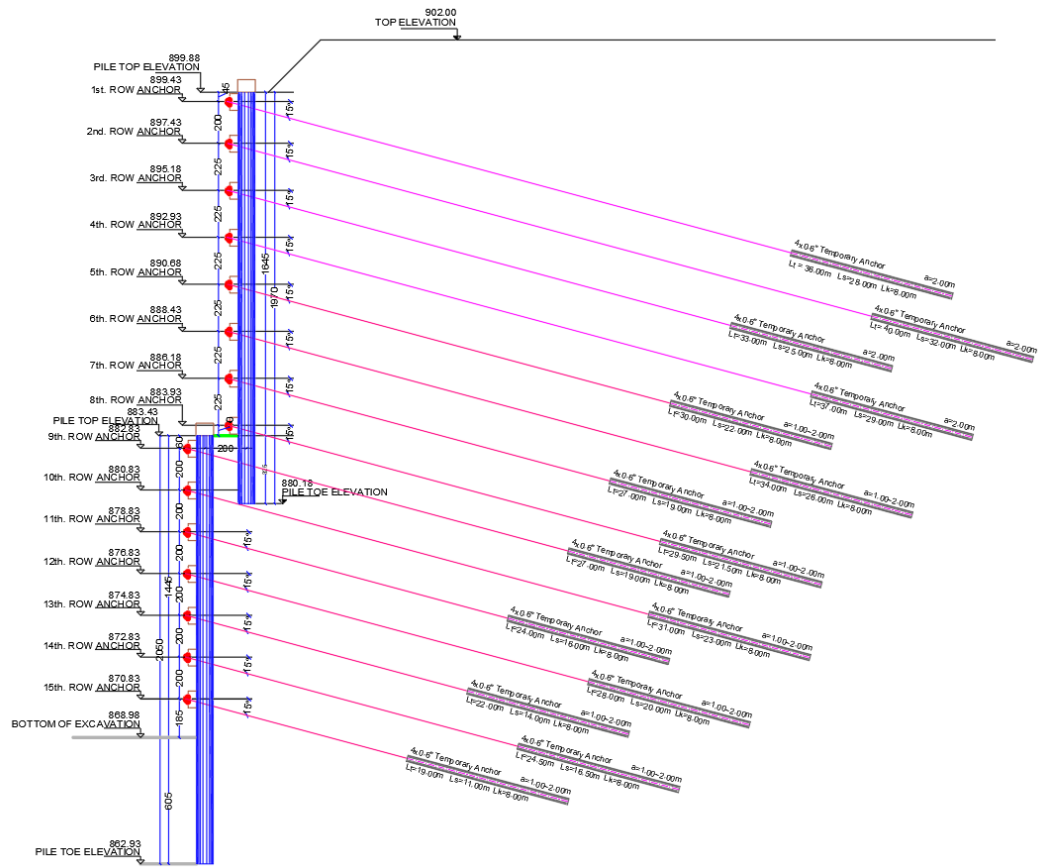


Figure B.4 Cross section view of shoring system

## C. CONSTRUCTION PHOTOS



Figure C.1 Bored piles and installation of soil anchors



Figure C.2 Multi-Tier shoring system final stage



Figure C.3 Multi-Tier shoring system



Figure C.4 Multi-Tier shoring system



Figure C.5 Multi-Tier shoring system



Figure C.6 Multi-Tier shoring system

## D. PLAXIS 2D RESULTS

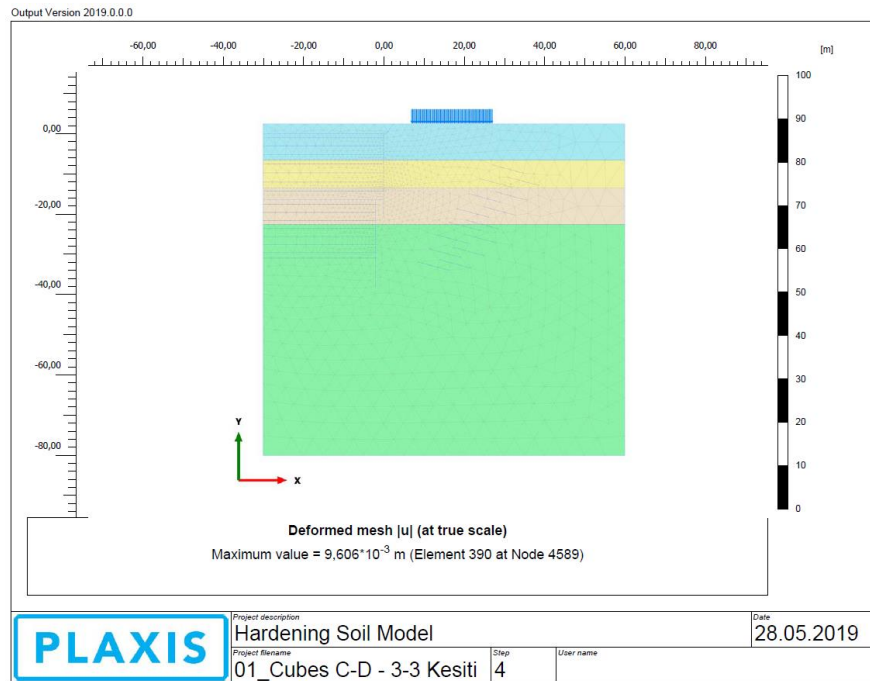


Figure D.1 Plaxis 2D deformed mesh original ground

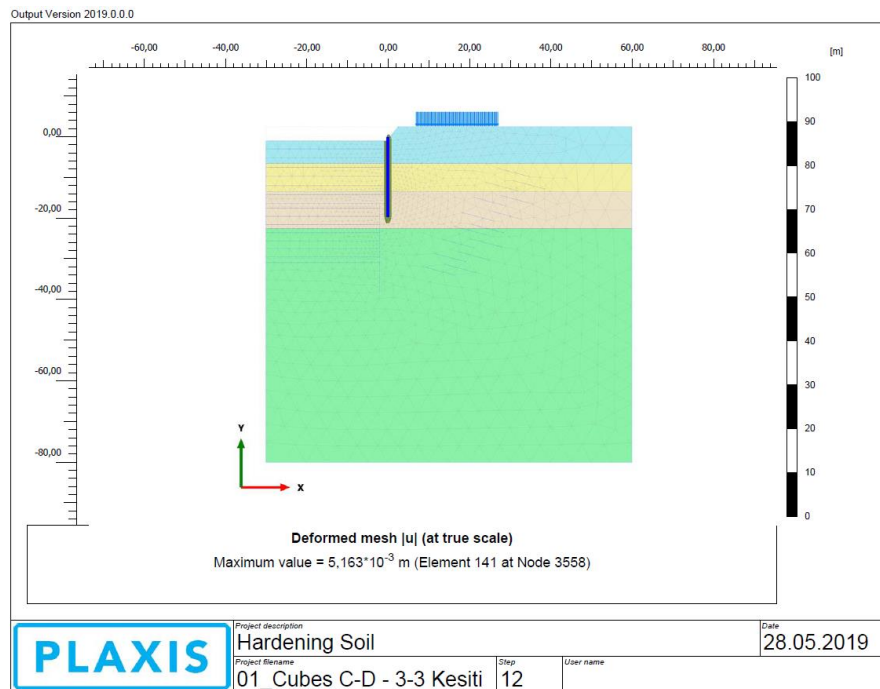


Figure D.2 Upper pile construction

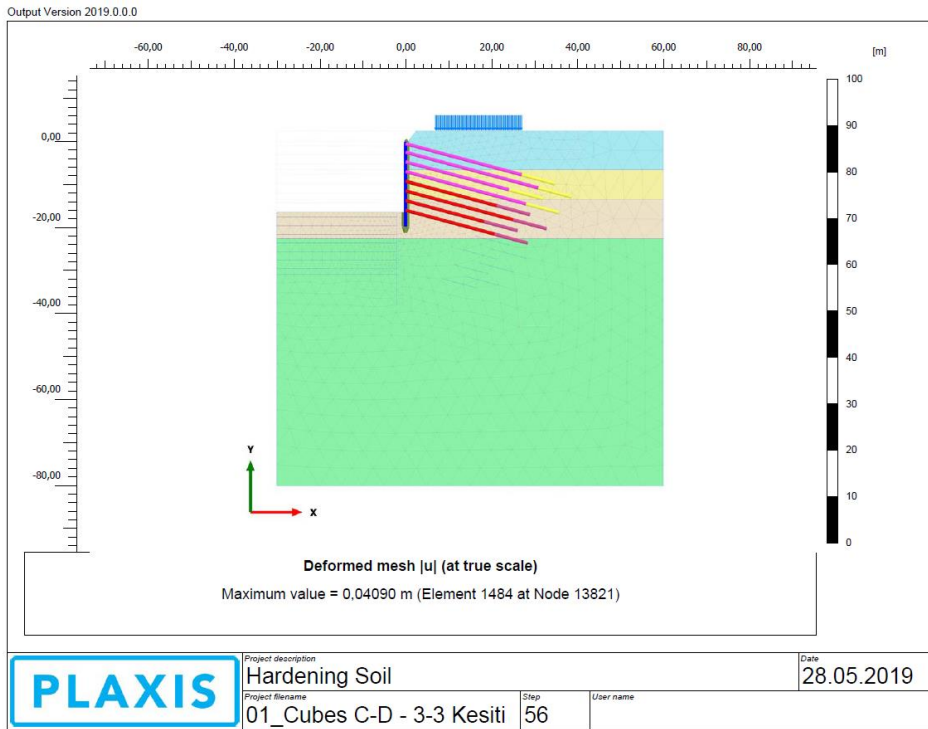


Figure D.3 Excavation and anchors construction steps until lower pile top level

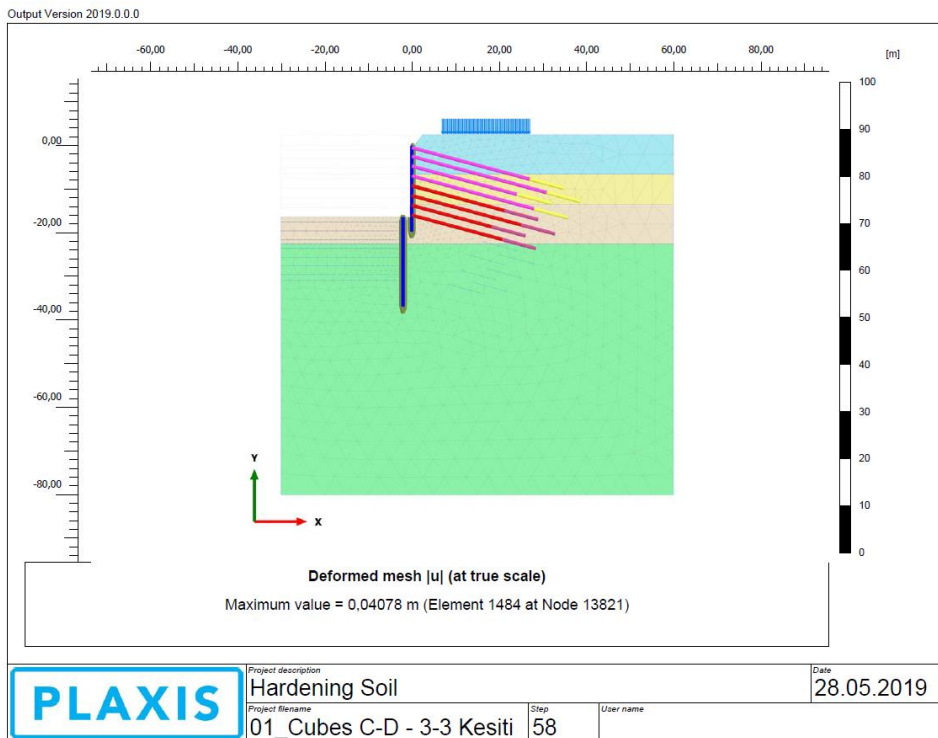


Figure D.4 Lower pile construction

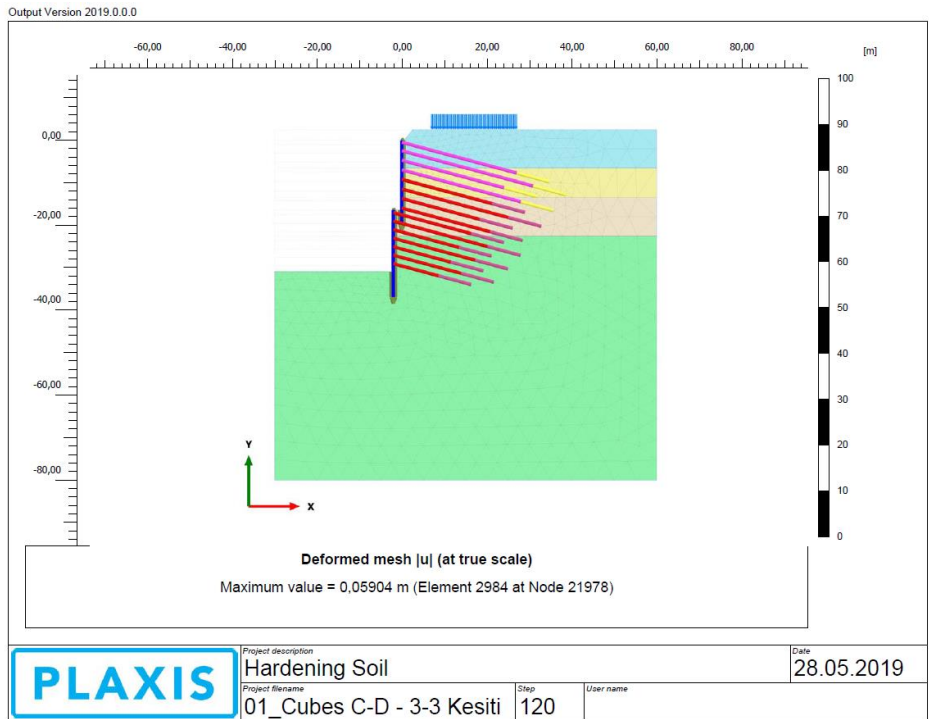


Figure D.5 Excavation and anchors construction steps until bottom level of excavation

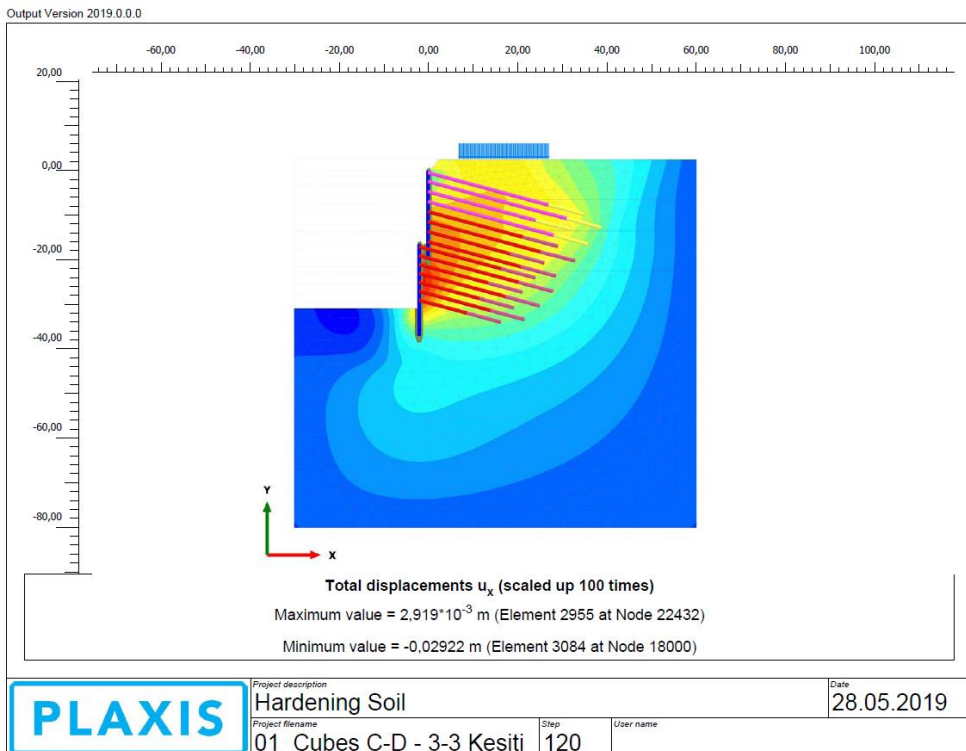


Figure D.6 Horizontal displacement of shoring system

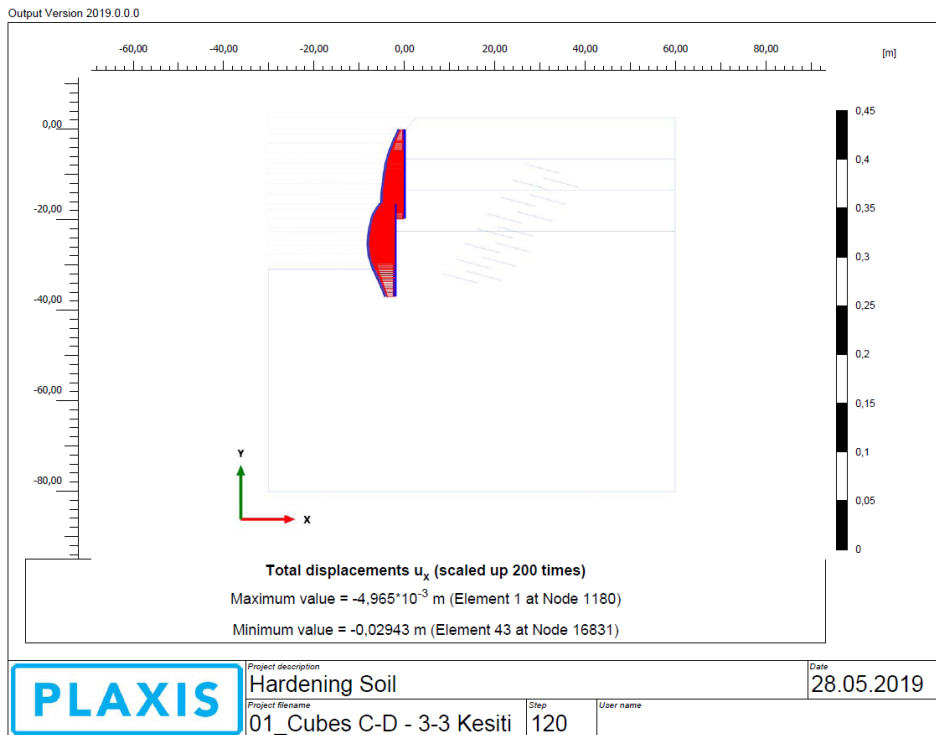


Figure D.7 Pile horizontal displacements



Figure D.8 Moment force diagram of piles

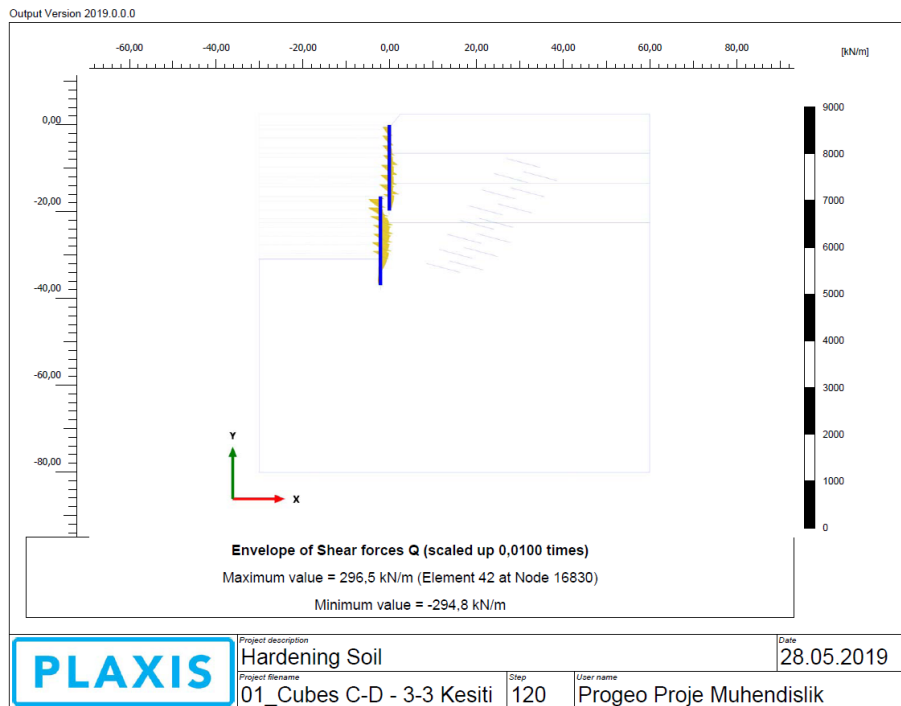


Figure D.9 Shear force diagram of piles

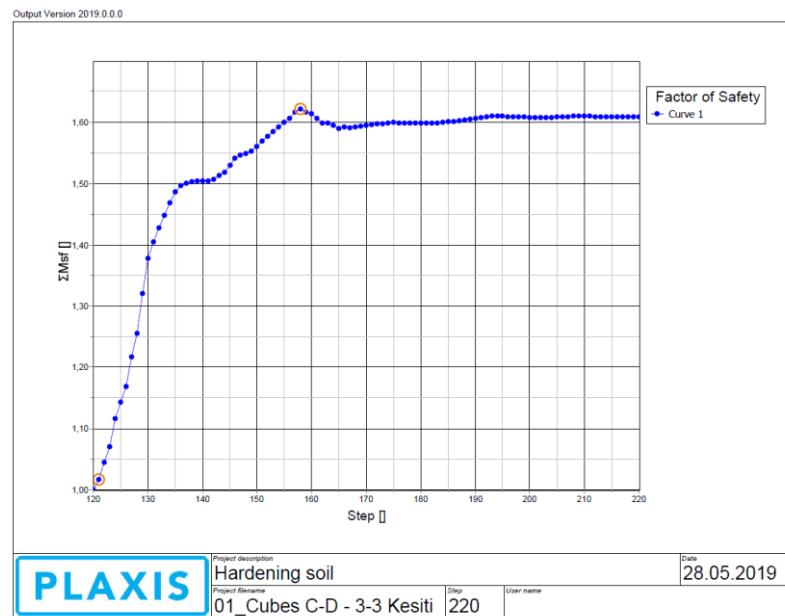


Figure D.10 Factor of safety of shoring system

## E. PLAXIS 2D RESULTS OF PARAMETRIC STUDIES

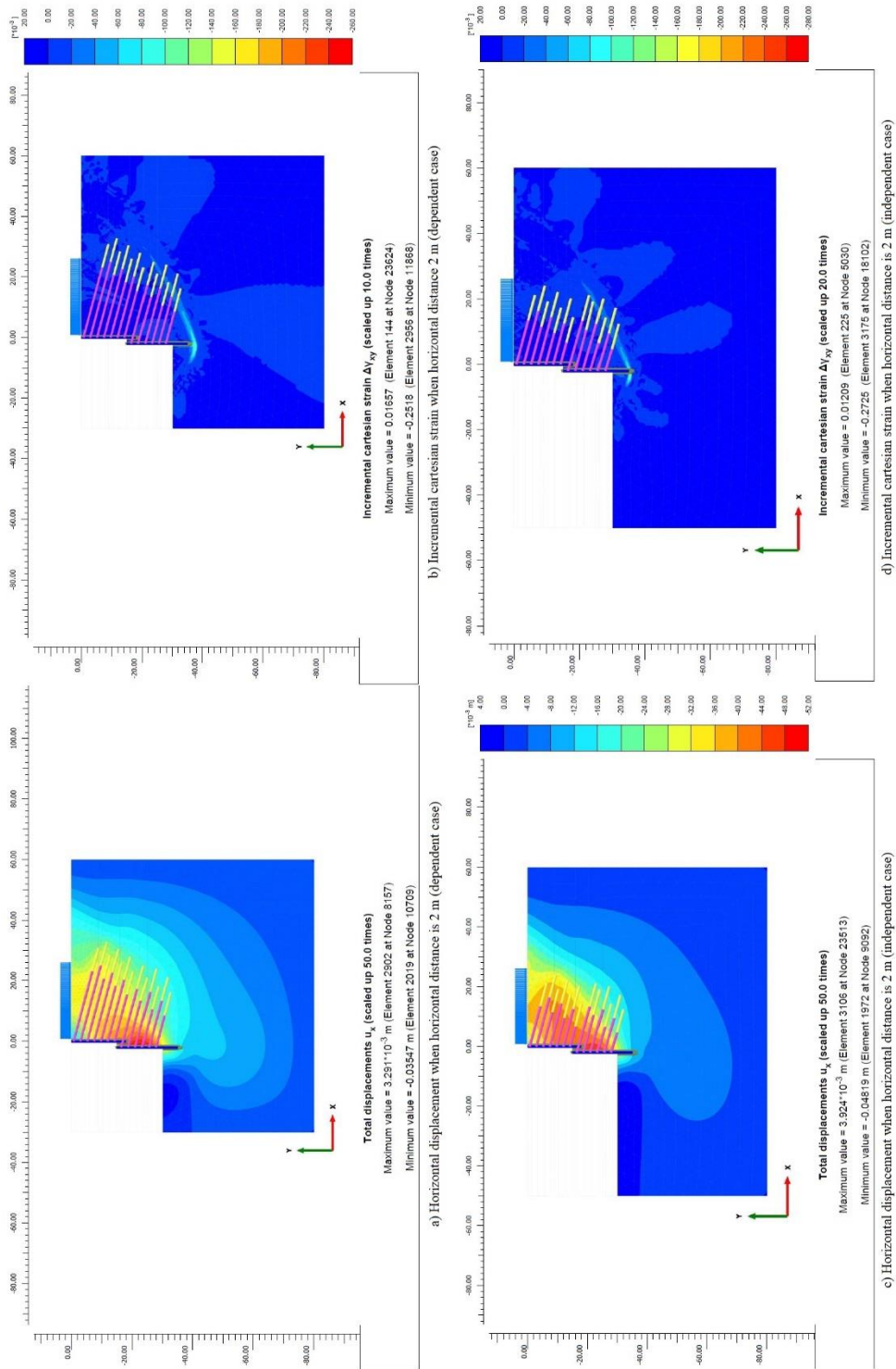


Figure E. 11 Plaxis results of parametric study (effect of lateral distance)

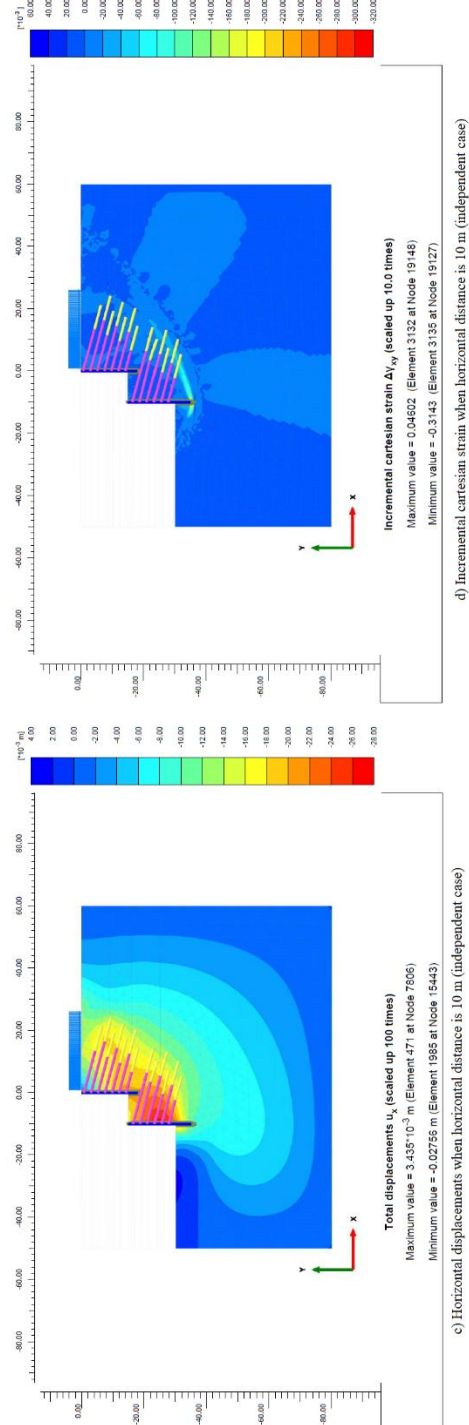
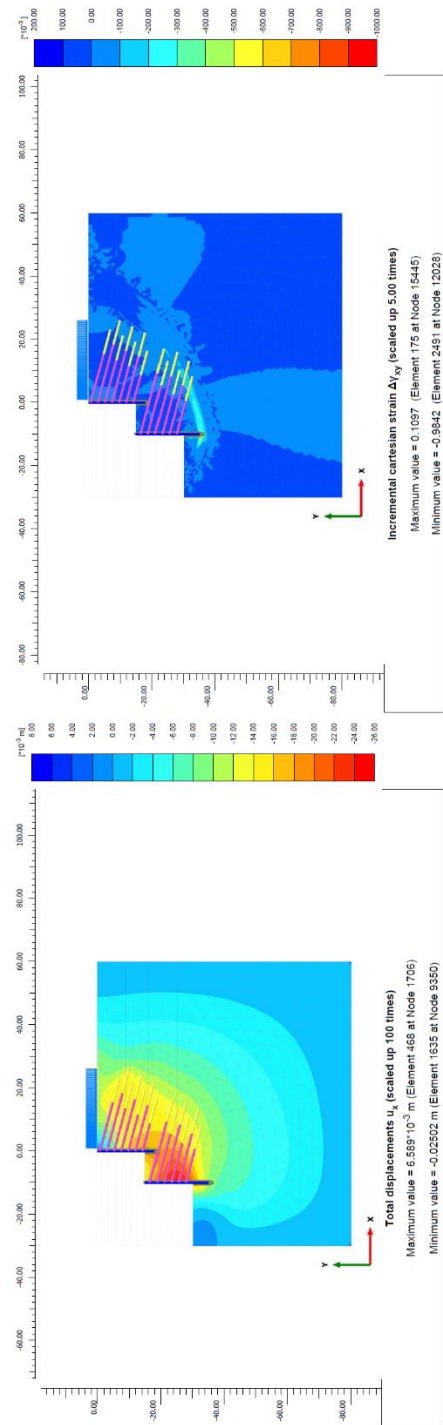


Figure E.12 Plaxis results of parametric study (effect of lateral distance)